THE ELASTIC RIGIDITIES OF RIBBED PLATES

by

ROBERT DRYDEN LITTLE

UNIVERSITY OF CAPE TOWN

1972

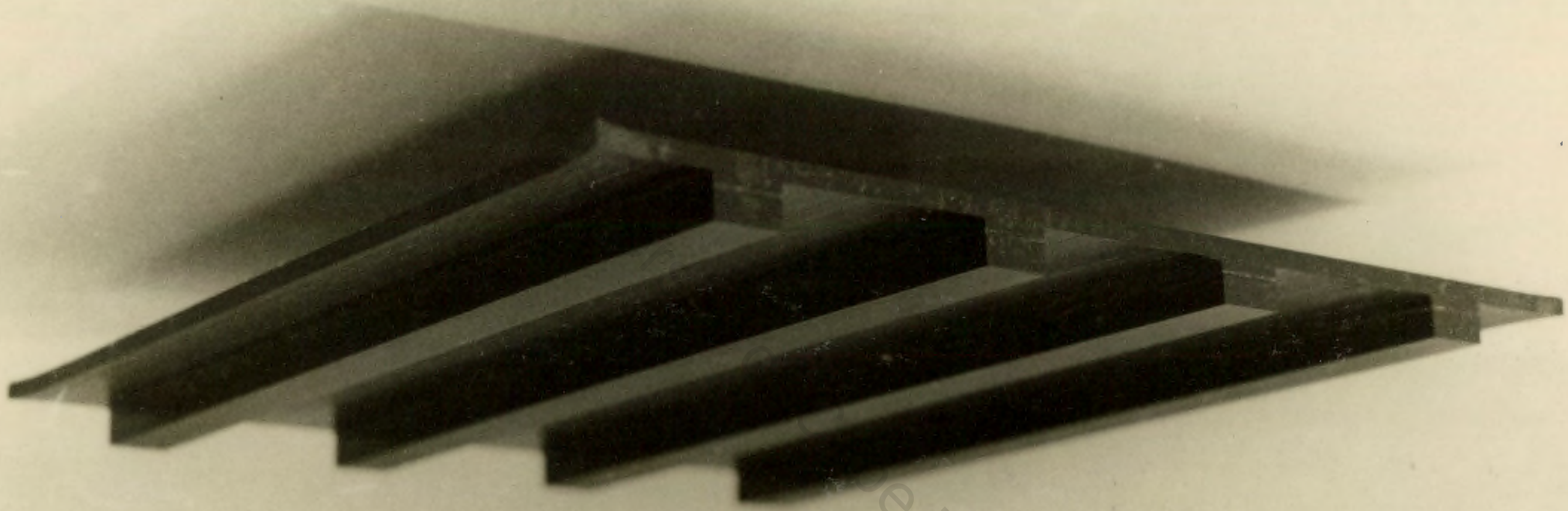

FOREWORD

This thesis is submitted in partial fulfilment of the requirements for the degree of Master of Science in Civil Engineering at the University of Cape Town. The writer attended courses in Skeletal Structures, Surface Structures, Advanced Prestressed Concrete, Engineering Optimisation, and Statistics. The writer wishes to acknowledge the help and encouragement of his supervisor, Mr. W.S. Doyle, M.Phil., who gave up so much of his time in guiding this thesis. The writer wishes to thank the technicians who helped with the experimental part of the work, especially Mr. P.W. Duxbury, who made the models with such care and patience. Thanks are also due to Miss L. Jennings who did the typing. Finally, the writer acknowledges the assistance of a bursary from the C.S.I.R.

SYNOPSIS

This thesis deals with the flexural and twisting rigidities of orthotropic plates. Asymmetrically stiffened plates are examples of technically orthotropic plates and are found in civil engineering structures such as bridges and ribbed floor slabs. The formulae for the rigidities as found in the literature are reviewed.

The writer has devised an experimental method of determining the rigidities. This involves a bending test using the Moiré technique and a twisting test. In the writer's method only one model is needed to determine all the rigidities. This is compared to other methods for which two or three models are needed.

Sixteen different models of asymmetrically stiffened plates with ribs running in one direction only were made. The flexural rigidities of eight of these models and the twisting rigidities of all sixteen models were determined. The objective of the tests was to compare the test values with the theoretical values. More specifically the objective can be defined as follows.

a. To determine how well an asymmetrically stiffened plate behaves as an orthotropic plate, i.e. how far apart may the ribs be spaced before the plate becomes a system of plate elements and beam elements.

b. To determine the influence, if any, on the rigidities D_x, D_1 and D_y of altering the spacing of the ribs of stiffened plates which have the same theoretical values of D_x.

c. To determine whether there is any difference between the rigidities D_{12} and D_{21}, which are the same for a true orthotropic plate and are usually assumed to be the same for an asymmetrically stiffened plate.

Conclusions are drawn on these points.

SYMBOLS

$a_{11}, a_{12}, \ldots, a_{66}$	coefficients of deformation in X,Y,Z system
$a'_{11}, a'_{12}, \ldots, a'_{66}$	coefficients of deformation in X',Y',Z' system
a_1, a_3	constants in 8th order theory
A_r	area in Bredt formula
AY, AZ	nodal spacings
$A_{11}, A_{12}, \ldots, A_{66}$	moduli of elasticity in X,Y,Z system
$A'_{11}, A'_{12}, \ldots, A'_{66}$	moduli of elasticity in X',Y',Z' system
A	rectangular plate length in X-direction
B	rectangular plate length in Y-direction
b	rib breadth
C	factor in the beam torsion constant
$D = \frac{Eh^3}{12(1-\upsilon^2)}$	flexural rigidity of isotropic plate
$D_x, D_y, D_1, D_{xy}, D_{ij}$	orthotropic plate rigidities
d	rib depth below flange
dx, dy, dz	infinitesimal distances in X,Y,Z system
$\frac{dw}{dx}, \frac{d^2w}{dy^2}, \frac{d^4w}{dx^4}, \frac{d^2\phi}{dz^2}$, etc.	are all partial derivatives
e_1, e_2, e_3, e_4	distances from a neutral axis
E	Young's modulus for an isotropic material
E_x, E_y, E_z	Young's moduli for an orthotropic material
$G = E/2(1+\upsilon)$	shear modulus for an isotropic material
G_{xy}, G_{xz}, G_{yz}	shear moduli for an orthotropic material
$H = D_1 + 2D_{xy}$	rigidity in the biharmonic equation
h	plate thickness
I	moment of inertia
J	beam torsion constant

k_x, k_y, k_{xy}	correction factors for variation in dimensions
k_M	Moiré method correction factor
M_x, M_y	plate bending moments per unit length
M_{xy}, M_{yx}	plate twisting moments per unit length
M_T	beam twisting moment
P	load
Q_x, Q_y	plate shear forces per unit length
q	distributed load per unit area
R = AY/AZ	aspect ratio of nodal pattern
s	rib spacing
s_x, s_y	spacing between ribs in the X and Y directions respectively
u, v, w	displacements in the X,Y,Z system
$\bar{V}$	elastic potential
X,Y,Z	cartesian co-ordinate axes, where XOY is the plane of the plate, and X is the direction of greatest stiffness
X',Y',Z'	cartesian co-ordinate axes, rotated with respect to X,Y,Z
γ_x, γ_y	torsional rigidities in the formulae for M_{xy} and M_{yx}
γ_{xy}, γ_{xz}, γ_{yz}	shear strains
ϵ_x, ϵ_y, ϵ_z	normal strains
σ_x, σ_y, σ_z	normal stresses
τ_{xy}, τ_{xz}, τ_{yz}	shear stresses
υ	Poisson's ratio for an isotropic material
υ_x, υ_y	Poisson's ratios for an orthotropic plate

INDEX

CHAPTER 1

THE ORTHOTROPIC PLATE

1. DEFINITION OF AN ORTHOTROPIC PLATE

To develop theories of the structural performance of engineering materials, we assume that they possess certain idealised natural physical properties. It is assumed that the material is a perfectly elastic body which will resume its initial form after unloading. Mathematically this elastic property is described by Hooke's Law. An isotropic body is one which consists of a homogeneous material with the same mechanical properties in all directions. Such material bodies very seldom exist. Most structural materials such as steel are composed of crystals of various kinds, orientations, and elastic properties in all directions. However considering relatively small sizes of crystals and their random distribution it may be assumed that the elastic behaviour of one piece of material is expressed by the average of the elastic properties of all crystals. On the basis of this assumption the material is considered to be isotropic.

Some materials have definite differences in elastic properties in different directions. These materials are called anisotropic or aelotropic. For instance materials used in the aircraft industry such as delta wood, avia-sandwich plates, textolit and others are all anisotropic materials. Sometimes fabrication methods make it necessary to consider conditions of anisotropy for structural materials.

Some sheets of metal show a marked anisotropy depending on the direction of rolling.

In the case where a body possesses principally different elastic properties in three perpendicular or orthogonal directions, it is called orthogonally-anisotropic, or orthotropic for short. Natural timber is a typical example of such a material. The number of elastic constants needed to describe an isotropic body is two, namely, Young's Modulus, E, and Poisson's ratio, υ. However, in an anisotropic body the number is higher with a maximum of 21.

The first and basic theoretical investigation in this field was by Cauchy who in 1828 gave generalised equations for the elasticity of anisotropic bodies. Gehring in 1860 investigated the thin anisotropic plate. Boussinesq considered equilibrium equations for anisotropic plates and bars in 1879. Voigt published a book in 1910 on the elastic properties of anisotropic crystals and found values of elastic constants. Geckeler in 1928 made further developments. All the above works were purely theoretical and were developed considering elements possessing properties of natural or true anisotropy.

A plate of constant thickness but with different elastic properties in mutually perpendicular directions is called naturally orthotropic. Structurally or technically orthotropic plates are those made usually of isotropic material but which are reinforced or stiffened in a particular direction or in mutually perpendicular directions. Examples are ribbed plates as in steel bridge decks, reinforced concrete flat and ribbed slabs as in bridges and large

buildings. The idea of the application of the theory of elasticity of orthotropic plates to reinforce concrete flat and ribbed slabs was proposed and developed by M.T. Huber in 1914.

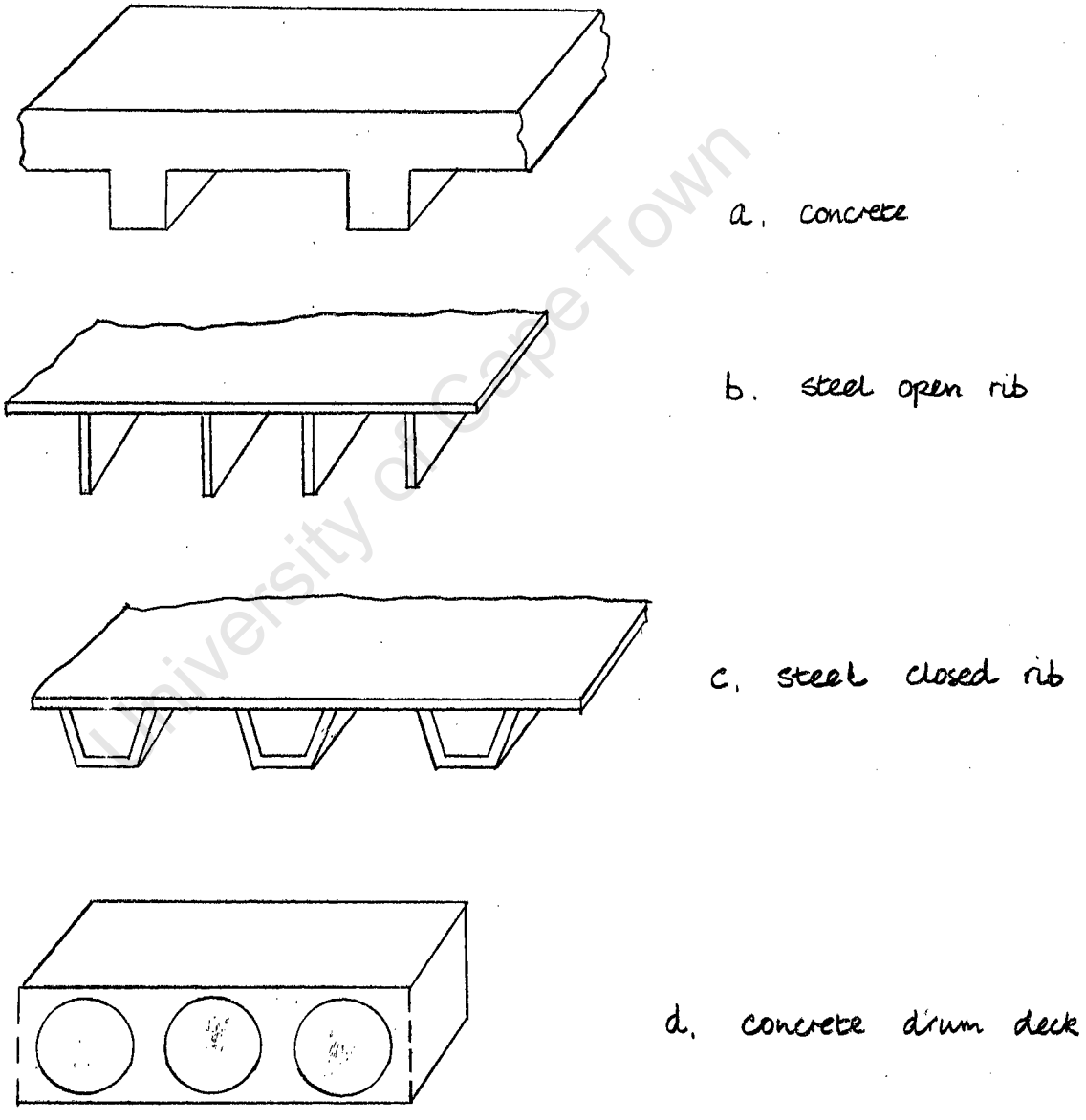

Fig. 1.1 Examples of technically orthotropic plates.

The advantage of orthotropic plate theory used in bridge design is that maximum use is made of the strength of materials, resulting in an economical design. The progress in methods of structural analysis has assisted the development of orthotropic bridges. In a composite beam and slab system for example, provided that the elements of the grid are spaced closely enough together, the structure will act as a truly orthotropic plate, not as a system of individual elements. In steel bridges, the saving in weight by using orthotropic decks in general exceeds the extra cost of construction especially for longer spans.

Orthotropic bridges are likely to be more architecturally satisfying due to their lower weight and, therefore, cleaner lines. The desirability of building orthotropic bridges has been demonstrated, and therefore any advance in the theory is also desirable.

2. HUBER'S EQUATION

The methods of analysis of orthotropic plates in bending fall into two categories. These are numerical methods, namely, finite differences and finite elements, and mathematical methods. Huber's theory is the basis of them all although it is refined by some authors, as will be seen in Chapter 2.

Before deriving Huber's equation it is in order to list the various categories of plates as given in Ref. 2. Plates are classified as follows:

(a) Thick plates in which a triaxial state of stress is developed, which is defined by the complete set of

differential equations of the 3-dimensional theory of elasticity. Plates for which the ratio of the thickness h to the least dimension on plan exceeds 1/5 can be taken as belonging to this class.

(b) Thin plates with small deflections, in which, under deformation due to transverse loading, the membrane stresses are very small in comparison with the flexural stresses (up to 5%). This class may be taken to comprise plates for which the ratio of the thickness h to the span does not exceed 1/5 and the deflection w does not become larger than h/5.

(c) Thin plates with large deflections ($w/h > 1/5$) are characterised by the fact that the flexural stresses are accompanied by relatively large tensile or compressive membrane stresses in the middle plane. These membrane stresses significantly affect the bending moments.

(d) Membranes are plates in which, under the action of transverse loading, bending moments are produced which are so small that they are negligible in comparison with the membrane stresses.

(e) Diaphragms are plate-like elements which are subjected to loading which acts in the middle plane of the element only.

Huber's equation only applies to thin plates with small deflections, and is based on the following assumptions (Ref. 4):

i. The material of the plate is perfectly elastic, i.e. the elastic response is independent of the load intensity and the stress-strain relationship is given by the law of Hooke.

ii. The material of the plate is perfectly homogeneous.

iii. Thickness is uniform and small in comparison with the other dimensions of the plate.

iv. Points of the plate lying initially on a normal to the plate middle-plane remain on the normal to the middle surface of the plate after bending.

v. Normal stresses in the direction transverse to the plane of the plate are negligible and the thickness of the plate does not undergo any deformation during bending.

vi. The deflections of the plate are small in comparison with its thickness; if the deflection parallel to the normal to the middle plane is denoted by w then curvatures of the middle surface of the plate are given by the second partial derivatives of w.

vii. The deflections of the plate are such that there is no normal strain in planes tangent to the middle surface.

viii. The body forces are either disregarded or assumed to be a part of the external load.

ix. The direction of external load is perpendicular to the plane of the plate.

Consider an orthotropic plate of uniform thickness. Let the principal directions of orthotropy lie along the X and Y axes of a rectangular system of coordinates X, Y, Z. Let the displacements of a point in the plate after bending be u, v, w, corresponding to the axes X, Y, Z.

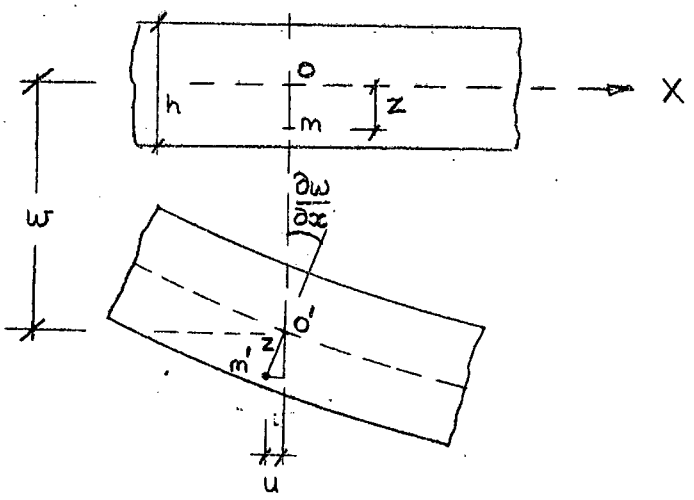

Fig. 1.2

With the notation in Fig. 1.2, point O' lies below point O due to assumption vii. Also if the angle through which the normal OM turns is small, we may say that

$$u = -z\frac{dw}{dx} \quad ; \quad v = -z\frac{dw}{dy}$$

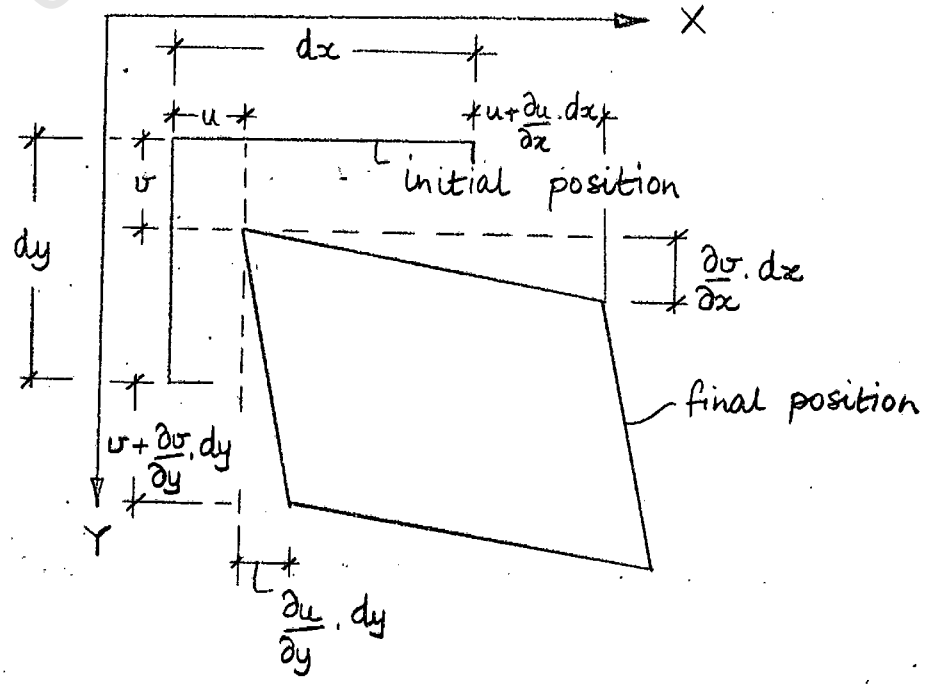

Fig. 1.3

where G_{xy} is the shear modulus in the XY plane. Solving Eqs 1.3 for σ_x and σ_y, we have

$$\sigma_x = \frac{E_x \epsilon_x}{(1-\upsilon_x \upsilon_y)} + \frac{\upsilon_y E_x \epsilon_y}{(1-\upsilon_x \upsilon_y)}$$

$$\sigma_y = \frac{E_y \epsilon_y}{(1-\upsilon_x \upsilon_y)} + \frac{\upsilon_x E_y \epsilon_x}{(1-\upsilon_x \upsilon_y)} \qquad \text{Eqs 1.4}$$

and $\tau_{xy} = G_{xy} \gamma_{xy}$

substituting Eqs 1.1 into Eqs 1.4 we have

$$\sigma_x = -z \frac{E_x}{(1-\upsilon_x \upsilon_y)} \cdot \frac{d^2w}{dx^2} - z \frac{\upsilon_y E_x}{(1-\upsilon_x \upsilon_y)} \cdot \frac{d^2w}{dy^2}$$

$$\sigma_y = -z \frac{E_y}{(1-\upsilon_x \upsilon_y)} \cdot \frac{d^2w}{dy^2} - z \frac{\upsilon_x E_y}{(1-\upsilon_x \upsilon_y)} \cdot \frac{d^2w}{dx^2} \qquad \text{Eqs 1.5}$$

$$\tau_{xy} = -z\, 2G_{xy} \frac{d^2w}{dxdy}$$

The stress distribution over an element of plate is shown in Fig. 1.4.

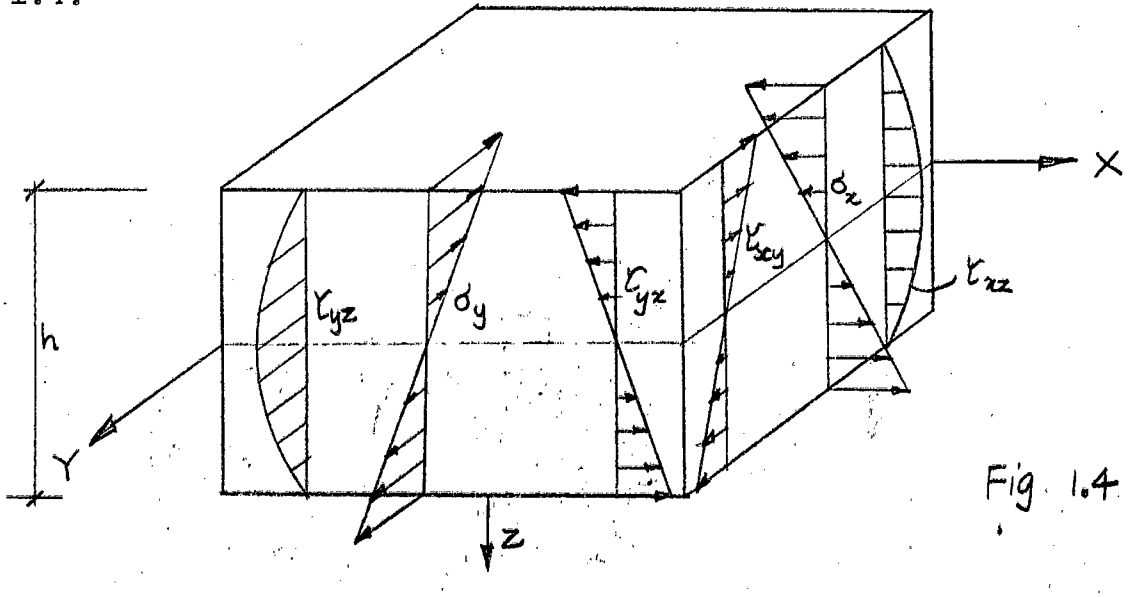

Fig 1.4

Taking any slice of thickness dz of the block in Fig. 1.4 it can be seen that for equilibrium

$$\tau_{xy} = \tau_{yx}$$

summing the moments due to the stresses acting on an element of the block of plate, we find the bending and twisting moments per unit length of the plate.

$$M_x = \int_{-h/2}^{h/2} \sigma_x \, z \, dz$$

$$= - \frac{E_x}{(1-\upsilon_x \, \upsilon_y)} \left[\frac{d^2w}{dx^2} + \upsilon_y \frac{d^2w}{dy^2} \right] \int_{-h/2}^{h/2} z^2 \, dz$$

$$= - \frac{E_x}{(1-\upsilon_x \, \upsilon_y)} \frac{h^3}{12} \left[\frac{d^2w}{dx^2} + \upsilon_y \frac{d^2w}{dy^2} \right]$$

$$= - D_x \left[\frac{d^2w}{dx^2} + \upsilon_y \frac{d^2w}{dy^2} \right] \qquad \text{Eq 1.6}$$

Similarly

$$M_y = - D_y \left[\frac{d^2w}{dy^2} + \upsilon_x \frac{d^2w}{dx^2} \right] \qquad \text{Eq 1.7}$$

where $D_y = \dfrac{E_y \, h^3}{12(1-\upsilon_x \, \upsilon_y)}$

$$M_{xy} = - \int_{-h/2}^{h/2} \tau_{xy} \, z \, dz = M_{yx}$$

$$= 2G_{xy} \frac{d^2w}{dxdy} \int_{-h/2}^{h/2} z^2 \, dz$$

$$= 2G_{xy} \frac{h^3}{12} \cdot \frac{d^2w}{dxdy}$$

$$= 2D_{xy} \frac{d^2w}{dxdy} \qquad \text{Eq 1.8}$$

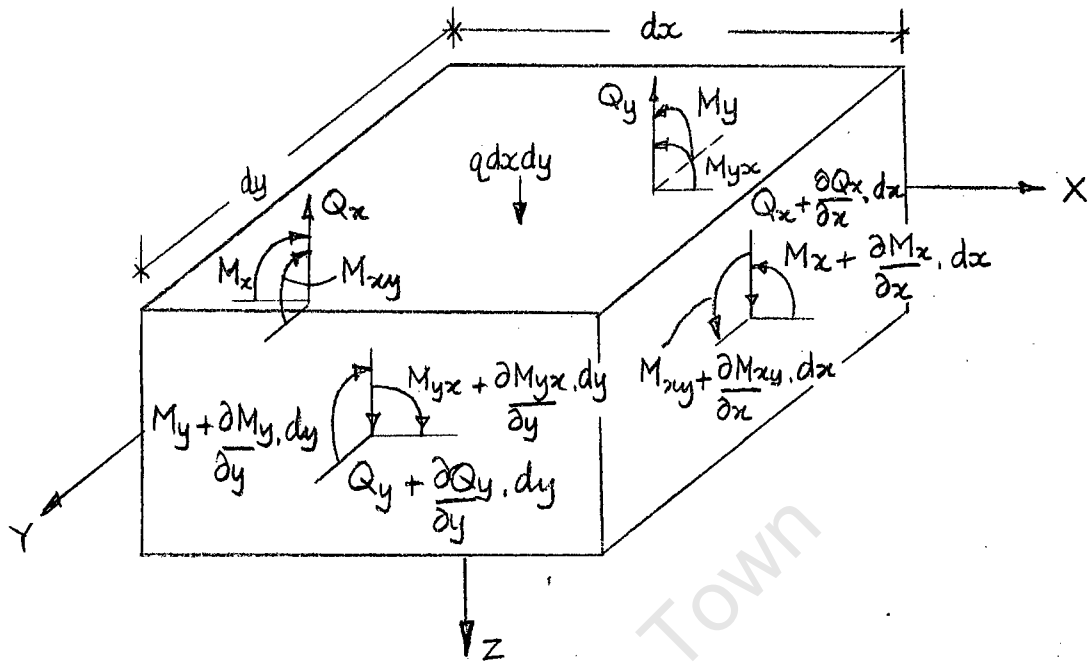

Fig. 1.5

The equations of equilibrium of an element of plate can now be established from Fig. 1.5. Q_x and Q_y are the shear forces per length and q is the distributed load on the element. Taking moments about the Y axis, and neglecting small terms

$$Q_x = \frac{dM_x}{dx} - \frac{dM_{yx}}{dy} \qquad \text{Eq 1.9}$$

Taking moments about the X axis,

$$Q_y = \frac{dM_y}{dy} - \frac{dM_{xy}}{dx} \qquad \text{Eq 1.10}$$

And summing the forces in the Z direction

$$\frac{dQ_x}{dx} + \frac{dQ_y}{dy} + q = 0 \qquad \text{Eq 1.11}$$

Differentiating Eqs 1.9 and 1.10 and substituting into Eq 1.11 gives

$$\frac{d^2M_x}{dx^2} - \frac{d^2M_{yx}}{dxdy} + \frac{d^2M_y}{dy^2} - \frac{d^2M_{xy}}{dxdy} + q = 0 \qquad \text{Eq 1.12}$$

$$\therefore \quad D_x \left[\frac{d^4w}{dx^4} + \upsilon_y \frac{d^4w}{dx^2dy^2}\right] + 4D_{xy} \frac{d^4w}{dx^2dy^2} + D_y \left[\frac{d^4w}{dy^4} + \upsilon_x \frac{d^4w}{dx^2dy^2}\right] = q$$

$$\therefore \quad D_x \frac{d^4w}{dx^4} + \left[\upsilon_y D_x + \upsilon_x D_y + 4D_{xy}\right] \frac{d^4w}{dx^2dy^2} + D_y \frac{d^4w}{dy^4} = q$$

$$\therefore \quad D_x \frac{d^4w}{dx^4} + 2H \frac{d^4w}{dx^2dy^2} + D_y \frac{d^4w}{dy^4} = q \qquad \text{Eq 1.13}$$

where $H = D_1 + 2D_{xy}$

and $D_1 = \upsilon_x D_y = \upsilon_y D_x$

Equation 1.13 is the differential equation of a bent orthotropic plate and is due to Huber. It can be expressed in finite difference form, or used to find a mathematical solution to any particular plate problem. The mathematical solution however is limited to a rectangular plate and has been solved for various boundary conditions. These may be clamped, simply supported, elastically supported, or free edges in various combinations. A finite difference or finite element solution can be found for a plate of any plan shape.

For all solutions it is necessary to know the values of the rigidities D_x, D_y, D_1 and D_{xy}. For a true orthotropic plate this amounts to knowing the values of E_x, E_y, G_{xy} and either υ_x or υ_y. For a technically orthotropic plate it is the geometry which changes with a rotation in the plane of the plate, not the material properties, and therefore the

problem is different.

3. THE EQUATIONS OF THE ISOTROPIC PLATE

For an isotropic plate of thickness h we have

$$E_x = E_y = E$$

$$\upsilon_x = \upsilon_y = \upsilon$$

and $$G_{xy} = G = \frac{E}{2(1+\upsilon)} .$$

Substituting these values into the moment equations 1.6, 1.7, 1.8 we have

$$M_x = -\frac{Eh^3}{12(1-\upsilon^2)}\left[\frac{d^2w}{dx^2} + \upsilon\frac{d^2w}{dy^2}\right]$$

$$= -D\left[\frac{d^2w}{dx^2} + \upsilon\frac{d^2w}{dy^2}\right]$$

$$M_y = -D\left[\frac{d^2w}{dy^2} + \upsilon\frac{d^2w}{dx^2}\right]$$

and $$M_{xy} = 2G\frac{h^3}{12}\cdot\frac{d^2w}{dxdy}$$

$$= 2\frac{E}{2(1+\upsilon)}\cdot\frac{h^3}{12}\cdot\frac{d^2w}{dxdy}$$

$$= \frac{Eh^3}{12(1-\upsilon^2)}\cdot(1-\upsilon)\cdot\frac{d^2w}{dxdy}$$

$$= D(1-\upsilon)\cdot\frac{d^2w}{dxdy}$$

$$= M_{yx}$$

Here $$D = \frac{Eh^3}{12(1-\upsilon^2)}$$

is known as the flexural rigidity of the isotropic plate.

The differential equation of the isotropic plate becomes

$$\frac{d^4w}{dx^4} + 2\frac{d^4w}{dx^2dy^2} + \frac{d^4w}{dy^4} = \frac{q}{D}$$

since $D_x = D_y = D$

and $H = D_1 + 2D_{xy}$

$= \upsilon D + D(1-\upsilon)$

$= D$

The isotropic plate is thus a special case of the orthotropic plate. For a solution of an isotropic plate only two elastic constants must be known, namely E and υ. For an orthotropic plate however there are four unknowns, namely D_x, D_y, D_1 and D_{xy}. Formulae for these for various technically orthotropic plates due to different authors are given in Chapter 2.

CHAPTER 2

THEORETICAL VALUES OF THE ORTHOTROPIC PLATE CONSTANTS

1. GENERAL

In this chapter recommended formulae for the rigidities D_x, D_y, D_1, D_{xy} and H are surveyed. These depend on the various authors' opinions and on the different types of technically orthotropic plates which they are discussing. Although only one type of plate was tested experimentally in this thesis, rigidity formulae are given below for other types as well since they are often relevant. Formulae are given under the author's name, and a summary appears at the end of the chapter. Formulae will be translated into the writer's symbols, and the X direction is always taken as the direction of greatest flexural stiffness, D_x.

Summarizing the formulae for a true orthotropic plate of uniform thickness h, obtained in Chapter 1,

$$D_x = \frac{E_x I}{(1-\upsilon_x \upsilon_y)}$$

$$D_y = \frac{E_y I}{(1-\upsilon_x \upsilon_y)}$$

Eqs 2.1

$$D_1 = \upsilon_x D_y = \upsilon_y D_x$$

$$D_{xy} = G_{xy} \frac{h^3}{12}$$

where $I = \frac{h^3}{12}$ = the moment of inertia for a beam of

rectangular section, depth h, and unit width.

In general for technically orthotropic plates, υ_x and υ_y are not true Poisson's ratios, since they depend on the geometry of the structure as well as the material properties. They are defined as

$$\upsilon_x = \frac{D_{12}}{D_y} \quad ; \quad \upsilon_y = \frac{D_{21}}{D_x}$$

where D_{12} and D_{21} are the rigidities in the formulae

$$M_x = - D_x \frac{d^2w}{dx^2} - D_{12} \frac{d^2w}{dy^2}$$

$$M_y = - D_y \frac{d^2w}{dy^2} - D_{21} \frac{d^2w}{dx^2}$$

Most authors assume that

$$D_1 = D_{12} = D_{21}$$

which is true for a true orthotropic plate.

It is necessary to define two more rigidities, namely γ_x and γ_y, in order to avoid confusion in this chapter. They are defined by

$$M_{xy} = \gamma_x \frac{d^2w}{dxdy}$$

and $$M_{yx} = \gamma_y \frac{d^2w}{dxdy}$$ Eqs 2.2

For a true orthotropic plate

$$\gamma_x = \gamma_y = 2D_{xy} = 2G_{xy} \frac{h^3}{12}$$

For a technically orthotropic plate, in general

$$\gamma_x \neq \gamma_y$$

Therefore, from Eqs 1.12, 1.13

$$2H = 2D_1 + \gamma_x + \gamma_y \qquad \text{Eq 2.3}$$

and we now define D_{xy} for a technically orthotropic plate as

$$2D_{xy} = \frac{\gamma_x + \gamma_y}{2} \qquad \text{Eq 2.4}$$

This distinction between D_{xy}, γ_x and γ_y is not always drawn in the literature; sometimes $2D_{xy}$ is used when γ_x is meant.

2. FROM TIMOSHENKO AND WOINOWSKY-KRIEGER

Timoshenko and Woinowsky-Krieger (Ref. 1) only devote a short section to orthotropic plates, giving values for the rigidities and a mathematical solution for a rectangular plate simply supported on all four sides. All mathematical solutions are complex, and as an illustration, the solution in Ref. 1 is given below.

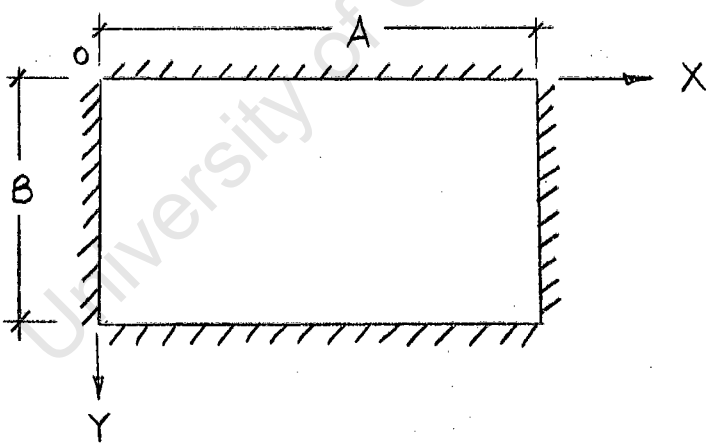

Fig. 2.1

The solution is for a uniformly distributed load, q, over the whole plate. Taking the axes as shown in Fig. 2.1, and representing the load by a double trigonometric series, Eq 1.13 becomes

$$D_x \frac{d^4w}{dx^4} + 2H \frac{d^4w}{dx^2dy^2} + D_y \frac{d^4w}{dy^4}$$

$$= \frac{16}{\pi} q \sum_{m=1,3,5..}^{\infty} \sum_{n=1,3,5...}^{\infty} \frac{1}{mn} \sin \frac{m\pi x}{A} \sin \frac{n\pi y}{B}$$

The deflection is found to be

$$w = \frac{16}{\pi} q \sum_{m=1,3,5...}^{\infty} \sum_{n=1,3,5...}^{\infty} \frac{\sin \frac{m\pi x}{A} \sin \frac{n\pi y}{B}}{mn \left(\frac{m^4}{A^4} D_x + \frac{2m^2n^2}{A^2B^2} H + \frac{n^4}{B^4} D_y \right)}$$

The curvatures, moments, etc. can be derived from this expression for any point in the plate. The impression that the writer has gained of these mathematical solutions is that sometimes the series converge slowly and sometimes not.

On the subject of rigidity formulae for various types of plate, Timoshenko says at the outset that, in particular, all values of torsional rigidity D_{xy} based on purely theoretical considerations should be regarded as a first approximation, and a direct test is recommended to obtain more reliable values. Various types of plate mentioned are as follows:

Plates with many stiff ribs

A. Symmetrically stiffened plates

The following theory is taken from Leknitskii (Ref. 5)

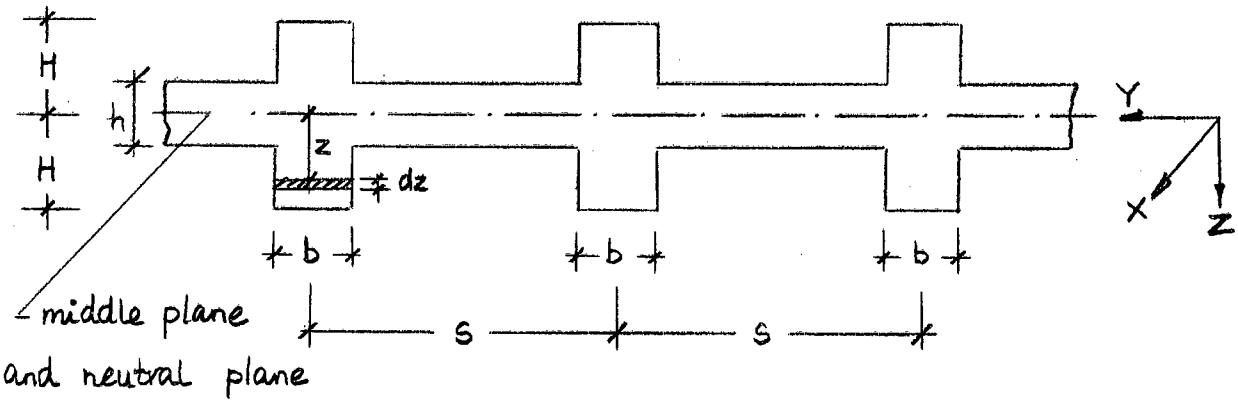

Fig. 2.2

For an isotropic plate reinforced on two sides by parallel stiff ribs

$$D_x = \frac{Eh^3}{12(1-\upsilon^2)} + \frac{E'I}{s}$$

$$D_y = \frac{Eh^3}{12(1-\upsilon^2)} = D \qquad \text{Eqs 2.5}$$

$$H = D$$

where I is the moment of inertia of a pair of ribs about an axis in the middle plane and E' is the Young's modulus for the rib material. The formula for D_x comes from the equation for the moment per unit length, as follows:

$$M_x = \int_{-h/2}^{h/2} \sigma_x z\, dz + 2\int_{h/2}^{H} \sigma_x \frac{b}{s} z\, dz$$

$$\therefore \quad M_x = -\int_{-h/2}^{h/2} \frac{E}{(1-\upsilon^2)}\left[\frac{d^2w}{dx^2} + \upsilon\frac{d^2w}{dy^2}\right] z^2\, dz$$

$$- 2\int_{h/2}^{H} \frac{E'b}{s}\frac{d^2w}{dx^2} z^2\, dz$$

$$= -\left[\frac{Eh^3}{12(1-\upsilon^2)} + \frac{E'I}{s}\right]\frac{d^2w}{dx^2} - \frac{\upsilon\, Eh^3}{12(1-\upsilon^2)}\cdot\frac{d^2w}{dy^2}$$

$$= -D_x\frac{d^2w}{dx^2} - D_{12}\frac{d^2w}{dy^2}$$

In the Y-direction the stiffeners are assumed to have no effect on the bending. The M_y equation is therefore the same as for an isotropic plate.

$$M_y = -\frac{Eh^3}{12(1-\upsilon^2)}\cdot\frac{d^2w}{dy^2} - \frac{\upsilon\, Eh^3}{12(1-\upsilon^2)}\cdot\frac{d^2w}{dx^2}$$

$$= -D_y\frac{d^2w}{dy^2} - D_{21}\frac{d^2w}{dx^2}$$

Here $D_{12} = D_{21} = D_1 = \upsilon D$

$$H = D_1 + 2D_{xy}$$

$$= \upsilon D + D(1-\upsilon) = D$$

Notice that he is assuming that D_{xy} is the torsional stiffness of the plate alone; the stiffness of the ribs is ignored.

For plates reinforced by two sets of mutually perpendicular ribs, symmetrically distributed on both sides of the middle plane, the following formulae are given

$$D_x = \frac{Eh^3}{12(1-\upsilon^2)} + \frac{E'\,I_x}{s_x}$$

$$D_y = \frac{Eh^3}{12(1-\upsilon^2)} + \frac{E''\,I_y}{s_y} \qquad \text{Eqs 2.6}$$

$$H = \frac{Eh^3}{12(1-\upsilon^2)} = D$$

It is assumed that the axes of the ribs are parallel to the principal directions; E' and E" are the Young's moduli for the ribs parallel to X and to Y; I_x and I_y are the moments of inertia of the ribs about lines in the middle plane of the plate; s_x and s_y are the rib spacings.

B. Asymmetrically stiffened plates

We now consider a slab reinforced asymmetrically by equidistant ribs running in one direction only. Timoshenko states that the theory as given in Chapter 1 can only give a rough idea of the actual state of stress and strain in the slab. This is because confusion arises over the position of a neutral plane. Before proceeding to the formulae for the rigidities as given in Timoshenko, some comments on the position of neutral planes are in order.

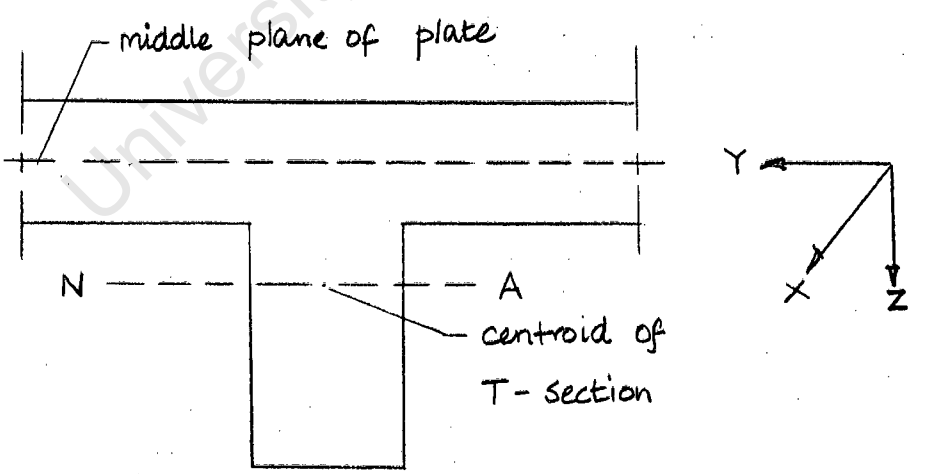

Fig. 2.3

Consider a moment M_x acting on the T-section shown. If the T-section were a beam, it would bend about a neutral axis passing through the centroid of the T-section. Now

imagine a moment M_y acting in the YZ plane. The plate part of the structure will want to bend about a neutral surface which is the same as the middle plane of the plate. Where the plate lies on top of and is part of the beam, the neutral surface will move down in some manner. However, the bending in the X and Y directions is not independent.

Consider, for example, an element of material at the level of the middle plane of the plate. M_x would apply a stress σ_x on the element causing a compression $\epsilon_x = \frac{\sigma_x}{E}$ and an extension $\epsilon_y = - \upsilon \frac{\sigma_x}{E}$ if the element were unrestrained in the Y direction. The strain ϵ_y affects the neutral surface for bending in the YZ plane. Similarly M_y affects the neutral axis for bending in the XZ plane. The true position of the neutral surfaces might be something like those shown in Fig. 2.4.

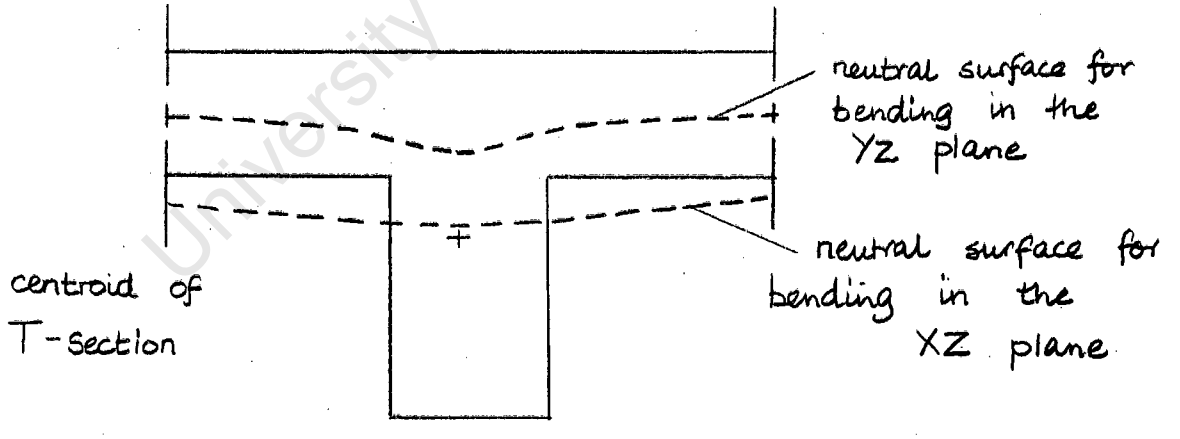

Fig. 2.4

It is not necessary that the two neutral surfaces be the same. This would mean that at any point in the structure where the strain $\epsilon_x = 0$, the strain ϵ_y is also zero. If the surfaces were the same, it would imply that $D_x = D_y$ as is proved below.

Consider a piece of irregular plate (Fig. 2.5) which has its surface bounded by lines parallel to the X direction. Consider a length A in the Y direction and unit length in the X direction. Give it an assumed neutral surface.

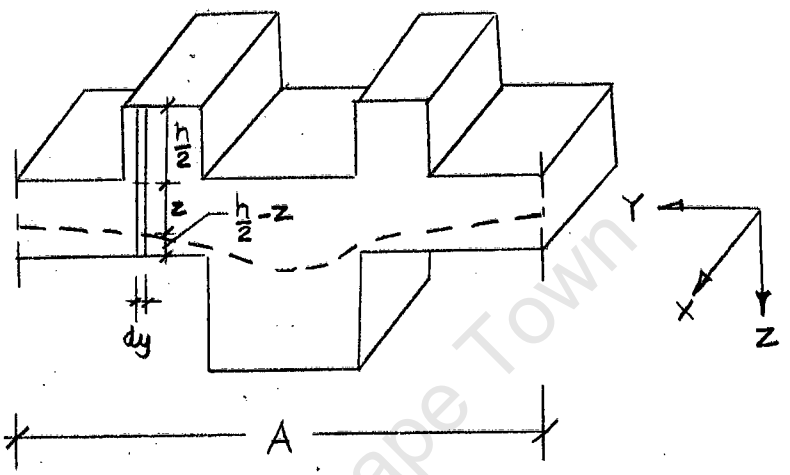

Fig. 2.5

Divide it into elementary strips of width dy, depth h, and let the distance from the centroid of a strip to the neutral surface be z. Then

$$I_x = \int_o^A \left[\frac{h^3}{12} + hz^2\right] dy$$

$$\therefore \quad \frac{I_x}{A} = \frac{1}{A} \int_o^A \left[\frac{h^3}{12} + hz^2\right] dy = \bar{I}_x$$

= a moment of inertia per unit length of the cross section

$$\text{Also } I_y = 1.\left[\frac{h^3}{12} + hz^2\right]$$

$$\therefore \quad \bar{I}_y = \frac{1}{A} \int_o^A \left[\frac{h^3}{12} + hz^2 \right] dy$$

= average moment of inertia in the Y direction, per unit length

$$= \bar{I}_x$$

$\therefore$ A common neutral surface implies equal moments of inertia in the X and Y directions, i.e. $D_x = D_y$.

By experiment $D_x \neq D_y$, therefore the neutral surfaces are not the same.

This also implies that one cannot estimate the value of D_y of the section shown in Fig. 2.6, for example, by taking sections parallel to the XZ plane and averaging the results. Formulae for D_x and D_y of sections such as this are given in Ref. 4.

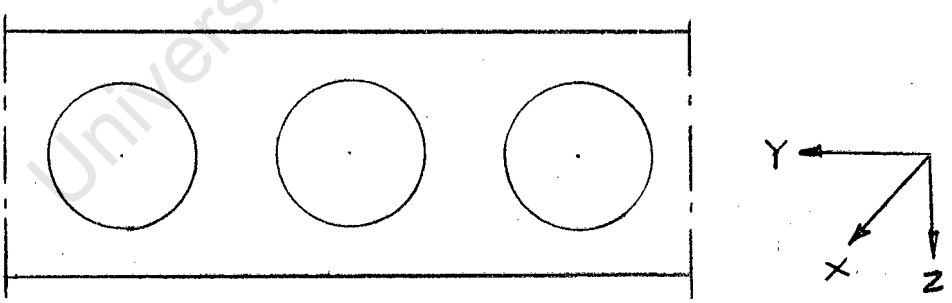

Fig. 2.6

To return to Timoshenko, the rigidity formulae (proposed by Huber) for an asymmetrically stiffened plate are as follows

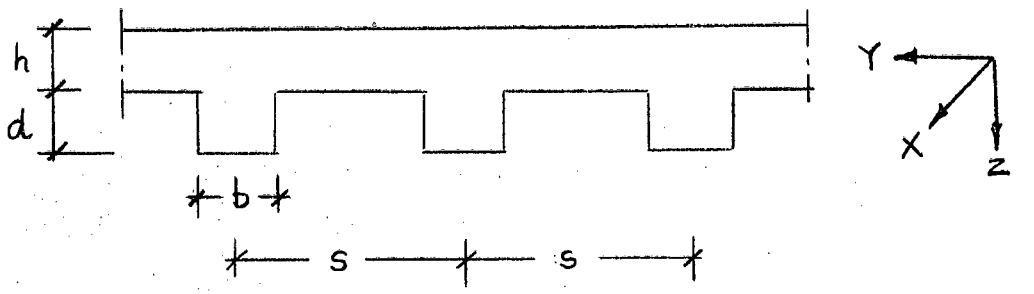

Fig. 2.7

Let I_x be the moment of inertia of a T-section of width s, and $\alpha = h/(h+d)$.

$$\text{Then } D_x = \frac{EI_x}{s}$$

$$D_y = \frac{Eh^3}{12} \cdot \frac{s}{(s-b+\alpha^3 b)}$$

$$D_1 = 0$$

$$2D_{xy} = D(1-\upsilon) + \frac{GJ}{2s}$$

Eqs 2.7

In the formula for D_x the plate contribution to I_x is not divided by $(1-\upsilon^2)$. The explanation for D_y is given in Section 2 on Huber. In general the formulae for D_x, D_y and D_1 neglect the effect of Poisson's ratio.

In the formula for D_{xy}, J is the torsion constant of one rib. The slab and the rib are assumed to resist the torsional moment separately. No additional stiffness due to their continuity is allowed. J is defined as in the usual theory of twisting of beams (see for example Ref. 6) where, if θ = the angle of twist per unit length of the beam and M_T = the twisting moment

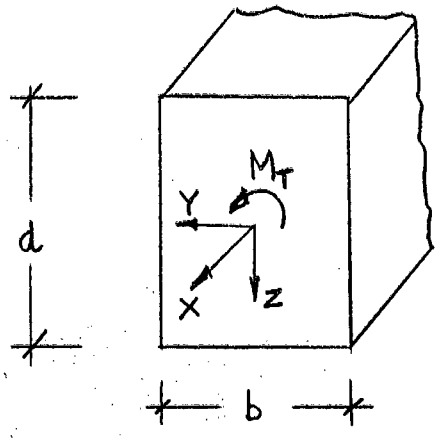

Fig. 2.8

$$M_T = G.J.\theta \qquad \text{Eq 2.8}$$

For a rectangular beam cross-section

$$J = b^3d.C \qquad (b < d)$$

$$J = bd^3.C \qquad (d < b)$$

where C is a constant depending on the ratio b : d. When b = d, C = 0,1406. As the ratio b/d increases, C increases, asymptotically approaching the value C = $^1/3$ as b/d tends to infinity.

C. Reinforced Concrete Slabs (due to M.T. Huber)

Let E_s = Young's modulus of steel

E_c = Young's modulus of concrete

υ_c = Poisson's ratio of concrete

$n = E_s/E_c$

For a slab with two way reinforcement in the directions X and Y it is assumed that

$$D_x = \frac{E_c}{(1-\upsilon_c^2)} \left[I_{cx} + (n-1).I_{sx}\right]$$

$$D_y = \frac{E_c}{(1-\upsilon_c^2)} \left[I_{cy} + (n-1).I_{sy}\right]$$

Eqs 2.9

$$D_1 = \upsilon_c . \sqrt{D_x D_y}$$

$$D_{xy} = \frac{(1-\upsilon_c)}{2} . \sqrt{D_x D_y}$$

where I_{cx} is the moment of inertia of the slab material

I_{sx} that of the reinforcement taken about the neutral axis in the section x = constant

I_{cy}, I_{sy} are the respective values for the section y = constant.

$$H = D_1 + 2D_{xy} = \sqrt{D_x D_y}$$ Eq 2.10

Eq 1.13 now becomes

$$D_x \frac{d^4w}{dx^4} + 2\sqrt{D_x D_y} \frac{d^4w}{dx^2 dy^2} + D_y \frac{d^4w}{dy^4} = q$$

By introducing a new variable

$$y_1 = y \sqrt[4]{D_x / D_y}$$

Eq 1.13 reduces to

$$\frac{d^4w}{dx^4} + 2 \frac{d^4w}{dx^2 dy_1^2} + \frac{d^4w}{dy_1^4} = \frac{q}{D_x}$$

which can be solved as an isotropic plate. There was

therefore an end in view in choosing the formulae for D_1 and D_{xy}. The explanation for their choice, which is not a strictly theoretical derivation, is as follows.

For an isotropic plate

$$M_{xy} = D(1-\upsilon) \cdot \frac{d^2w}{dxdy} = M_{yx}$$

For a technically orthotropic plate, however, in general $M_{xy} \neq M_{yx}$ since the torsional rigidities will be different in the X, Y directions. As a reasonable approximation for the rigidities consider the expression for an isotropic plate and substitute for the values of D and υ by certain middle values of D_x, D_y and υ_x, υ_y.

Choose these values as

$$D = \sqrt{D_x D_y}$$

$$\upsilon = \sqrt{\upsilon_x \upsilon_y}$$

Then $M_{xy} = (1-\sqrt{\upsilon_x \upsilon_y})\sqrt{D_x D_y} \cdot \frac{d^2w}{dxdy}$

or $2D_{xy} = (1-\sqrt{\upsilon_x \upsilon_y})\sqrt{D_x D_y}$

and $D_1 = \sqrt{\upsilon_x \upsilon_y} \cdot \sqrt{D_x D_y}$

$\therefore \quad H = D_1 + 2D_{xy} = \sqrt{D_x D_y}$

and it is assumed that

$$\upsilon_c = \sqrt{\upsilon_x \upsilon_y}$$

On the subject of the values of D_x and D_y in Eqs 2.9, it is clear that they are derived by transforming the section

to an equivalent concrete section and again assuming that

$$\upsilon_c = \sqrt{\upsilon_x \upsilon_y}$$

However Timoshenko notes that Eqs 2.9 are not independent of the state of the concrete. Any difference, for instance, in the reinforcement in the directions x and y will affect the ratio D_x/D_y much more after cracking of the concrete than before.

D. Plywood plates

A table of elastic constants for five types of plywood is given. This is useful as a test of a formula for G_{xy} for true orthotropic plates developed by Klöppel and Yamadá (Ref. 7).

$$G_{xy} = \frac{E_x E_y}{E_x + (1+2\upsilon_x)E_y} \qquad \text{Eq 2.11}$$

This is based on purely theoretical considerations. In the table below the test and theoretical values are compared.

Unit = 10^6 psi

Material	E_x Test	E_y Test	$\upsilon_x E_y$ Test	G_{xy} Test	G_{xy} Ref 7
Maple, 5-ply	1,87	0,60	0,073	0,159	0,429
Afara, 3-ply	1,96	0,165	0,043	0,110	0,146
Gaboon (Okoumé), 3-ply	1,28	0,11	0,014	0,085	0,099
Birch, 3- and 5-ply	2,00	0,167	0,077	0,17	0,144
Birch, with bakelite membranes	1,70	0,85	0,061	0,10	0,542

The agreement in general is seen to be bad. The theoretical G_{xy} varies from more than five times too small to 1,2 times too big. It is not known, however, how accurate the tests were. Klöppel and Yamadá probably would not claim that their formula is applicable to plywood plates as they are not true orthotropic plates. They are plates of constant thickness, however, and the table does suggest that the formula will not be valid for any technically orthotropic plates.

E. Gridworks

Orthotropic plate theory may also be applied to gridworks if the distances between the beams in both directions is small compared with the dimensions of the grid.

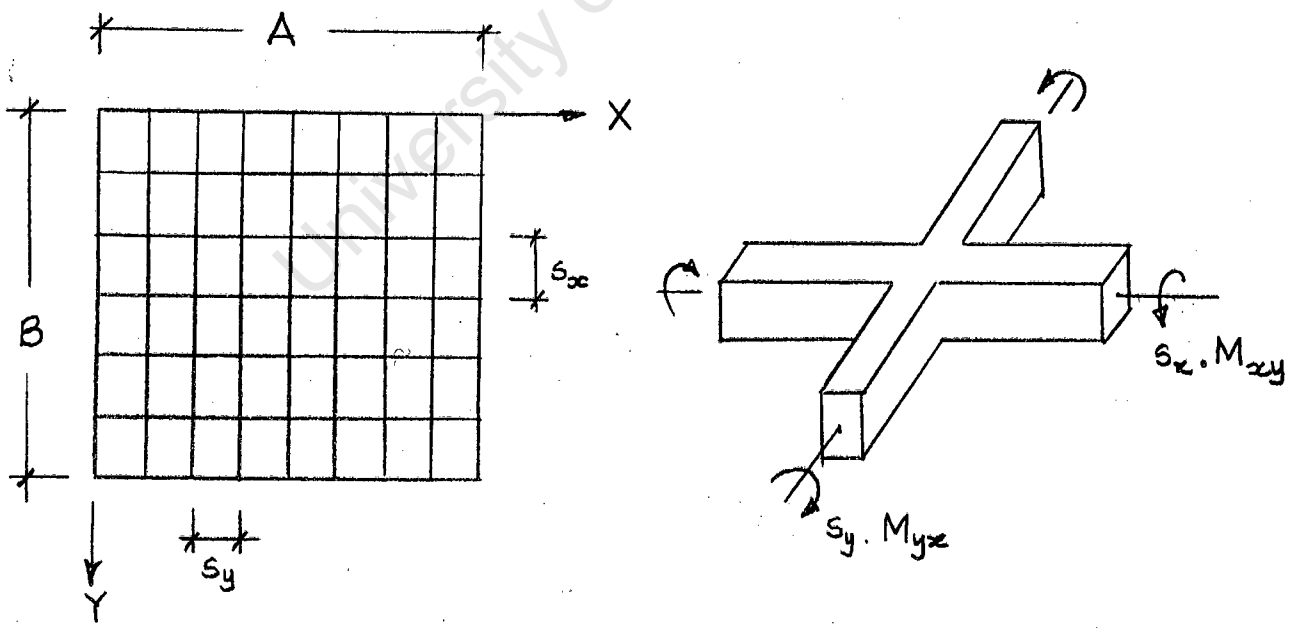

Fig. 2.9

The beams are supported at their ends and the load is applied normal to the XY plane. If EI_x, EI_y are the flexural

rigidities of beams parallel to the X,Y axes then

$$D_x = \frac{EI_x}{s_x} \quad ; \quad D_y = \frac{EI_y}{s_y}$$

D_1 is taken as zero since there is no slab to provide Poisson's ratio effects. For twisting we have

$$M_{xy} = \frac{GJ_x}{s_x} \cdot \frac{d^2w}{dxdy}$$

$$M_{yx} = \frac{GJ_y}{s_y} \cdot \frac{d^2w}{dxdy}$$

where J_x, J_y are the torsion constants of the beams in the X,Y directions.

Substituting these expressions into the equation of equilibrium Eq 1.12

$$\frac{d^2M_x}{dx^2} - \frac{d^2M_{yx}}{dxdy} + \frac{d^2M_y}{dy^2} - \frac{d^2M_{xy}}{dxdy} + q = 0$$

We find that the D.E. for a gridwork is

$$D_x \frac{d^4w}{dx^4} + \left[\frac{GJ_x}{s_x} + \frac{GJ_y}{s_y}\right] \frac{d^4w}{dx^2dy^2} + D_y \frac{d^4w}{dy^4} = q$$

i.e. $2H = \frac{GJ_x}{s_x} + \frac{GJ_y}{s_y}$

$$= 4D_{xy}$$

$$\therefore \quad D_{xy} = \frac{GJ_x}{4s_x} + \frac{GJ_y}{4s_y}$$

F. Corrugated Plates

Plates made from isotropic material which have been given waves in one direction may be considered as approximately uniform and orthotropic if the number of waves is sufficiently large, or if the chord of the corrugations is small by comparison with the length of a side of the plate. The calculation of stiffness reduces, as for plates with parallel stiffeners, to the calculation of moments of inertia per unit length for the basic sections.

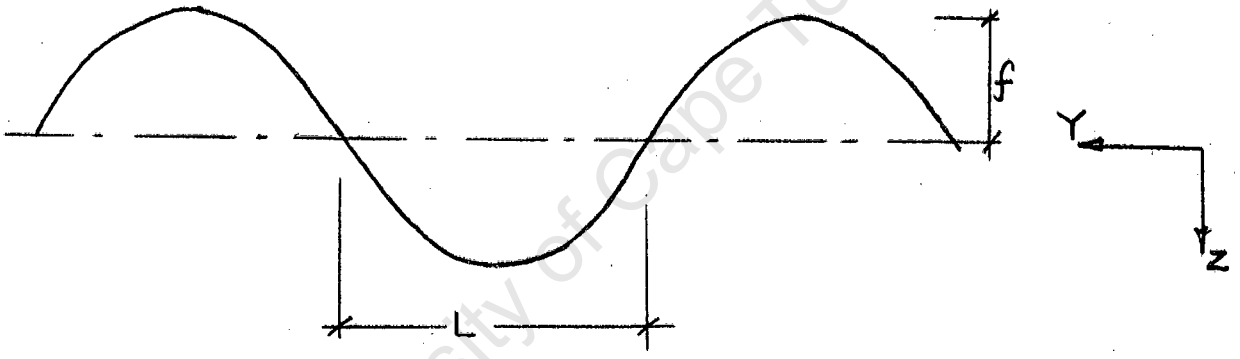

Fig. 2.10

Assuming the waves to be sinusoidal

$$z = f \sin \frac{\pi y}{L}$$

Let the arc length be s, the plate thickness h.

Then $D_x = EI$; $D_y = \frac{L}{s} \frac{Eh^3}{12(1-\upsilon^2)}$

$D_1 = 0$; $H = 2D_{xy} = \frac{s}{L} \frac{Eh^3}{12(1+\upsilon)}$

in which approximately

$$s = L.\left[1 + \frac{\pi^2 f^2}{4L^2}\right]$$

$$I = \frac{f^2 h}{2} \cdot \left[1 - \frac{0,81}{1 + 2,5\left(\frac{f}{2L}\right)^2}\right]$$

3. FROM M.T. HUBER

Huber's work is summarised in his books (Ref. 14, 15) where he develops his well-known theory and derives various mathematical solutions to problems. His rigidities for asymmetrically stiffened plates were given under Timoshenko (section 2.) where υ was taken as zero as a first approximation. This assumption is not so bad for concrete as for steel ($\upsilon = 0,3$). However, the writer has seen the following ranges for υ of concrete given, namely 0,1 - 0,2; 0,15 - 0,25; 0,2 - 0,3. These are substantial compared to steel. Rowe (Ref. 22) states that considerable errors occur in the calculation of the transverse moments in concrete bridges if υ is not taken into account.

In Ref. 14 appear the only formulae for υ_x and υ_y with a rational explanation which the writer has seen.

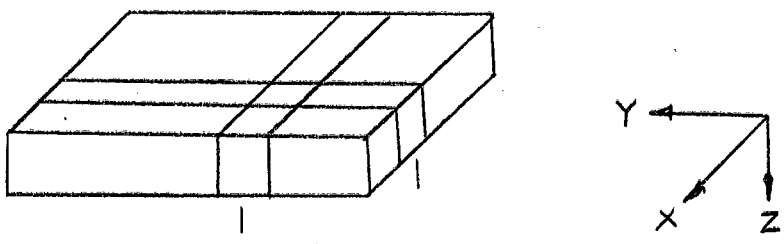

Fig. 2.11

As an introduction consider a true orthotropic plate.

Imagine the plate to be divided into X-strips and Y-strips of unit width, and denote the bending stiffnesses by $D'_x = E_x I$ and $D'_y = E_y I$. Then we get for the curvatures of the two strips the following equations

$$\frac{1}{r_x} = \frac{M_x}{D'_x} \quad ; \quad \frac{1}{r_y} = \frac{M_y}{D'_y}$$

where r_x and r_y are the radii of curvature. The interdependence of the strips and the plate prohibit the free lateral strain, and hence there is a change in curvature. The moment M_x has a reducing influence on the curvature of the Y-strips, and similarly M_y reduces the curvature of the X-strips. Apparently we may write by analogy with the isotropic plate

$$\frac{1}{r_x} = \frac{M_x}{D'_x} - \upsilon_y \frac{M_y}{D'_y}$$

$$\frac{1}{r_y} = \frac{M_y}{D'_y} - \upsilon_x \frac{M_x}{D'_x} \qquad \text{Eqs 2.12}$$

Now consider a plate made of isotropic material but which is stiffened by ribs

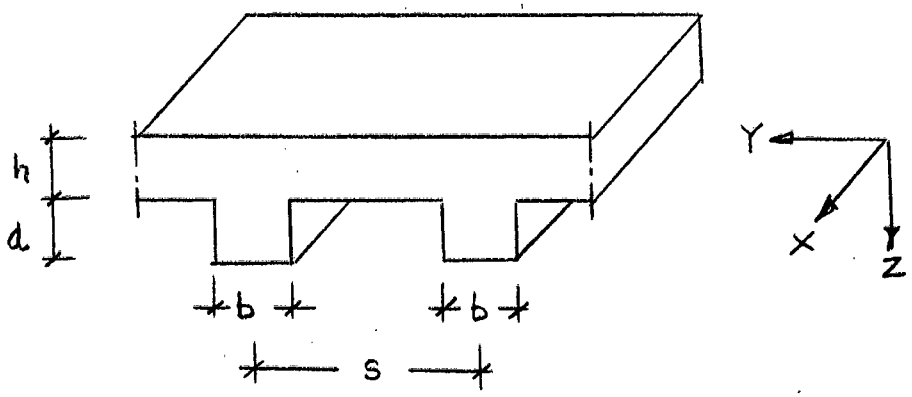

Fig. 2.12

Denote the bending stiffness of a unit cross-section width of an imaginary plate formed by putting ribs together by

$$D_y^r = \frac{E(h+d)^3}{12(1-\upsilon^2)}$$

Denote the stiffness of the plate alone by

$$D_y^p = \frac{Eh^3}{12(1-\upsilon^2)}$$

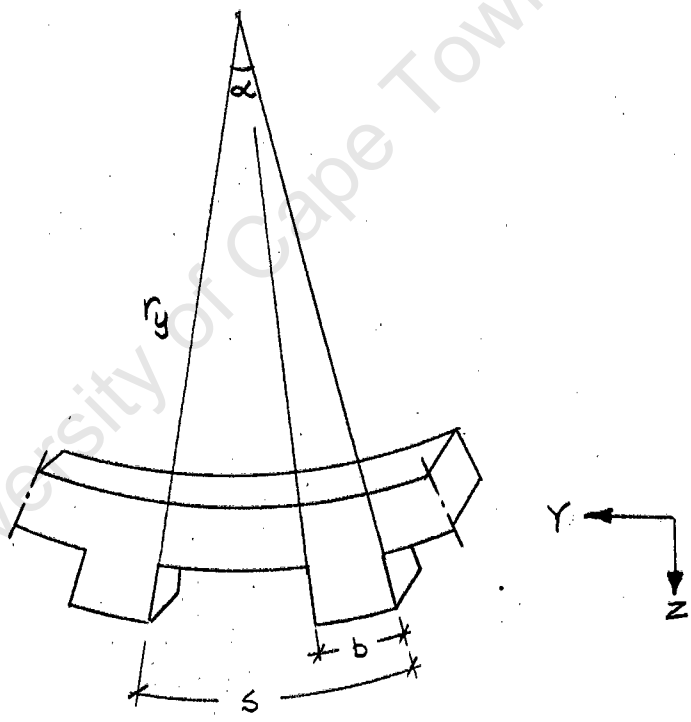

Fig. 2.13

From Fig. 2.13

$$\alpha = \frac{s}{r_y} \quad \text{and} \quad \frac{1}{r_y} = \frac{M_y}{D_y}$$

Then for a constant moment $M_y = 1$

$$\alpha = \frac{s}{D_y} = \frac{s-b}{D_y^p} + \frac{b}{D_y^r}$$

$$\therefore \quad D_y = D_y^p \cdot \frac{s}{(s-b) + \frac{D_y^p}{D_y^r} \cdot b} \qquad \text{Eq 2.13}$$

This is one of Eqs 2.7 as in Timoshenko (section 2.)

When $\frac{h^3}{(h+d)^3}$ is small

$$D_y = D_y^p \frac{s}{(s-b)} \qquad \text{Eq 2.14}$$

Now consider the ribbed plate to be divided into X- and Y-strips as before. Due to the action of moment M_y alone onto an element of the plate there should be caused in the Y-direction the curvature $\frac{M_y}{D_y'^p}$

where $D_y'^p = \frac{Eh^3}{12}$ is the beam bending stiffness of the Y-strip of plate. All stiffnesses marked with a ' are the beam bending stiffnesses. In the X-direction there should be caused a curvature of $-\upsilon \frac{M_y}{D_y'^p}$

Now imagine the ribs to be added to the plate. In the Y-direction the curvature is reduced in the ratio $D_y'^p : D_y'$, i.e. it becomes $\frac{M_y}{D_y'}$

In the X-direction the curvature is affected to a greater extent by the ribs, and will be reduced in ratio $D_x'^p : D_x'$.

It becomes $-\upsilon \frac{D_x'^p}{D_x'} \frac{M_y}{D_y'^p}$.

Using Eq 2.14 we may write it as

$$-\upsilon \frac{D'^{p}_{x}}{D'_{x}} \cdot \frac{s}{s-b} \cdot \frac{M_y}{D'_y}$$

Hence $$\upsilon_y = \upsilon \frac{D'^{p}_{x}}{D'_{x}} \cdot \frac{s}{s-b} \qquad \text{Eq 2.15}$$

To derive a value for υ_x, imagine a moment M_x alone to act. This causes in the X-direction a curvature of $\frac{M_x}{D'_x}$ and in the Y-direction a curvature of $-\upsilon \frac{M_x}{D'_x}$ where $D'_x = \frac{EI_x}{s}$.

The curvature in the Y-direction is now reduced in the ratio of (s-b) : s to allow for the stiffening effect of the ribs, and becomes $-\upsilon \frac{s-b}{s} \cdot \frac{M_x}{D'_x}$

Hence $$\upsilon_x \doteq \upsilon \frac{(s-b)}{s} \qquad \text{Eq 2.16}$$

Eq 2.15 can be rewritten as

$$\upsilon_y = \upsilon \frac{h^3 s}{12 I_x} \cdot \frac{s}{(s-b)} \qquad \text{Eq 2.17}$$

where I_x is the moment of inertia of the T-section.

Huber's values for D_{12} and D_{21} would become

$$D_{21} = \upsilon \frac{h^3 s}{12 I_x} \cdot \frac{s}{(s-b)} \cdot D_x = \upsilon D \frac{s}{(s-b)} \qquad \text{Eq 2.18}$$

$$D_{12} = \upsilon \frac{s-b}{s} D_y \doteq \upsilon D \qquad \text{Eq 2.19}$$

Cornelius (Ref. 16) recommends that for bridges with concrete slabs and relatively small steel ribs

$$\frac{\upsilon_x}{\upsilon_y} = \frac{D_x}{D_y} \text{ with } \upsilon_{max} = \upsilon_{concrete}$$

When the ribs become large $\upsilon_x = \upsilon_y = 0$.

4. FROM TROITSKY

Troitsky's book (Ref. 3) deals with the theory and design of steel bridge decks. Several methods of solution are given, one of which is to replace the deck by a theoretically orthotropic plate, which he terms the method of elastic equivalence. This is based on Huber's equation. The structural geometry of the deck may have many forms. The deck plate may be stiffened by torsionally weak ribs such as rectangular, I, channel, or angle sections, or by torsionally stiff ribs which are hollow sections of various shapes. Often the deck will have stiff ribs in one direction and weak ribs in the perpendicular direction. The deck plate may also be a concrete slab instead of a steel plate.

The way of comparing weak and stiff decks is by calculating the value of α, which is equal to 1 for an isotropic plate.

$$\alpha = \frac{H}{\sqrt{D_x D_y}}$$

Examples of relatively stiff and weak decks are given in Fig. 2.14. An asterisk signifies a possible simplifying assumption in the calculations, e.g. $D_y = 0$ may be used if

the ratio of D_x to D_y is very large.

In Fig. 2.15 taken from Ref. 3, Troitsky's formulae for rigidities and moments are given.

Cases	$D_x \frac{d^4w}{dx^4} + 2H \frac{d^4w}{dx^2dy^2} + D_y \frac{d^4w}{dy^4} = q$
$H > \sqrt{D_x D_y}$ * $D_y = 0$	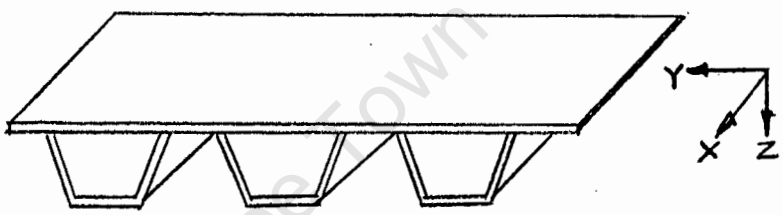
$H = \sqrt{D_x D_y}$	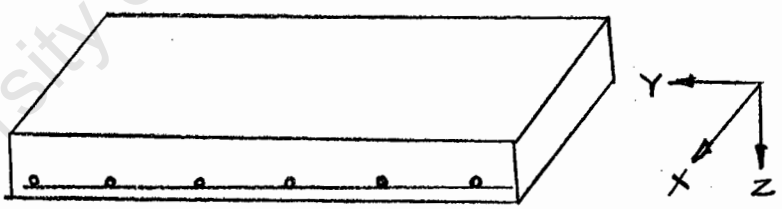
$H < \sqrt{D_x D_y}$ * $H = 0$ * $D_y = H = 0$	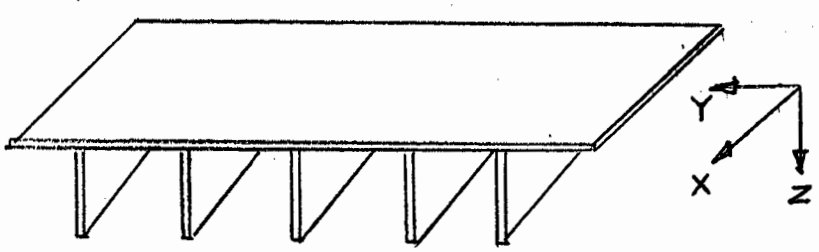

Fig. 2.14

Fig. 2.15

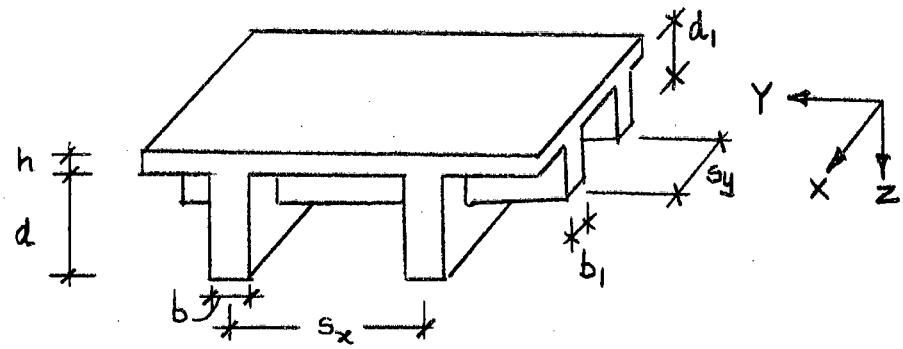

$$D_x = \frac{EI_x}{s_x}$$

$$D_y = \frac{EI_y}{s_y}$$

$$2D_{xy} = \frac{G}{6}\left[\frac{b^3 d}{s_x} + \frac{b_1^3 d_1}{s_y}\right]$$

$$H = \frac{Eh^3}{12(1-\upsilon^2)} + 2D_{xy} \qquad \text{Eqs 2.20}$$

$$M_x = -D_x\left[\frac{d^2w}{dx^2} + \upsilon\frac{d^2w}{dy^2}\right]$$

$$M_y = -D_y\left[\frac{d^2w}{dy^2} + \upsilon\frac{d^2w}{dx^2}\right]$$

$$M_{xy} = 2D_{xy}\frac{d^2w}{dxdy}$$

Notice that in D_x and D_y the plate portion is not divided by $(1-\upsilon^2)$, and that in M_x and M_y, υ is used instead of υ_x and υ_y. In the formula for D_{xy} the torsion constant J is taken as

$$J = \frac{1}{3}b^3 d + \frac{1}{3}b_1^3 d_1$$

The constant C is therefore always taken as 1/3. This is an approximation due to Föppl (Ref. 8) which is meant to increase the stiffness to allow for the continuity between rib and slab or between the elements of the rib if, for example, the rib is an I-section. It should only be applicable to thin steel sections.

Notice also that in the M_{xy} equation the stiffness of the plate is ignored.

Hollow sections

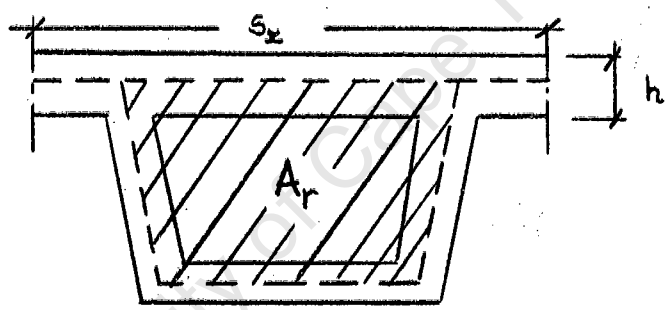

Fig. 2.16

For hollow sections the value of H is very different from the formula for open sections.

$$D_x = \frac{EI_x}{s_x} \quad , \quad D_y = \frac{Eh^3}{12(1-\upsilon^2)}$$

$$2H = G \frac{4 A_r^2}{\Sigma \frac{ds}{\delta}} \qquad \text{(from Bredt formula)}$$

δ is the variable thickness of the wall.

A_r is the mean of the areas enclosed by the outer and inner boundaries of the cross-section of the wall.

s_p is the total perimeter of the wall measured at the centre line.

Note that again the plate portion of the value of D_x is not divided by $(1-\upsilon^2)$. The rib is assumed not to increase the value of D_y.

Exact theory of stiffened plates

Orthogonally stiffened plates may be replaced by an equivalent orthotropic plate of constant thickness when the ribs are disposed symmetrically with respect to the middle plane of the plate. When the stiffeners are located only on one side of the plate the unknown location of the neutral surfaces of the bending stresses increases the complexity of determining the rigidities. The analysis of the problem can be extended to include the effect of the strain in the middle plane of the plate which produces additional shear stresses disregarded in Huber's method.

Therefore Huber's theory presents only an approximate solution of the problem. Investigations by Pfluger, Trenks, Giencke, and Massonnet resulted in the development of the exact theory of orthogonally stiffened plates. They find that the governing D.E. is of the 8th order.

$$D_1 \frac{d^8w}{dx^8} + D_2 \frac{d^8w}{dx^6dy} + D_3 \frac{d^8w}{dx^4dy^4} + D_4 \frac{d^8w}{dx^2dy^6} + D_5 \frac{d^8w}{dy^8} = q$$

where the constants D_1, D_2, .. D_5 are expressed by the geometric and elastic characteristics of the plate and ribs. However the solution of this equation requires a very

laborious calculation which seems to be almost impossible.

Giencke attempted to determine rigorously the effective torsional rigidity of the stiffened plate. He found that Huber's formula

$$2H = \upsilon_x D_y + \upsilon_y D_x + 4D_{xy}$$

should contain additional terms to show the influence of the eccentricity of the ribs with respect to the middle plane of the plate, and called this "the apparent torsional rigidity". However, Massonnet found that this value proposed by Giencke was excessive. This is expanded on later in this chapter.

Generally, the stresses obtained by rigorous methods are somewhat lower than those obtained from Huber's approximate theory. The computation procedures involved in working with the above 8th order D.E. are considered by Troitsky to be far too complicated to be considered for practical application in design at this stage of the development of the exact theory. The simplified theory has proved its application in the practical design of bridges.

5. FROM BARES AND MASSONNET

Ref. 4 is concerned with the theory and design of concrete beam-and-slab and hollow section bridges. Elastic theory is used to derive the Guyon-Massonnet-Bares method of lateral distribution coefficients. The underlying solution is a mathematical one, resulting in tables which are used for design. To use the tables two stiffness parameters are needed. These are the parameter of lateral stiffness β, and the torsional parameter α. They are defined as follows.

$$\beta = \frac{B}{A} \cdot \frac{D_x}{D_y}$$

$$\alpha = \frac{H}{\sqrt{D_x D_y}}$$

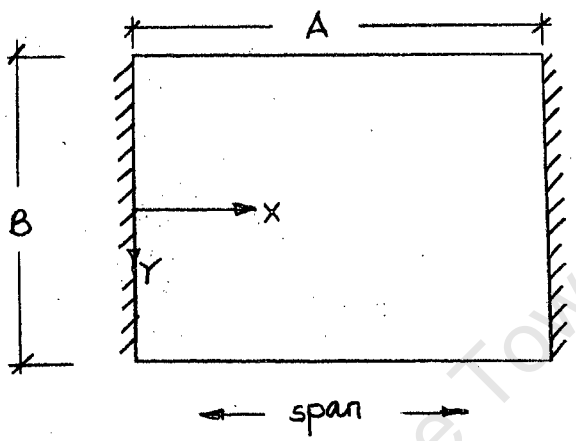

Fig. 2.17

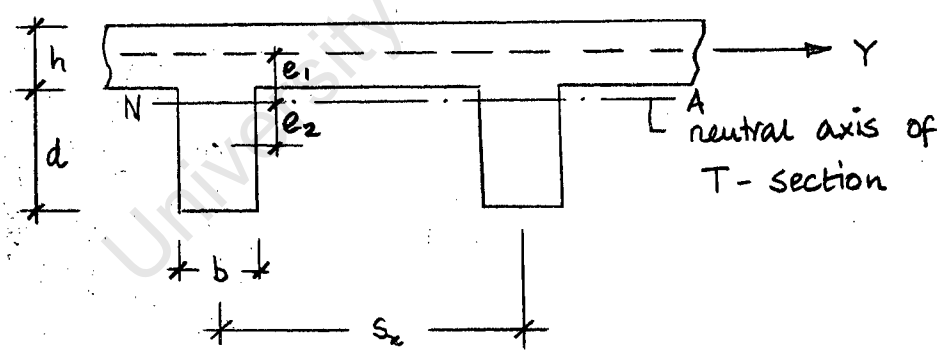

Fig. 2.18

For grillages υ is always taken as zero, but for composite beam-and-slab sections the portion of the rigidity caused by the slab should be divided by the factor $(1-\upsilon^2)$. Their formulae are therefore

$$D_x = \frac{E}{s_x} b \frac{d^3}{12} + \frac{E}{s_x} bd\, e_2^2 + \frac{E}{(1-\upsilon^2)}\left[\frac{h^3}{12} + h\, e_1^2\right]$$

$$D_y = \frac{E}{(1-\upsilon^2)} \cdot \frac{h^3}{12} = D$$

Eqs 2.21

$$D_1 = \upsilon D$$

$$H = D_1 + 2D_{xy} = \upsilon D + D(1-\upsilon) + \frac{GJ_x}{2s_x}$$

$$= D + \frac{GJ_x}{2s_x}$$

Notice that D_1 is not considered negligible and put equal to zero. As in Timoshenko the torsional stiffness is obtained by summing the stiffnesses of the slab and the beam acting separately.

If there are beams running in both the X and Y directions then the formulae become

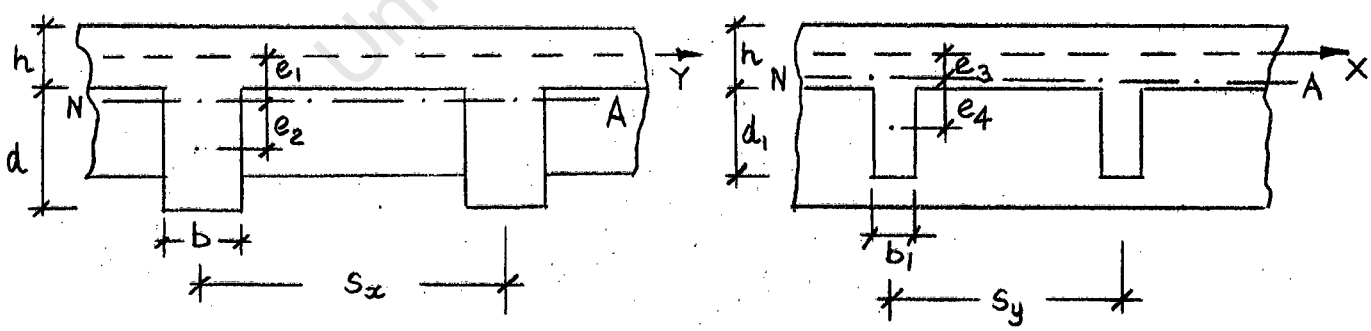

Fig. 2.19

D_x as before

$$D_y = \frac{E}{s_y} b_1 \frac{d_1^3}{12} + \frac{E}{s_y} b_1 \cdot d_1 \cdot e_4^2 + \frac{E}{(1-\upsilon^2)}\left[\frac{h^3}{12} + h\, e_3^2\right]$$

$$D_1 = \upsilon D$$

$$2H = 2D_1 + 4D_{xy}$$

$$= 2\,\upsilon\,D + D(1-\upsilon) + \frac{GJ_x}{s_x} + D(1-\upsilon) + \frac{GJ_y}{s_y}$$

$$= 2D + \frac{GJ_x}{s_x} + \frac{GJ_y}{s_y}$$

$$\therefore \quad H = D + \frac{GJ_x}{2s_x} + \frac{GJ_y}{2s_y} \qquad \text{Eqs 2.22}$$

At this stage it should be pointed out that there is an anomaly in the formulae for the torsional stiffness of a beam and that for a plate. This is mentioned in the literature but the writer has not come across an explanation. Broadly speaking, the anomaly lies in the fact that the stiffness of a beam is twice that of an equivalent plate section.

Consider an element of isotropic plate, thickness h.

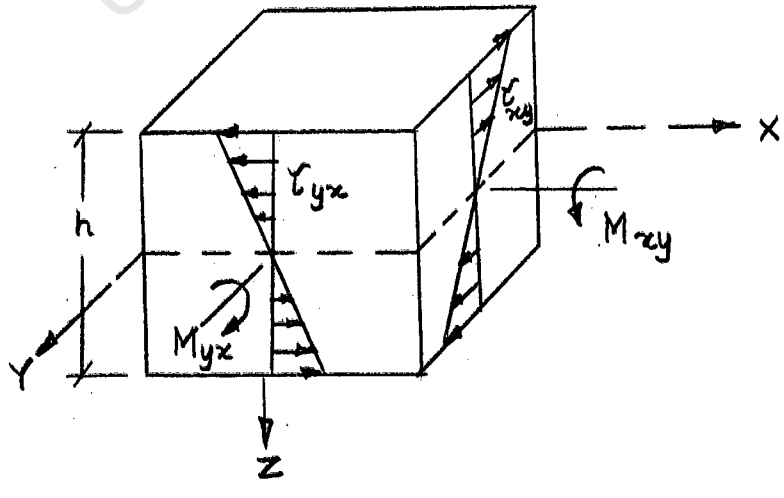

Fig. 2.20

Isotropic plate element.

As in Chapter 1, we have

$$\tau_{xy} = G\,\gamma_{xy}$$

$$\gamma_{xy} = \frac{du}{dy} + \frac{dv}{dx}$$

$$= -2\,z\,\frac{d^2w}{dxdy}$$

$$M_{xy} = -\int_{-h/2}^{h/2} \tau_{xy}\, z\, dz$$

$$= +\int_{-h/2}^{h/2} G.2\,\frac{d^2w}{dxdy}.\,z^2\,dz$$

$$= 2\,G\,\frac{h^3}{12}\,\frac{d^2w}{dxdy} = D(1-\upsilon)\,\frac{d^2w}{dxdy}$$

$$\therefore\quad 2D_{xy} = 2.G.\frac{h^3}{12} = D(1-\upsilon)$$

$$\text{or}\quad D_{xy} = \frac{Gh^3}{12}$$

Now consider a beam being twisted by a moment M_T through an angle θ per unit length.

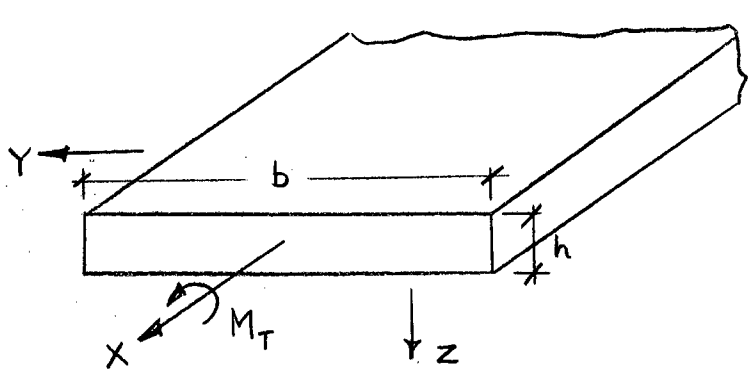

Fig. 2.21

From the classical theory of torsion

$$M_T = G.J.\theta$$

where $J = \frac{bh^3}{3}$ as $b/h \rightarrow \infty$

θ corresponds exactly to $\frac{d^2w}{dxdy}$

M_{xy} is a moment per unit length in the Y direction and has the units of force; M_T is a moment with units of force x distance. Let the ratio b/h of the beam become very large and consider an element of the beam of unit length in the Y direction. To compare the two expressions for moment M_T must be divided by b :

$$\frac{M_T}{b} = \frac{G\,b\,h^3}{3b}\,\theta = \frac{G\,h^3}{3}\cdot\frac{d^2w}{dxdy}$$

$$M_{xy} = 2\,\frac{G\,h^3}{12}\cdot\frac{d^2w}{dxdy} = \frac{G\,h^3}{6}\cdot\frac{d^2w}{dxdy}$$

The conclusion is that to find the torsional stiffness of a slab or of the slab part of a beam-and-slab structure the equivalent beam stiffness must be divided by 2.

6. FROM HUFFINGTON

Huffington (Ref. 9) has done a deep study of the rigidities of symmetrically and asymmetrically stiffened plates. His application is to plates with relatively small stiffeners, i.e. the value of D_x/D_y is low. These are more common in aircraft and ship building. When we say that a technically orthotropic plate is replaced by an equivalent orthotropic plate of constant thickness, the equivalence can

be defined in several ways. It could mean that either the deflection or one of the strain components of the actual and equivalent plates be the same at some point. It could mean that the mean difference of deflections or strain components of the two plates be zero. Huffington uses a third form on which to base equivalence, namely, that the total strain energies of the two plates be equal.

A. Symmetrically stiffened plates

Determination of D_x

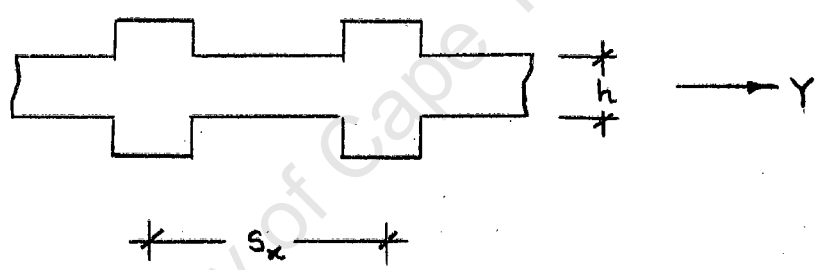

Fig. 2.22

Considering a stiffened plates simply supported at x = 0 and x = A, and infinitely long in the Y direction, loaded by a U.D.L., Huffington derives a very large expression for D_x. This depends on the elastic and geometric properties of the section, and on the span in the X direction, A. However as A is increased from zero, D_x swiftly approaches an asymptotic value. This is

$$D_x = D + \frac{EI_s}{s_x}$$

where I_s is the moment of inertia of the pair of stiffeners with respect to the middle plane of the plate. This value of D_x is the same as given by Leknitskii and others.

Determination of D_y

To determine D_y consider the stiffened plate as being simply supported at y = 0 and y = B, and infinitely long in the X-direction.

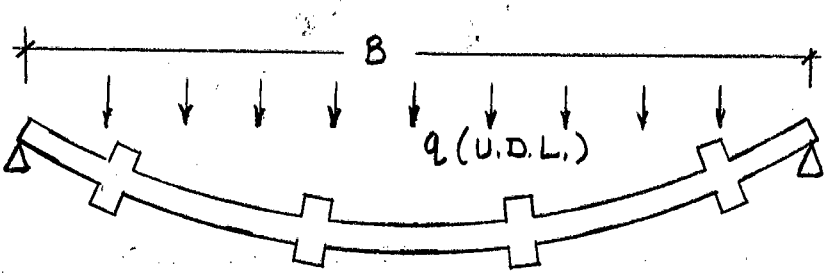

Fig. 2.23

The moment-curvature relationship is

$$M_y = -D(y)\frac{d^2w}{dy^2} = \frac{q}{2}\cdot(By - y^2)$$

where D(y) is the variable flexural rigidity of the stiffened plate. A lower bound to D_y is found by putting D(y) = D. This is a common value used by others. An upper bound to D_y is found from

$$D(y) = \frac{E[h(y)]^3}{12(1-\upsilon^2)} \qquad \text{Eq 2.23}$$

where h(y) is the total thickness of the plate-stiffener combination, subject to the following limitation. When the ratio of stiffener height to stiffener width is greater than unity, a reduced height of the order of the stiffener width should be employed.

By strain energy considerations the value of D_y becomes

$$D_y = \frac{B^5}{30\int_0^b \frac{(By-y^2)^2}{D(y)}\,dy} \qquad \text{Eq 2.24}$$

The evaluation of the integral in the above equation can be tedious when the number of stiffeners is large. However D_y rapidly approaches an asymptotic value as the number of stiffeners increases, as expected.

Determination of D_{xy}

The method given for this is really a reference to another method. It is not clear what is done. The formula for D_{xy} is given as

$$2D_{xy} = \frac{GK}{2}$$

where K = torsion constant obtained by the membrane analogy, relaxation methods, or some empirical method.

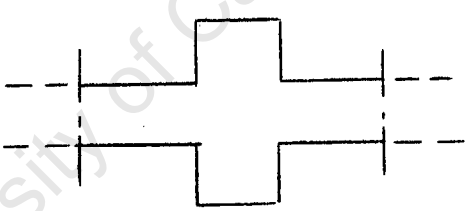

Fig. 2.24

It is not clear whether the section in Fig. 2.24 is regarded as a beam and K found accordingly. The anomaly between the stiffness of beams and slabs causes most of the confusion.

Determination of D_1

A very large expression is derived for D_1, in which the span dimension, A, appears. As A increases to ∞, D_1 takes on the limiting value

$$D_1 = \upsilon D$$

This value has been recommended by others.

B. Asymmetrically stiffened plates

For these plates, D_x may be determined as in section 5 (p. 45). For D_y Huffington says that a judicious selection of continuous functions to represent the neutral surface and the effective thickness h(y) must be made, otherwise the method is as for symmetrically stiffened plates. D_{xy} is determined as in section 1. above. D_1 requires modification but it is not stated whether the limiting case

$$D_1 = \upsilon D$$

is materially affected.

7. FROM GIENCKE

Giencke (Ref. 11) was involved in the derivation of the more exact 8th order theory already mentioned.

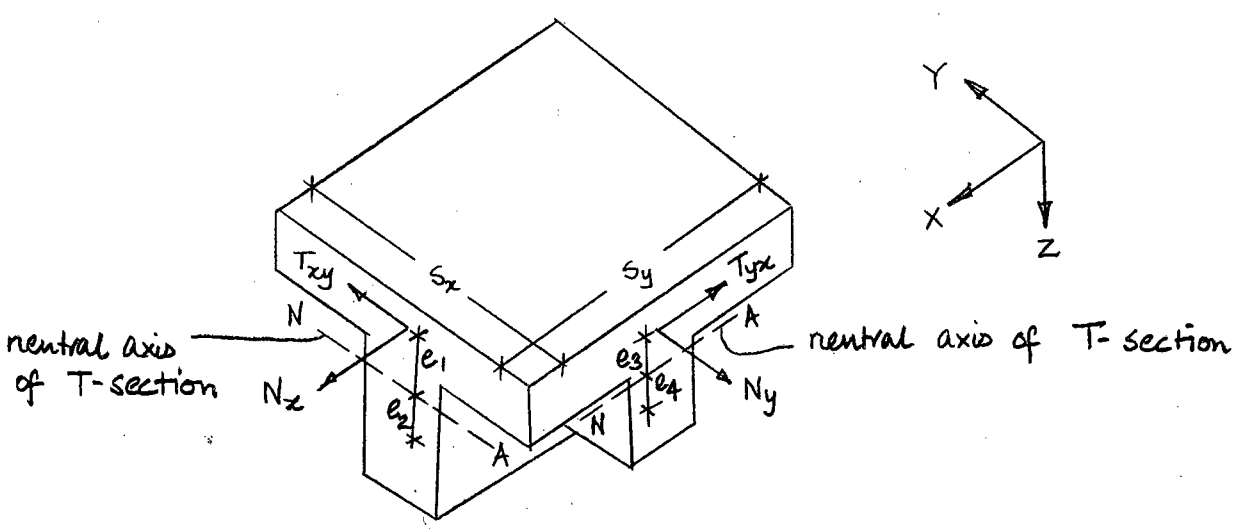

Fig. 2.25

Basically, it involves considering the in-plane forces in the slab or plate as well as the other forces, M_x, M_y, Q_x, Q_y, M_{xy}, M_{yx}. Three differential equations in the displacements u, v, and w are found. These are combined into one 8th order D.E. in terms of w only. Using this theory, Giencke proposes corrections to the 4th order theory. The moment equations become

$$M_x^* = -D_x \frac{d^2w}{dx^2} - \upsilon \left[D + e_1 e_3 \frac{Eh}{(1-\upsilon^2)} \right] \frac{d^2w}{dy^2} \qquad \text{Eq 2.25}$$

$$M_y^* = -D_y \frac{d^2w}{dy^2} - \upsilon \left[D + e_1 e_3 \frac{Eh}{(1-\upsilon^2)} \right] \frac{d^2w}{dx^2} \qquad \text{Eq 2.26}$$

$$M_{xy}^* = \left[D(1-\upsilon) + \frac{GJ_x}{s_x} + \frac{e_1(e_1+e_3)}{2} \cdot \frac{Eh}{(1+\upsilon)} \right] \frac{d^2w}{dxdy} \qquad \text{Eq 2.27}$$

$$M_{yx}^* = \left[D(1-\upsilon) + \frac{GJ_y}{s_y} + \frac{e_3(e_1+e_3)}{2} \cdot \frac{Eh}{(1+\upsilon)} \right] \frac{d^2w}{dxdy} \qquad \text{Eq 2.28}$$

where E is the modulus of the plate material if the rib and plate materials are different.

From the above equations

$$H^* = D + \frac{GJ_x}{2s_x} + \frac{GJ_y}{2s_y} + \upsilon e_1 e_3 \frac{Eh}{(1-\upsilon^2)} + \frac{(e_1+e_3)^2 Eh}{4(1+\upsilon)} \qquad \text{Eq 2.29}$$

Massonnet (Ref. 12, 4) finds that Giencke's values are too large. He finds that the values e_1, e_3 in the above formulae should be replaced by values ranging between e_1, e_3 and zero. The actual values depend on the boundary conditions and the loading. His values for the rigidities are (with the

notation in Figs. 2.19, 2.25)

$$D_x^* = D_x + (e_1-a_1)^2 E.\left[h + \frac{bd}{s_x}\right] \qquad \text{Eq 2.30}$$

$$D_y^* = D_y + (e_3-a_3)^2 E.\left[h + \frac{b_1 d_1}{s_y}\right] \qquad \text{Eq 2.31}$$

$$D_1^* = \upsilon\left[D + a_1 a_3 \frac{Eh}{(1-\upsilon^2)}\right] \qquad \text{Eq 2.32}$$

$$\gamma_x^* = D(1-\upsilon) + \frac{GJ_x}{s_x} + \frac{a_1(a_1+a_3)}{2} \cdot \frac{Eh}{(1+\upsilon)} \qquad \text{Eq 2.33}$$

$$\gamma_y^* = D(1-\upsilon) + \frac{GJ_y}{s_y} + \frac{a_3(a_1+a_3)}{2} \cdot \frac{Eh}{(1+\upsilon)} \qquad \text{Eq 2.34}$$

$$H^* = D + \frac{GJ_x}{2s_x} + \frac{GJ_y}{2s_y} + \upsilon a_1 a_3 \frac{Eh}{(1-\upsilon^2)} + (a_1+a_3)^2 \frac{Eh}{4(1+\upsilon)} \qquad \text{Eq 2.35}$$

where $o < a_1 < e_1$ and $o < a_3 < e_3$

and a_1, a_3 depend on the boundary conditions and the loading. Unfortunately, without going through the 8th order theory it is impossible to give meanings to a_1, a_3; they must just be accepted as terms in the equations.

For cylindrical (pure) bending in the X direction (M_x = const, M_y = O)

$$D_x^* = D_x \qquad D_y^* = D_y = D$$

$$H^* = D + \frac{GJ_x}{2s_x} + \frac{GJ_y}{2s_y} + \upsilon e_1 e_3 \frac{Eh}{(1-\upsilon^2)} + (e_1+e_3)^2 \frac{Eh}{4(1+\upsilon)} \qquad \text{Eqs 2.36}$$

For pure twisting, i.e. $\frac{d^2w}{dx^2} = \frac{d^2w}{dy^2} = 0$

and $\frac{d^2w}{dxdy} \neq 0$ at all points.

$$a_1 = a_3 = 0$$

$$\therefore \quad D_x^* = D_x + e_1^2 E\left[h + \frac{bd}{s_x}\right]$$

$$D_y^* = D_y + e_3^2 E\left[h + \frac{b_1 d_1}{s_x}\right] \qquad \text{Eqs 2.37}$$

$$H^* = D + \frac{GJ_x}{2s_x} + \frac{GJ_y}{2s_y} = H$$

In general, the rigidities obtained from the ordinary 4th order theory are always the minimum values.

8. FROM ADOTTE

Adotte (Ref. 10) deals with asymmetrically stiffened plates of any kind, steel or concrete, and gives what he terms "a second order" theory for them. This second order theory takes into account the in-plane forces in the plate or slab part of the structure, and so has the same base as the 8th order theory. In his method the bending and in-plane forces are found separately. Finite differences are used to obtain solutions. Basically, two general operator patterns are derived which are applied to the nodes in the structure. There are two sets of simultaneous equations to be solved. The unknowns at each node are the deflection, w, and Airy's stress function, F. By choosing values of F and then solving for the values of w, and then substituting in the values of w to recalculate the values of F, and so

on, the plate is solved.

Huber's equation (1.13) forms part of one of the general operators so, as with most other methods, values are needed for D_x, D_y and H. These are given by Adotte as

$$D_x = \frac{E\,I_x}{s_x(1-\upsilon^2)} \qquad D_y = \frac{E\,I_y}{s_y(1-\upsilon^2)}$$

$$H = \tfrac{1}{2}(D_x + D_y) \qquad \text{Eqs 2.38}$$

where I_x, I_y are the moments of inertia of the repeating sections in the X,Y directions. These are said to come from the standard theory of elasticity. Dividing the whole of I_x, I_y by $(1-\upsilon^2)$ is likely to overestimate D_x, D_y. The only place where the writer has seen the formula for H given above is in Marcus's equation

$$D_x \frac{d^4w}{dx^4} + (D_x + D_y) \frac{d^4w}{dx^2dy^2} + D_y \frac{d^4w}{dy^4} = q$$

which was discounted and replaced by Huber.

9. OTHER AUTHORS

In this section references on the subject of orthotropic plates are given, but which contain no new ideas on the values of the rigidities.

Zienkiewicz and Cheung (Ref. 17) among others produced an orthotropic rectangular element stiffness matrix for use in a finite element analysis. Values of D_x, D_y, D_1 and D_{xy} are needed for substitution into this matrix. An alternative method is to use isotropic plate elements and beam elements.

Bares (Ref. 2) gives solutions in tabular form for various values of D_x/D_y and various load and support conditions. In Ref. 20 he presents his version of the more exact theory and describes some experimental work on an orthotropic slab.

Leknitskii (Ref. 5) is concerned with mathematical solutions of anisotropic plates with various shapes, support conditions, and loadings. He gives rigidity formulae for plates with many stiff ribs, plywood plates, corrugated plates, and plates with the modulus E varying generally through the thickness.

Some mathematical solutions for bridge decks using the more exact theory appear in Ref. 13, 18, 19. The views on rigidity formulae follow those of Cornelius and Giencke.

10. SUMMARY

In the experimental part of this work tests are done on homogeneous, asymmetrically stiffened plates with ribs running in one direction only. In the summary below are the rigidities for this type of orthotropic plate only.

A. Values for D_x

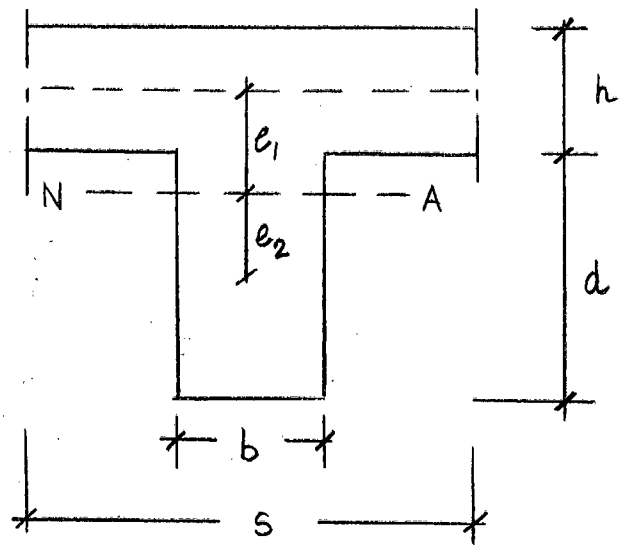

Fig. 2.26

i. $$D_x = \frac{E}{s}\left[\frac{bd^3}{12} + bd\, e_2^2\right] + \frac{E}{(1-\upsilon^2)}\left[\frac{h^3}{12} + h\, e_1^2\right]$$ **Eq 2.39**

This is the most general formula.

ii. $$D_x^* = D_x + (e_1-a_1)^2 . E.\left[h + \frac{bd}{s}\right]$$ **Eq 2.40**

where D_x is as in (i) above, and $o < a_1 < e_1$.

This is Massonnet's 8th order correction.

iii. $$D_x = \frac{EI_x}{s}$$ **Eq 2.41**

iv. $$D_x = \frac{EI_x}{s(1-\upsilon^2)}$$ **Eq 2.42**

where I_x is the moment of inertia of the T-section about its neutral axis, are approximations which can be used if

a. υ is very small)
)
b. the plate contribution to) for formula (iii)
)
I_x is small)

c. the beam contribution to)
) for formula (iv)
I_x is small)

B. Values of D_y

i. $$D_y = \frac{Eh^3}{12(1-\upsilon^2)} = D \qquad \text{Eq 2.43}$$

This is a safe formula which some consider conservative.

ii. $$D_y = \frac{E\,h^3\,s}{12(s-b+\alpha^3 b)} \qquad \text{Eq 2.44}$$

where $\alpha = h/(h+d)$

This is Huber's formula

iii. $$D < D_y < \frac{B}{30\int_0^B \frac{(By-y^2)^2}{D(y)}\,dy} \qquad \text{Eq 2.45}$$

where B is the span in the Y direction

where $D(y) = \frac{E[h(y)]^3}{12(1-\upsilon^2)}$

where h(y) is the total thickness of the plate stiffener combination subject to the following limitation. When the ratio of stiffener height to stiffener width is greater than unity a reduced height of the order of the stiffener width should be used.

This was Huffington's recommendation for symmetrically stiffened plates, and was really applied to plates with simply supported edges.

C. Values of D_1

i. $D_1 = \upsilon D$ Eq 2.46

This is the commonly accepted one and seems the most reasonable.

ii. $D_1 = \upsilon . D + \upsilon . e_1 . e_3 . \frac{Eh}{(1-\upsilon^2)} = \upsilon D$ Eq 2.47

This is Giencke's approximate formula from 8th order theory, and is put in to show that no change is made to the value of D_1 by this theory when the ribs run in one direction only ($e_3 = o$).

iii. $D_1 = O$ Eq 2.48

This is a first approximation used if υ is small or if the contribution of the plate to D_x is small.

D. Values of γ_x, γ_y, and D_{xy}

i. $\gamma_x = D(1-\upsilon) + G . \frac{J}{s}$

$\gamma_y = D(1-\upsilon)$ Eqs 2.49

$2D_{xy} = D(1-\upsilon) + G . \frac{J}{2s}$

This is the usual set of formulae. γ_x represents the

sum of the torsional rigidities of the plate and the beam taken separately. There is no formula which allows for their additional strength due to continuity, except for ii. below, which is really for thin steel sections.

For steel ribs joined to a concrete slab by shear connectors or joined to a steel deck plate by bolts there may well be a negligible continuity effect.

ii. $$\gamma_x = D(1-\upsilon) + G\frac{bd^3}{3s}$$

$$\gamma_y = D(1-\upsilon) \qquad \text{Eqs 2.50}$$

$$2D_{xy} = D(1-\upsilon) + G\frac{bd^3}{6s}$$

In the formula for γ_x the beam contribution is calculated with C = 1/3, irrespective of the ratio d/b.

iii. $$\gamma_x = D(1-\upsilon) + \frac{e_1^2\,Eh}{2(1+\upsilon)} + \frac{GJ}{s}$$

$$\gamma_y = D(1-\upsilon) \qquad \text{Eqs 2.51}$$

$$2D_{xy} = D(1-\upsilon) + \frac{e_1^2\,Eh}{4(1+\upsilon)} + \frac{GJ}{2s}$$

These formulae come from the 8th order approximation due to Giencke. For Massonnets formulae replace e_1 by a_1, where $o < a_1 < e_1$, in the above equations.

CHAPTER 3

GENERAL ANISOTROPIC ELASTIC THEORY APPLIED TO ORTHOTROPIC PLATES

Statements such as "The bending of orthotropic plates is characterised by four independent elastic constants D_x, D_y, D_1 and D_{xy}", are sometimes made in the literature. This can be misleading because there are actually nine elastic constants which characterise an orthotropic plate, but usually only four are needed in a bending analysis.

In Chapter 1 the relationships between stress and strain in an orthotropic plate were stated in Eqs 1.3. There the co-ordinate system X,Y,Z corresponded to the directions of principal stiffness. It will be seen that the stress-strain relationships are more complicated when this is not the case, and hence the moment equations (1.6, 1.7, 1.8) acquire extra terms. The method of finding the moments in directions other than the directions of principal stiffness will be given. One application of this is that it can be used to determine the rigidities of orthotropic plates by experiment.

The basic theory in this chapter comes from Ref. 23. We begin by considering the state of stress and strain in a continuous anisotropic body.

1. The State of Stress in a Continuous Solid Body

The state of stress at any given point of a continuous body is determined entirely by the components of stress in 3

mutually perpendicular planes which pass through the chosen point. Choosing a mutually perpendicular set of axes X,Y,Z the stress components are defined as in Fig. 3.1.

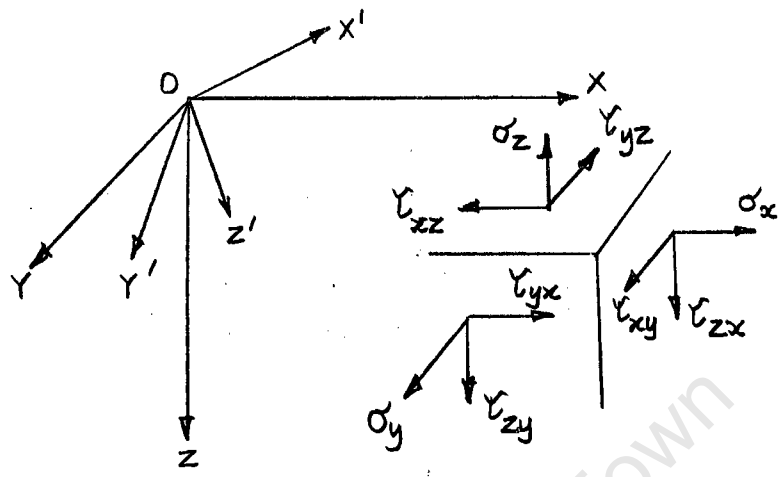

Fig. 3.1

We can find by projection the components of stress in a new orthogonal system X',Y',Z'. The position of the new system with respect to the first system is determined by Table 3.1 of direction cosines. In the table α_1 = cos (XOX') γ_2 = cos (ZOY') and so forth.

TABLE 3.1

Direction cosines

	X	Y	Z
X'	α_1	β_1	γ_1
Y'	α_2	β_2	γ_2
Z'	α_3	β_2	γ_3

The stresses in the new coordinate system (i.e. on the

areas normal to the X',Y' and Z' axes) are

$$\sigma'_x = \sigma_x\alpha_1^2 + \sigma_y\beta_1^2 + \sigma_z\gamma_1^2 + 2\tau_{yz}\beta_1\gamma_1 + 2\tau_{xz}\alpha_1\gamma_1 + 2\tau_{xy}\alpha_1\beta_1$$

$$\tau'_{yz} = \sigma_x\alpha_2\alpha_3 + \sigma_y\beta_2\beta_3 + \sigma_z\gamma_2\gamma_3 + \tau_{yz}(\beta_2\gamma_3 + \beta_3\gamma_2)$$

$$+ \tau_{xz}(\alpha_2\gamma_3 + \alpha_3\gamma_2) + \tau_{xy}(\alpha_2\beta_3 + \alpha_3\beta_2)$$

Eqs 3.1

The expressions for σ'_y, σ'_z, τ'_{xz}, τ'_{xy} are obtained by cyclic permutation of the indices of α, β and γ. The formulae for the transition from the system X',Y',Z' to X,Y,Z have the form:

$$\sigma_x = \sigma'_x\alpha_1^2 + \sigma'_y\alpha_2^2 + \sigma'_z\alpha_3^2 + 2\tau'_{yz}\alpha_2\alpha_3 + 2\tau'_{xz}\alpha_1\alpha_3 + 2\tau'_{xy}\alpha_1\alpha_2$$

$$\tau_{yz} = \sigma'_x\beta_1\gamma_1 + \sigma'_y\beta_2\gamma_2 + \sigma'_z\beta_3\gamma_3 + \tau'_{yz}(\beta_2\gamma_3 + \beta_3\gamma_2)$$

$$+ \tau'_{xz}(\beta_1\gamma_3 + \beta_3\gamma_1) + \tau'_{xy}(\beta_1\gamma_2 + \beta_2\gamma_1)$$

Eqs 3.2

As before, cyclic permutation of α, β and γ gives the remaining stress component formulae.

2. Strain

The state of deformation in the neighbourhood of a given point of a continuous body is determined by six components of strain : 3 components of relative normal strain which we denote by ϵ with one index which indicates the direction of the strain; 3 components of relative shear strain which we denote by γ with 2 indices.

For the transition from one orthogonal coordinate system X,Y,Z to another X',Y',Z', the components of strain transform according to formulae of type (3.1). Here we substitute

ϵ for σ and $\frac{1}{2}\gamma$ for τ.

$$\epsilon'_x = \epsilon_x\alpha_1^2 + \epsilon_y\beta_1^2 + \epsilon_z\gamma_1^2 + \gamma_{yz}\beta_1\gamma_1 + \gamma_{xz}\alpha_1\gamma_1 + \gamma_{xy}\alpha_1\beta_1$$

$$\gamma'_{yz} = 2\epsilon_x\alpha_2\alpha_3 + 2\epsilon_y\beta_2\beta_3 + 2\epsilon_z\gamma_2\gamma_3 + \gamma_{yz}(\beta_2\gamma_3 + \beta_3\gamma_2)$$
$$+ \gamma_{xz}(\alpha_2\gamma_3 + \alpha_3\gamma_2) + \gamma_{xy}(\alpha_2\beta_3 + \alpha_3\beta_2).$$

Eqs 3.3

and conversely,

$$\epsilon_x = \epsilon'_x\alpha_1^2 + \epsilon'_y\alpha_2^2 + \epsilon'_z\alpha_3^2 + \gamma'_{yz}\alpha_2\alpha_3 + \gamma'_{xz}\alpha_1\alpha_3 + \gamma'_{xy}\alpha_1\alpha_2$$

$$\gamma_{yz} = 2\epsilon'_x\beta_1\gamma_1 + 2\epsilon'_y\beta_2\gamma_2 + 2\epsilon'_z\beta_3\gamma_3 + \gamma'_{yz}(\beta_2\gamma_3 + \beta_3\gamma_2)$$
$$+ \gamma'_{xz}(\beta_1\gamma_3 + \beta_3\gamma_1) + \gamma'_{xy}(\beta_1\gamma_2 + \beta_2\gamma_1)$$

Eqs 3.4

We denote the components of displacement of the particles of a continuous body along the axes of the Cartesian coordinate system X,Y,Z by u,v,w. In the case of small displacements of a continuous body, it is possible to neglect the squares and products of the derivatives of the displacements. We have:

$$\epsilon_x = \frac{du}{dx} \qquad \epsilon_y = \frac{dv}{dy} \qquad \epsilon_z = \frac{dw}{dz}$$

$$\gamma_{yz} = \frac{dv}{dz} + \frac{dw}{dy} \qquad \gamma_{xz} = \frac{dw}{dx} + \frac{du}{dz}$$

$$\gamma_{xy} = \frac{du}{dy} + \frac{dv}{dx}$$

Eqs 3.5

Formulae and equations given above are valid for both elastic and inelastic continuous bodies; their derivations can be found in any text on the theory of elasticity.

3. The Generalized Hooke's Law

We assume that the components of strain are linear functions of the components of stress. In other words, it is assumed that a continuous body satisfies the generalized Hooke's Law. When no elements of elastic symmetry are present in the general case of a homogeneous anisotropic body, the equations which express the generalized Hooke's Law in Cartesian coordinates X,Y,Z have the form:

$$\epsilon_x = a_{11}\sigma_x + a_{12}\sigma_y + a_{13}\sigma_z + a_{14}\tau_{yz} + a_{15}\tau_{xz} + a_{16}\tau_{xy}$$

$$\epsilon_y = a_{21}\sigma_x + a_{22}\sigma_y + a_{23}\sigma_z + a_{24}\tau_{yz} + a_{25}\tau_{xz} + a_{26}\tau_{xy}$$

.....

$$\gamma_{xy} = a_{61}\sigma_x + a_{62}\sigma_y + \ldots \qquad \ldots + a_{66}\tau_{xy}$$

Eqs 3.6

These equations contain 36 coefficients a_{ij}, called the coefficients of deformation. By solving the above equations for the stress components σ_x, σ_y, ..., τ_{xy} we obtain an equivalent form for the equations of the generalized Hooke's Law:

$$\sigma_x = A_{11}\epsilon_x + A_{12}\epsilon_y + A_{13}\epsilon_z + A_{14}\gamma_{yz} + A_{15}\gamma_{xz} + A_{16}\gamma_{xy}$$

$$\sigma_y = A_{21}\epsilon_x + A_{22}\epsilon_y + A_{23}\epsilon_z + A_{24}\gamma_{yz} + A_{25}\gamma_{xz} + A_{26}\gamma_{xy}$$

.....

$$\tau_{xy} = A_{61}\epsilon_x + A_{62}\epsilon_y + \ldots \qquad \ldots + A_{66}\gamma_{xy}$$

Eqs 3.7

The constants A_{ij} are called the moduli of elasticity. If an elastic potential exists, the number of elastic constants in the most general case of anisotropy is reduced to 21. Such

an elastic potential exists when the variation of the body under deformation occurs isothermally or adiabatically. We shall assume that the variations of deformation occur isothermally.

Denoting the elastic potential by $\bar{V}$ (equal to the potential energy of deformation per unit of volume), we have the following relations:

$$\sigma_x = \frac{d\bar{V}}{d\epsilon_x} \quad , \quad \sigma_y = \frac{d\bar{V}}{d\epsilon_y} \quad , \ \ldots \qquad \ldots , \quad \tau_{xy} = \frac{d\bar{V}}{d\gamma_{xy}} \ .$$

By differentiating the above with respect to ϵ_x, ϵ_y, ... γ_{xy}, we obtain

$$\frac{d\sigma_x}{d\epsilon_y} = \frac{d\sigma_y}{d\epsilon_x} \qquad \frac{d\sigma_x}{d\epsilon_z} = \frac{d\sigma_z}{d\epsilon_x}$$

and so forth.

Hence it follows that

$A_{21} = A_{12}$, $A_{31} = A_{13}$, ... , $A_{65} = A_{56}$,

or, in general $A_{ij} = A_{ji}$ $(i,j = 1,2, \ldots ,6)$

Similar relations hold for the coefficients of deformation, i.e. $a_{ij} = a_{ji}$ $(i,j = 1,2, \ldots ,6)$.

4. The Elastic Potential

In the general case the expression for the elastic potential has the form:

$$\begin{aligned}\bar{V} = {} & \tfrac{1}{2}a_{11}\sigma_x^2 + a_{12}\sigma_x\sigma_y + a_{13}\sigma_x\sigma_z + a_{14}\sigma_x\, yz + a_{15}\sigma_x\tau_{xz} \\ & + a_{16}\sigma_x\tau_{xy} + \tfrac{1}{2}a_{22}\sigma_y^2 + a_{23}\sigma_y\sigma_z + a_{24}\sigma_y\,\tau_{yz} \\ & + a_{25}\sigma_y\tau_{xz} + a_{26}\sigma_y\tau_{xy} + \tfrac{1}{2}a_{33}\sigma_z^2 + a_{34}\sigma_z\tau_{yz}\end{aligned}$$

$$+ a_{35}\sigma_z\tau_{xz} + a_{36}\sigma_z\tau_{xy} + \tfrac{1}{2}a_{44}\tau_{yz}^2 + a_{45}\tau_{yz}\tau_{xz}$$

$$+ a_{46}\tau_{yz}\tau_{xy} + \tfrac{1}{2}a_{55}\tau_{xz}^2 + a_{56}\tau_{xz}\tau_{xy} + \tfrac{1}{2}a_{66}\tau_{xy}^2$$

Eq 3.8

Or, more briefly,

$$\overline{V} = \tfrac{1}{2}(\sigma_x\epsilon_x + \sigma_y\epsilon_y + \ \ldots \ + \tau_{xy}\gamma_{xy}) \qquad \text{Eq 3.9}$$

Or, in terms of the strains alone

$$\overline{V} = \tfrac{1}{2}A_{11}\epsilon_x^2 + A_{12}\epsilon_x\epsilon_y + \ \ldots \ + A_{16}\epsilon_x\gamma_{xy}$$

$$+ \tfrac{1}{2}A_{22}\epsilon_y^2 + \ \ldots \ + A_{26}\epsilon_y\gamma_{xy} + \ \ldots \ + \tfrac{1}{2}A_{66}\gamma_{xy}^2$$

Eq 3.10

We find the potential energy of deformation for the whole body by means of integration over its volume w:

$$V = \iiint_w \overline{V}\, dw \ .$$

5. The Technical Elastic Constants

The coefficients of deformation, a_{ij}, can be written in terms of the Young's moduli, Poisson coefficients and shear moduli

I. $a_{11} = \frac{1}{E_{xx}} \qquad a_{22} = \frac{1}{E_{yy}} \qquad a_{33} = \frac{1}{E_{zz}}$

II. $a_{12} = -\frac{\upsilon_{yx}}{E_{yy}} = -\frac{\upsilon_{xy}}{E_{xx}} \ , \qquad a_{23} = -\frac{\upsilon_{zy}}{E_{zz}} = -\frac{\upsilon_{yz}}{E_{yy}}$

$$a_{13} = -\frac{\upsilon_{xz}}{E_{xx}} = -\frac{\upsilon_{zx}}{E_{zz}}$$

III. $a_{44} = \frac{1}{G_{yz}} \qquad a_{55} = \frac{1}{G_{xz}} \qquad a_{66} = \frac{1}{G_{xy}}$

IV. $a_{56} = \frac{\mu_{xy,zx}}{G_{xz}} = \frac{\mu_{zx,xy}}{G_{xy}}$

$a_{46} = \frac{\mu_{xy,yz}}{G_{yz}} = \frac{\mu_{yz,xy}}{G_{xy}}$

$a_{45} = \frac{\mu_{zx,xy}}{G_{yz}} = \frac{\mu_{yz,zx}}{G_{xz}}$

V. $a_{14} = \frac{\eta_{yz,x}}{E_{xx}} = \frac{\eta_{x,yz}}{G_{yz}}$ $\qquad a_{25} = \frac{\eta_{zx,y}}{E_{yy}} = \frac{\eta_{y,zx}}{G_{xz}}$

$a_{36} = \frac{\eta_{xy,z}}{E_{zz}} = \frac{\eta_{z,xy}}{G_{xy}}$

VI. $a_{24} = \frac{\eta_{yz,y}}{E_{yy}} = \frac{\eta_{y,yz}}{G_{yz}}$ $\qquad a_{35} = \frac{\eta_{zx,z}}{E_{zz}} = \frac{\eta_{z,zx}}{G_{xz}}$

$a_{16} = \frac{\eta_{xy,x}}{E_{xx}} = \frac{\eta_{x,xy}}{G_{xy}}$ $\qquad a_{34} = \frac{\eta_{yz,z}}{E_{zz}} = \frac{\eta_{z,yz}}{G_{yz}}$

$a_{15} = \frac{\eta_{zx,x}}{E_{xx}} = \frac{\eta_{x,zx}}{G_{xz}}$ $\qquad a_{26} = \frac{\eta_{xy,y}}{E_{yy}} = \frac{\eta_{y,xy}}{G_{xy}}$

Here E_{xx}, E_{yy}, E_{zz} are the Young's moduli (for tension-compression with respect to the directions x,y,z; G_{yz}, G_{xz}, G_{xy} are the shear moduli for planes which are parallel to the coordinates yoz, xoz, xoy;

υ_{yx}, υ_{zy}, υ_{xz}, υ_{xy}, υ_{yz}, υ_{zx} are the Poisson coefficients which characterize the transverse compression for tension in the direction of the axis of the first coordinate (thus, υ_{yx} is a coefficient which characterizes the decrease in the x direction for tension in the y direction, and so on).

$\mu_{zx,yz}$, $\mu_{xy,yz}$, ... , $\mu_{yz,xy}$ we call the coefficients of Chentsov. They characterize the shear in the planes which are parallel to the coordinates and which induce tangential stresses parallel to the other coordinate planes.

Thus for example $\mu_{zx,yz}$ characterizes the shear in the plane parallel to the yz plane which induces the stress τ_{zx}, and so forth.

Finally, $\eta_{yz,x}$, $\eta_{zx,x}$, ... , $\eta_{xy,z}$ are called the coefficients of nutual influence of the first kind, and $\eta_{x,yz}$, $\eta_{y,yz}$, ... , $\eta_{z,xy}$ are called the coefficients of mutual influence of the second kind. The first characterize the stretching in the directions parallel to the axes which are induced by the tangential stresses; the second are shears in the planes parallel to the coordinates under the influence of normal stresses.

6. Elastic Symmetry

If the internal composition of a material possesses symmetry of any kind, then symmetry can be observed in its elastic properties. This can be extended to bodies with structural symmetry. If an anisotropic body possesses an elastic symmetry then the equations of the generalized Hooke's Law are simplified.

We find the simplifications by applying the following method. We refer the body to the first coordinate system X,Y,Z, and then to the second coordinate system X',Y',Z', which is symmetric to the first. Since the directions of similar axes of both systems are equivalent with respect to elastic properties, the equations of the generalized Hooke's Law and the expression of elastic potential will have the same form in both the first and second systems; the corresponding elastic constants entering into their composition also will be identical.

For the first system (X,Y,Z)

$$\overline{V} = \tfrac{1}{2}a_{11}\sigma_x^2 + a_{12}\sigma_x\sigma_y + \quad \ldots \quad + \tfrac{1}{2}a_{66}\tau_{xy}^2$$

For the second coordinate system (X',Y',Z')

$$\overline{V} = \tfrac{1}{2}a_{11}\sigma_x'^2 + a_{12}\sigma_x'\sigma_y' + \quad \ldots \quad + \tfrac{1}{2}a_{66}\tau_{xy}'^2$$

Since one and the same quantity is being discussed, we have

$$\tfrac{1}{2}a_{11}\sigma_x^2 + a_{12}\sigma_x\sigma_y + \quad \ldots \quad + \tfrac{1}{2}a_{66}\tau_{xy}^2$$

$$= \tfrac{1}{2}a_{11}\sigma_x'^2 + a_{12}\sigma_x'\sigma_y' + \quad \ldots \quad + \tfrac{1}{2}a_{66}\tau_{xy}'^2$$

We express σ_x', σ_y', ..., τ_{xy}' in terms of σ_x, σ_y, ..., τ_{xy}, using formulae of type (3.1). Equating coefficients for σ_x^2, $\sigma_x\sigma_y$, ..., τ_{xy}^2 in the left and right sides, we find that some coefficients a_{ij} are equal to zero and others are connected by definite relations. As a result, bodies possessing elastic symmetry have less than 21 independent elastic constants. Considering the elastic potential expressed in terms of the components of strain we can find the relationship between the moduli A_{ij} in the same way.

7. Elastic Symmetry in an Orthotropic Material

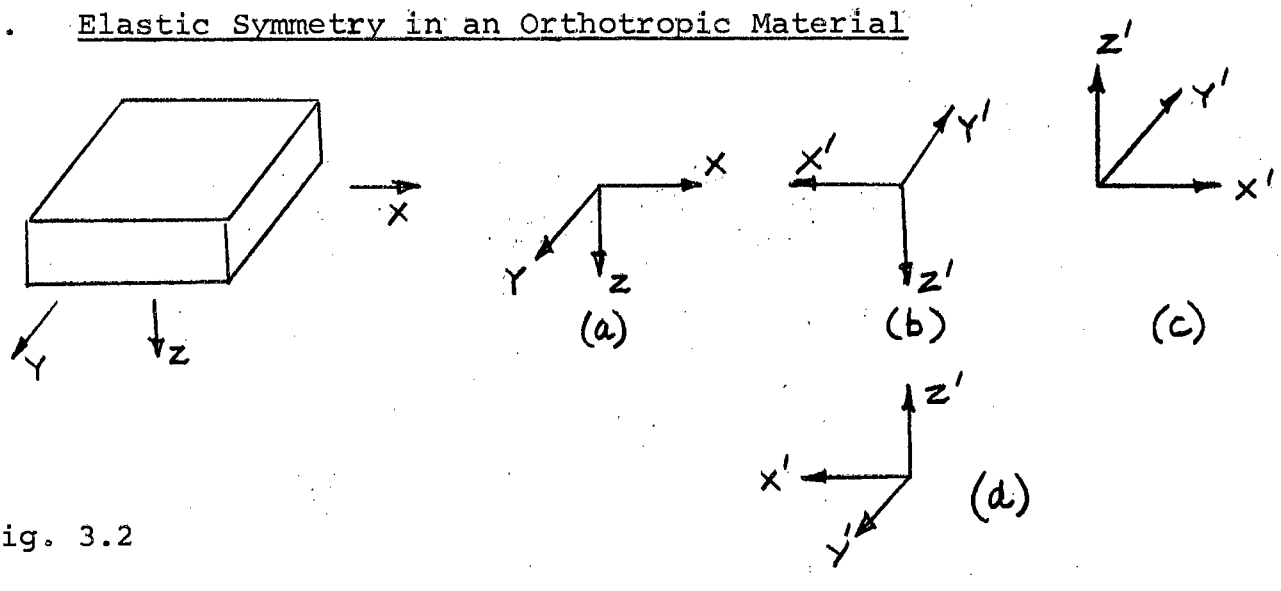

Fig. 3.2

Let X and Y be the principal directions in the orthotropic plate as in Fig. 3.2(a). It can be seen that the axis system (X,Y,Z) can be rotated in 3 possible ways (Fig. 3.2(b), (c), (d)) so that the new coordinate system (X',Y',Z') is equivalent with respect to elastic properties.

i. For the rotation from system 3.2(a) to 3.2(b) the table of direction cosines is:

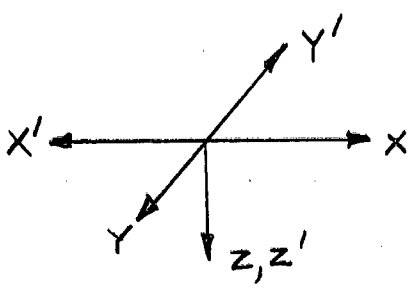

Fig. 3.3

	X	Y	Z
X'	-1	0	0
Y'	0	-1	0
Z'	0	0	1

From Eqs 3.1 we have

$$\sigma'_x = \sigma_x \qquad \tau'_{yz} = -\tau_{yz}$$

$$\sigma'_y = \sigma_y \qquad \tau'_{xz} = -\tau_{xz}$$

$$\sigma'_z = \sigma_z \qquad \tau'_{xy} = \tau_{xy}$$

Equating $\bar{V}$ for the two systems

$$\begin{aligned}\bar{V} = {} & \tfrac{1}{2}a_{11}\sigma_x^2 + a_{12}\sigma_x\sigma_y + a_{13}\sigma_x\sigma_z + a_{14}\sigma_x\tau_{yz} \\ & + a_{15}\sigma_x\tau_{xz} + a_{16}\sigma_x\tau_{xy} + \tfrac{1}{2}a_{22}\sigma_y^2 + a_{23}\sigma_y\sigma_z \\ & + a_{24}\sigma_y\tau_{yz} + a_{25}\sigma_y\tau_{xz} + a_{26}\sigma_y\tau_{xy} + \tfrac{1}{2}a_{33}\sigma_z^2 \\ & + a_{34}\sigma_z\tau_{yz} + a_{35}\sigma_z\tau_{xz} + a_{36}\sigma_z\tau_{xy} + \tfrac{1}{2}a_{44}\tau_{yz}^2 \\ & + a_{45}\tau_{yz}\tau_{xz} + a_{46}\tau_{yz}\tau_{xy} + \tfrac{1}{2}a_{55}\tau_{xz}^2 + a_{56}\tau_{xz}\tau_{xy} \\ & + \tfrac{1}{2}a_{66}\tau_{xy}^2\end{aligned}$$

$$= \tfrac{1}{2}a_{11}\sigma_x^2 + a_{12}\sigma_x\sigma_y + a_{13}\sigma_x\sigma_z - a_{14}\sigma_x\tau_{yz}$$
$$- a_{15}\sigma_x\tau_{xz} + a_{16}\sigma_x\tau_{xy} + \tfrac{1}{2}a_{22}\sigma_y^2 + a_{23}\sigma_y\sigma_z$$
$$- a_{24}\sigma_y\tau_{yz} - a_{25}\sigma_y\tau_{xz} + a_{26}\sigma_y\tau_{xy} + \tfrac{1}{2}a_{33}\sigma_z^2$$
$$- a_{34}\sigma_z\tau_{yz} - a_{35}\sigma_z\tau_{xz} + a_{36}\sigma_z\tau_{xy} + \tfrac{1}{2}a_{44}\tau_{yz}^2$$
$$+ a_{45}\tau_{yz}\tau_{xz} - a_{46}\tau_{yz}\tau_{xy}^2 + \tfrac{1}{2}a_{55}\tau_{xz} - a_{56}\tau_{xz}\tau_{xy}$$
$$+ \tfrac{1}{2}a_{66}\tau_{xy}^2$$

Equating coefficients of like terms:

$$a_{14} = a_{15} = a_{24} = a_{25} = a_{34} = a_{35} = a_{46} = a_{56} = 0$$

ii. For the rotation from system 3.2(a) to 3.2(c) the table of direction cosines is:

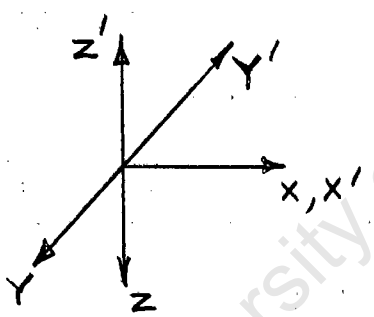

	X	Y	Z
X'	1	0	0
Y'	0	-1	0
Z'	0	0	-1

Fig. 3.4

From Eqs 3.1 we have

$$\sigma'_x = \sigma_x \qquad \tau'_{yz} = \tau_{yz}$$
$$\sigma'_y = \sigma_y \qquad \tau'_{xz} = -\tau_{xz}$$
$$\sigma'_z = \sigma_z \qquad \tau'_{xy} = -\tau_{xy}$$

Proceeding as in i. above this yields:

$$a_{15} = a_{16} = a_{25} = a_{26} = a_{35} = a_{36} = a_{45} = a_{46} = 0$$

iii. For the rotation from 3.2(a) to 3.2(d) no new information emerges because iii. can be seen to be the sum of rotations i. and ii.

For an orthotropic material in which the axis system (X,Y,Z) corresponds to the directions of principal stiffness the matrix of coefficients of deformation therefore simplifies to:

$$[a_{ij}] = \begin{bmatrix} a_{11} & a_{12} & a_{13} & 0 & 0 & 0 \\ & a_{22} & a_{23} & 0 & 0 & 0 \\ & & a_{33} & 0 & 0 & 0 \\ & & & a_{44} & 0 & 0 \\ \text{SYM} & & & & a_{55} & 0 \\ & & & & & a_{66} \end{bmatrix}$$

The moduli of elasticity, A_{ij}, can be found in the same manner as a_{ij}. The elastic potential is expressed in terms of the components of strain instead of stress; this is the only difference. The simplified matrix of moduli of elasticity becomes:

$$[A_{ij}] = \begin{bmatrix} A_{11} & A_{12} & A_{13} & 0 & 0 & 0 \\ & A_{22} & A_{23} & 0 & 0 & 0 \\ & & A_{33} & 0 & 0 & 0 \\ & & & A_{44} & 0 & 0 \\ \text{SYM} & & & & A_{55} & 0 \\ & & & & & A_{66} \end{bmatrix}$$

8. The Transformation of Elastic Constants under a transformation of the coordinate system

The elastic constants which enter into equations of the generalized Hooke's Law of an anisotropic body depend on the direction of the axes of the coordinate system. If the direction of the axes varies, then the elastic constants vary. Only in the case of an isotropic body are the constants invariant in any orthogonal coordinate system. When studying the state of stress of an anisotropic body the following question arises: if we know the elastic constants expressed in one coordinate system, what are the corresponding constants in another more convenient system?

This question can be answered by applying the method already used for the simplification of the expressions of the elastic potential and for the equations of the generalized Hooke's Law when elastic symmetry is present. Let the elastic constants for the system X,Y,Z be known. It is required to determine the constants in the new system X',Y',Z'. The position of the new system with respect to the old is defined by the table of direction cosines. We write the expressions for the elastic potential $\overline{V}$ expressed in the systems X,Y,Z and X',Y',Z'. By equating these expressions, we obtain an equation on the left side of which are the components of stress or strain in the old system; on the right side are the same quantities for the new system. We express the components of stress or strain in the old coordinate system in terms of the components of stress or strain in the new coordinate system. Comparing the coefficients of the squares and products of the components

of stress or strain referred to the new system we obtain the desired formulae for the new elastic constants on the left and right sides of the equation.

We are primarily interested in the transformation of the moduli of elasticity, A_{ij}, since they enter into the equations for bending and twisting moments. The transformation of a_{ij} will be given here but not derived.

Let the system X,Y,Z be that of the principal stiffnesses. In this system the planes XZ, XY and YZ are all planes of elastic symmetry. In the new system X',Y',Z', where Z' corresponds to Z, there is only one plane of elastic symmetry, which is the XY plane. The matrix of the moduli of elasticity is that corresponding to rotation i. in Section 8 above, and is:

$$\left[A'_{ij}\right] = \begin{bmatrix} A'_{11} & A'_{12} & A'_{13} & 0 & 0 & A'_{16} \\ & A'_{22} & A'_{23} & 0 & 0 & A'_{26} \\ & & A'_{33} & 0 & 0 & A'_{36} \\ & & & A'_{44} & A'_{45} & 0 \\ \text{SYM} & & & & A'_{55} & 0 \\ & & & & & A'_{66} \end{bmatrix}$$

The table of direction cosines for the rotation about the Z axis is:

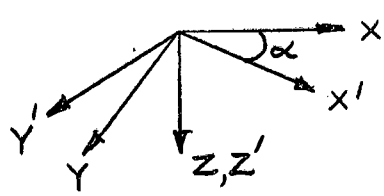

	x	y	z
x'	cos α	sin α	0
y'	-sin α	cos α	0
z'	0	0	1

Fig. 3.5

We have

$$\begin{aligned}\bar{\bar{V}} &= \tfrac{1}{2}A_{11}\epsilon_x^2 + A_{12}\epsilon_x\epsilon_y + A_{13}\epsilon_x\epsilon_z + \tfrac{1}{2}A_{22}\epsilon_y^2 \\ &\quad + A_{23}\epsilon_y\epsilon_z + \tfrac{1}{2}A_{33}\epsilon_z^2 + \tfrac{1}{2}A_{44}\gamma_{yz}^2 + \tfrac{1}{2}A_{55}\gamma_{xz}^2 \\ &\quad + \tfrac{1}{2}A_{66}\gamma_{xy}^2 \\ &= \tfrac{1}{2}A'_{11}\epsilon_x'^2 + A'_{12}\epsilon_x'\epsilon_y' + A'_{13}\epsilon_x'\epsilon_z' + A'_{16}\epsilon_x'\gamma_{xy}' \\ &\quad + \tfrac{1}{2}A'_{22}\epsilon_y'^2 + A'_{23}\epsilon_y'\epsilon_z' + A'_{26}\epsilon_y'\gamma_{xy}' + \tfrac{1}{2}A'_{33}\epsilon_z'^2 \\ &\quad + A'_{36}\epsilon_z'\gamma_{xy}' + \tfrac{1}{2}A'_{44}\gamma_{yz}'^2 + A'_{45}\gamma_{yz}'\gamma_{xz}' + \tfrac{1}{2}A'_{55}\gamma_{xz}'^2 \\ &\quad + \tfrac{1}{2}A'_{66}\gamma_{xy}'^2 \quad .\end{aligned}$$

From the table of direction cosines

$$\epsilon_x = \epsilon_x' \cos^2\alpha + \epsilon_y' \sin^2\alpha - \gamma_{xy}' \cos\alpha\sin\alpha$$

$$\epsilon_y = \epsilon_x' \sin^2\alpha + \epsilon_y' \cos^2\alpha + \gamma_{xy}' \cos\alpha\sin\alpha$$

$$\epsilon_z = \epsilon_z'$$

$$\gamma_{yz} = \gamma_{yz}' \cos\alpha + \gamma_{xz}' \sin\alpha$$

$$\gamma_{xz} = -\gamma_{yz}' \sin\alpha + \gamma_{xz}' \cos\alpha$$

$$\gamma_{xy} = 2\epsilon_x' \cos\alpha\sin\alpha - 2\epsilon_y' \cos\alpha\sin\alpha + \gamma_{xy}' (\cos^2\alpha - \sin^2\alpha)$$

Substituting these into the expression for $\bar{\bar{V}}$, we get the following relationships between A'_{ij} and A_{ij}:

$$A'_{11} = A_{11}\cos^4\alpha + (2A_{12} + 4A_{66})\cos^2\alpha\sin^2\alpha + A_{22}\sin^4\alpha$$

$$A'_{12} = A_{12}(\cos^4\alpha + \sin^4\alpha) + (A_{11} - 4A_{66} + A_{22})\cos^2\alpha\sin^2\alpha$$

$$A'_{13} = A_{13}\cos^2\alpha + A_{23}\sin^2\alpha$$

$$A'_{16} = \left[-A_{11}\cos^2\alpha + A_{22}\sin^2\alpha + (A_{12} + 2A_{66})\cos 2\alpha\right] \frac{\sin 2\alpha}{2}$$

$$A'_{22} = A_{11}\sin^4\alpha + (2A_{12} + 4A_{66})\cos^2\alpha\sin^2\alpha + A_{22}\sin^4\alpha$$

$$A'_{23} = A_{13}\sin^2\alpha + A_{23}\cos^2\alpha$$

$$A'_{26} = \left[-A_{11}\sin^2\alpha + A_{22}\cos^2\alpha - (A_{12} + 2A_{66})\cos 2\alpha\right] \frac{\sin 2\alpha}{2}$$

$$A'_{33} = A_{33}$$

$$A'_{36} = (A_{23} - A_{13})\cos\alpha\sin\alpha$$

$$A'_{44} = A_{44}\cos^2\alpha + A_{55}\sin^2\alpha$$

$$A'_{45} = (A_{44} - A_{55})\cos\alpha\sin\alpha$$

$$A'_{55} = A_{44}\sin^2\alpha + A_{55}\cos^2\alpha$$

$$A'_{66} = A_{66}\cos^2 2\alpha + (A_{11} - 2A_{12} + A_{22})\cos^2\alpha\sin^2\alpha$$

Eqs 3.11

The relationships between the coefficients of deformation, a'_{ij}, in the system X',Y',Z' and a_{ij} in the system X,Y,Z can be derived as for the moduli of elasticity A_{ij}. The only difference is that $\bar{V}$ must be expressed in terms of the components of stress instead of strain. The transformation rules are as follows:

$$a'_{11} = a_{11}\cos^4\alpha + (2a_{12} + a_{66})\cos^2\alpha\sin^2\alpha + a_{22}\sin^4\alpha$$

$$a'_{12} = a_{12}(\cos^4\alpha + \sin^4\alpha) + (a_{11} + a_{22} - a_{66})\cos^2\alpha\sin^2\alpha$$

$$a'_{13} = a_{13}\cos^2\alpha + a_{23}\sin^2\alpha$$

$$a'_{16} = \left[-2a_{11}\cos^2\alpha + 2a_{22}\sin^2\alpha + (2a_{12} + a_{66})\cos 2\alpha\right] \frac{\sin 2\alpha}{2}$$

$$a'_{22} = a_{11}\sin^4\alpha + (2a_{12} + a_{66})\cos^2\alpha\sin^2\alpha + a_{22}\cos^4\alpha$$

$$a'_{23} = a_{13}\sin^2\alpha + a_{23}\cos^2\alpha$$

$$a'_{26} = \left[-2a_{11}\sin^2\alpha + 2a_{22}\cos^2\alpha - (2a_{12} + a_{66})\cos 2\alpha\right] \cdot \frac{\sin 2\alpha}{2}$$

$$a'_{33} = a_{33}$$

$$a'_{36} = 2(a_{23} - a_{13})\cos\alpha\sin\alpha$$

$$a'_{44} = a_{44}\cos^2\alpha + a_{55}\sin^2\alpha$$

$$a'_{55} = a_{44}\sin^2\alpha + a_{55}\cos^2\alpha$$

$$a'_{66} = a_{66}\cos^2 2\alpha + 4(a_{11} - 2a_{12} + a_{22})\cos^2\alpha\sin^2\alpha$$

Eqs 3.12

The moduli of elasticity A'_{ij} correspond to a general set of axes X',Y',Z' but where X' and Y' always lie in the plane of the plate. It can be seen from Eqs 3.11 that in the special case where X' and Y' are the principal elastic directions, then $\alpha = 0$ and

$$A'_{16} = A'_{26} = A'_{36} = A'_{45} = 0$$

and for the other moduli

$$A'_{ij} = A_{ij} .$$

9. Moments in thin orthotropic plates

In the bending theory of thin orthotropic plates, the stress σ_z is taken as zero since it must be zero on the surface of the plate, and is assumed not to build up to an amount which will affect the strains ϵ_x, ϵ_y, and γ_{xy}. This means that the values of a_{13}, a_{23}, a_{33} are not used in analysis, and this in turn means that the values of A_{13}, A_{23}, A_{33} are not used. It also means that A_{11}, A_{12}, A_{22} have their values altered. To show this consider the X,Y,Z

system for which the alternative matrices of a_{ij} are

$$[a_{ij}] = \begin{bmatrix} a_{11} & a_{12} & a_{13} & 0 & 0 & 0 \\ & a_{22} & a_{23} & 0 & 0 & 0 \\ & & a_{33} & 0 & 0 & 0 \\ & & & a_{44} & 0 & 0 \\ \text{SYM} & & & & a_{55} & 0 \\ & & & & & a_{66} \end{bmatrix} \quad \text{or} \quad \begin{bmatrix} a_{11} & a_{12} & 0 & 0 & 0 \\ & a_{22} & 0 & 0 & 0 \\ & & a_{44} & 0 & 0 \\ \text{SYM} & & & a_{55} & 0 \\ & & & & a_{66} \end{bmatrix}$$

Here the values of a_{ij} are as given in section 5. The values of A_{ij} are now found by $[A_{ij}] = [a_{ij}]^{-1}$. Comparing values of A_{ij} for the alternatives:

	Thin plate		Orthotropic body
A_{11} =	$\frac{E_x}{(1-\upsilon_{xy}\upsilon_{yx})}$	or	$\frac{E_x(1-\upsilon_{yz}\upsilon_{zy})}{(1-\upsilon_{yz}\upsilon_{zy}-\upsilon_{xy}\upsilon_{yx}-\upsilon_{xz}\upsilon_{zx}-2\upsilon_{xy}\upsilon_{yz}\upsilon_{zx})}$
A_{12} =	$\frac{E_x\upsilon_{yx}}{(1-\upsilon_{xy}\upsilon_{yx})}$	or	$\frac{E_x(\upsilon_{yx}-\upsilon_{zx}\upsilon_{yz})}{(1-\upsilon_{yz}\upsilon_{zy}-\upsilon_{xy}\upsilon_{yx}-\upsilon_{xz}\upsilon_{zx}-2\upsilon_{xy}\upsilon_{yz}\upsilon_{zx})}$
A_{22} =	$\frac{E_y}{(1-\upsilon_{xy}\upsilon_{yx})}$	or	$\frac{E_y(1-\upsilon_{xz}\upsilon_{zx})}{(1-\upsilon_{yz}\upsilon_{zy}-\upsilon_{xy}\upsilon_{yx}-\upsilon_{xz}\upsilon_{zx}-2\upsilon_{xy}\upsilon_{yz}\upsilon_{zx})}$
A_{66} =	G_{xy}	or	G_{xy}

In the thin plate theory the stresses become

$$\sigma_x = A_{11}\,\epsilon_x + A_{12}\,\epsilon_y$$

$$\sigma_y = A_{12}\,\epsilon_x + A_{22}\,\epsilon_y$$

$$\tau_{xy} = A_{66}\,\gamma_{xy}$$

The moments become

$$M_x = \int_{-h/2}^{h/2} \sigma_x \, z \, dz = -\left(D_{11} \frac{d^2w}{dx^2} + D_{12} \frac{d^2w}{dy^2} \right)$$

$$M_y = \int_{-h/2}^{h/2} \sigma_y \, z \, dz = -\left(D_{22} \frac{d^2w}{dy^2} + D_{12} \frac{d^2w}{dx^2} \right)$$

$$M_{xy} = \int_{-h/2}^{h/2} \tau_{xy} \, z \, dz = 2D_{66} \frac{d^2w}{dxdy}$$

where $D_{ij} = A_{ij} \frac{h^3}{12}$

The assumption that σ_z is zero therefore not only has the effect of removing a term from the equations for M_x and M_y, but also changes the values of D_{11}, D_{12} and D_{22}. In general the Poisson's ratios υ_{xz}, υ_{zx}, υ_{yz} and υ_{zy} are not equal to zero. One would expect the terms $\upsilon_{yz}\upsilon_{zy}$ and $\upsilon_{xz}\upsilon_{zx}$ to be of the same order as $\upsilon_{xy}\upsilon_{yx}$. Provided that none of the Poisson's ratios is negative, it can be seen that the thin plate theory underestimates the values of D_{11}, D_{12} and D_{22}. This is an error on the safe side if one is calculating the deflections.

The moment equations in the system X',Y',Z' are derived as follows in the thin plate theory

$$\sigma'_x = A'_{11} \epsilon'_x + A'_{12} \epsilon'_y + A'_{16} \gamma'_{xy}$$

$$\sigma'_y = A'_{12} \epsilon'_x + A'_{22} \epsilon'_y + A'_{26} \gamma'_{xy}$$

$$\tau'_{xy} = A'_{16} \epsilon'_x + A'_{26} \epsilon'_y + A'_{66} \gamma'_{xy}$$

$\therefore$ with the sign conventions as shown in Figs. 1.4, 1.5

$$M'_x = \int_{-h/2}^{h/2} \sigma'_x \, z \, dz = -\left(D'_{11} \frac{d^2w}{dx^2} + D'_{12} \frac{d^2w}{dy^2} + 2D'_{16} \frac{d^2w}{dxdy} \right)$$

$$M'_y = \int_{-h/2}^{h/2} \sigma'_y \, z \, dz = -\left(D'_{22} \frac{d^2w}{dy^2} + D'_{12} \frac{d^2w}{dx^2} + 2D'_{26} \frac{d^2w}{dxdy} \right)$$

$$M'_{xy} = -\int_{-h/2}^{h/2} \tau'_{xy} \, z \, dz = D'_{16} \frac{d^2w}{dx^2} + D'_{26} \frac{d^2w}{dy^2} + 2D'_{66} \frac{d^2w}{dxdy}$$

$$= M'_{yx}$$

10. Mohr's circle for moments

The stresses in the system X',Y',Z' are from Eqs 3.1

$$\sigma'_x = \sigma_x \cos^2\alpha + \sigma_y \sin^2\alpha + 2\tau_{xy} \cos\alpha \sin\alpha$$

$$\sigma'_y = \sigma_x \sin^2\alpha + \sigma_y \cos^2\alpha - 2\tau_{xy} \cos\alpha \sin\alpha$$

$$\tau'_{xy} = -\sigma_x \cos\alpha \sin\alpha + \sigma_y \cos\alpha \sin\alpha + \tau_{xy} (\cos^2\alpha - \sin^2\alpha)$$

These can be rewritten as

$$\sigma'_x = \frac{\sigma_y + \sigma_y}{2} + \frac{(\sigma_x - \sigma_y)}{2} \cos 2\alpha + \tau_{xy} \sin 2\alpha$$

$$\sigma'_y = \frac{\sigma_x + \sigma_y}{2} - \frac{(\sigma_x - \sigma_y)}{2} \cos 2\alpha - \tau_{xy} \sin 2\alpha$$

$$\tau'_{xy} = -\frac{(\sigma_x - \sigma_y)}{2} \sin 2\alpha + \tau_{xy} \cos 2\alpha$$

From the above the moments become

$$M'_x = \frac{(M_x + M_y)}{2} + \frac{(M_x - M_y)}{2} \cos 2\alpha - M_{xy} \sin 2\alpha$$

$$M'_y = \frac{(M_x + M_y)}{2} - \frac{(M_x - M_y)}{2}\cos 2\alpha + M_{xy}\sin 2\alpha$$

$$M'_{xy} = \frac{(M_x - M_y)}{2}\sin 2\alpha + M_{xy}\cos 2\alpha \qquad \text{Eqs 3.13}$$

The above moment equations have certain differences in the signs from the stress equations because of the way the moments and stresses were defined in Figs. 1.4, 1.5. These moment formulae can be represented by a Mohr circle construction as shown in Fig. 3.6. The form of M'_x, M'_y and M'_{xy} can be seen to be satisfied by rotating triangle OAB through an angle of 2α to positon OA'B'.

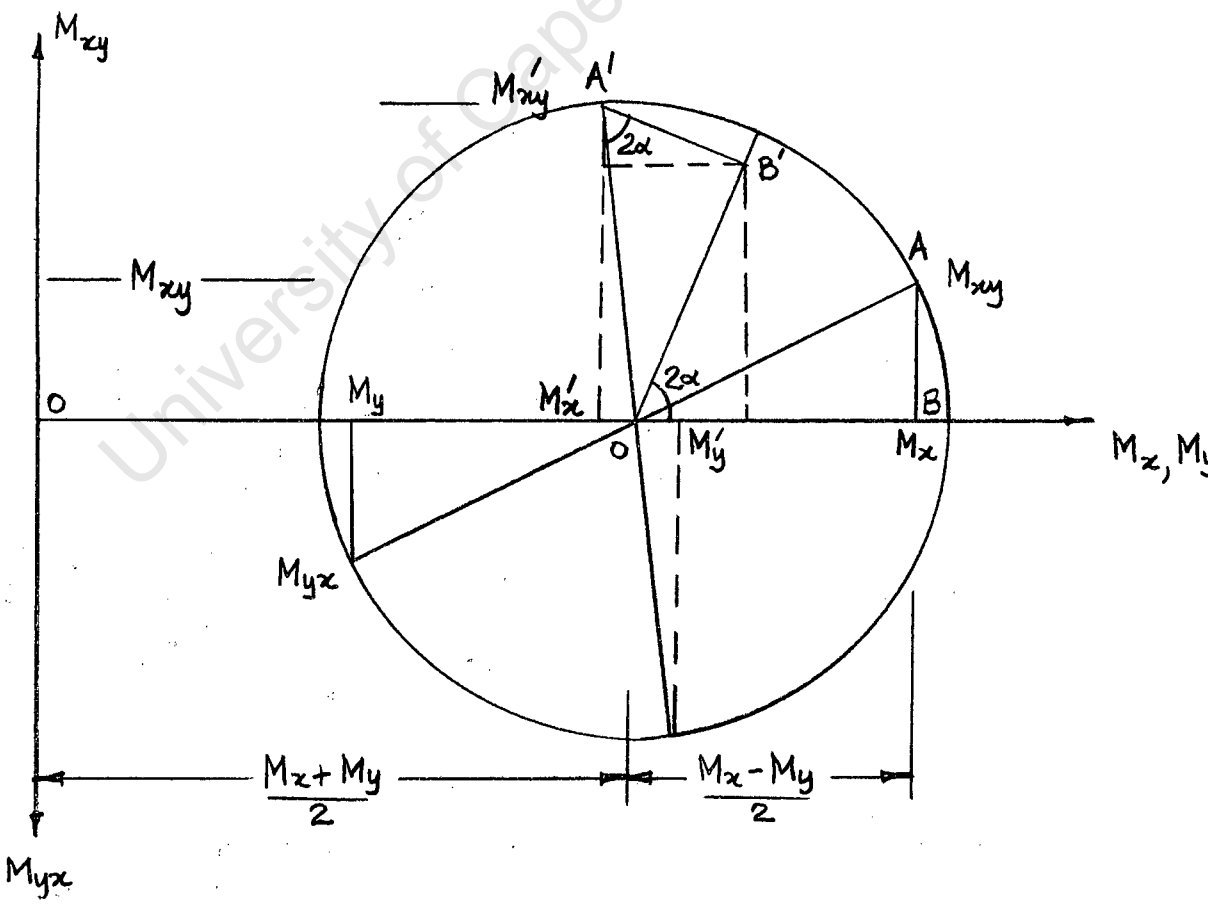

Fig. 3.6

When $M'_{xy} = 0$, then M'_x, M'_y are the principal bending moments, and the angle α is defined by

$$\tan 2\alpha = -\frac{2M_{xy}}{(M_x - M_y)}$$

The principal bending moments can be found from

$$M_{max},\ M_{min} = \frac{M_x + M_y}{2} \pm \sqrt{\left(\frac{M_x - M_y}{2}\right)^2 + \left(M_{xy}\right)^2}\ .$$

CHAPTER 4

EXPERIMENTAL METHODS OF FINDING THE RIGIDITIES

From a study of the literature it appears that only one method of finding the rigidities of an orthotropic plate has been used. This involves a twisting test and a minimum of two bending tests, and was developed by Bergsträsser (Ref. 24) in 1927. A minimum of three models is needed to determine all the rigidities D_x, D_y, D_1 and D_{xy}. This method will be described below.

The time taken to make a model is considerable if it is to be well made. The writer accordingly has devised a method for which only one model is needed to measure all the rigidities. This method, however, also has its limitations as will be seen.

1. Bergsträsser's Method

This method is described by Hearmon and Adams (Ref. 25) who used it for tests on plywood plates.

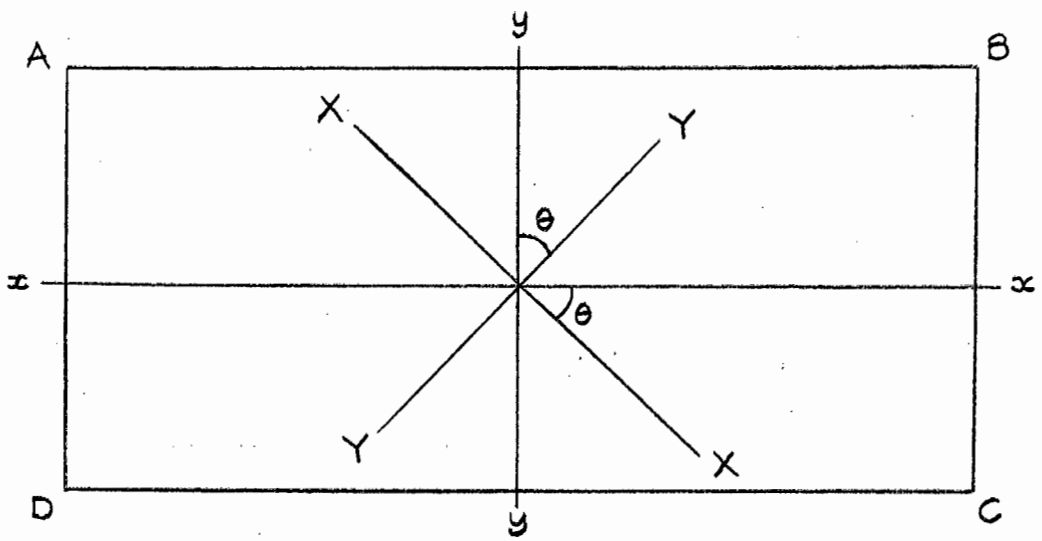

Fig. 4.1

Consider a plate ABCD cut from orthotropic material. Suppose the plate is subjected to uniform bending moments M_x per unit length of side along AD,BC, M_y per unit length along AB,CD and a uniform twisting moment M_{xy} per unit length along all four sides. The general expression for the deflection of a thin plate subject to these conditions is

$$\begin{aligned} h^3 w &= 6M_x (a'_{11}x^2 + a'_{12}y^2 + a'_{16}xy) \\ &\quad + 6M_y (a'_{12}x^2 + a'_{22}y^2 + a'_{26}xy) \\ &\quad + 6M_{xy}(a'_{16}x^2 + a'_{26}y^2 + a'_{66}xy) \end{aligned} \qquad \text{Eq 4.1}$$

where w is the small deflection, normal to the plane of the plate, of the point x,y relative to the origin of coordinates, where h is the plate thickness, and where a_{ij} are as defined in Eqs 3.12.

When $\theta = 0$ ($a'_{16} = a'_{26} = 0$) and when $M_{xy} = 0$, the deflection is symmetrical about the lines $x = 0$, $y = 0$, and antisymmetrical about these lines when $M_x = M_y = 0$, and $M_{xy} \neq 0$. The first case corresponds with pure bending, and the second with pure torsion.

When $\theta \neq 0$, then $a'_{16} \neq 0$, $a'_{26} \neq 0$ and, if $M_{xy} = 0$, some twisting will occur owing to the existence of the terms $a'_{16}xy$ and $a'_{26}xy$ in Eq 4.1. Similarly, if $M_x = M_y = 0$, some symmetrical bending will occur owing to the presence of the terms $a'_{16}x^2$ and $a'_{26}y^2$.

The Bending Test

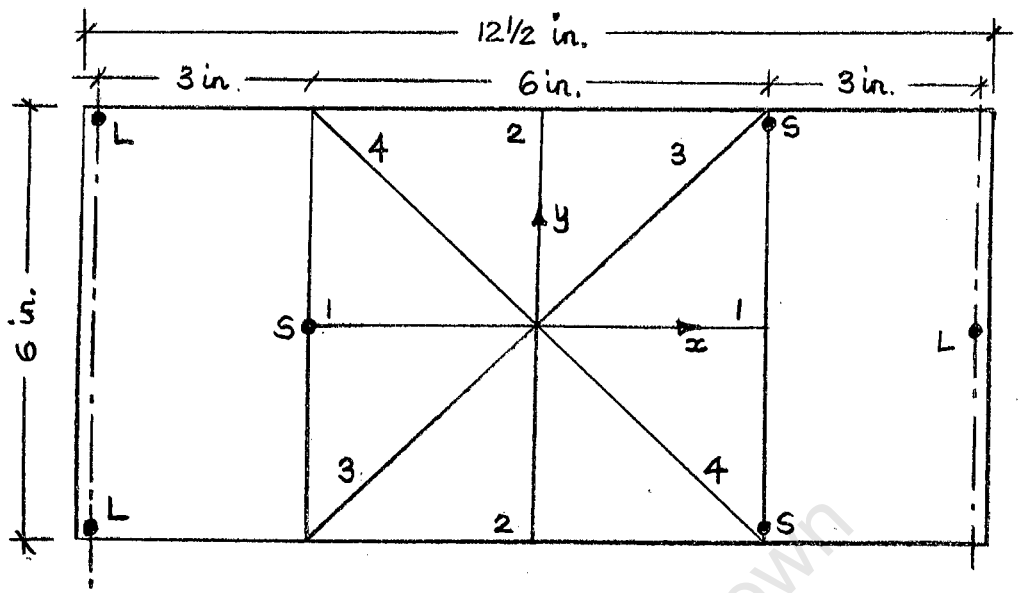

Fig. 4.2

The plate and its loading and support points are shown in Fig. 4.2. Ball-bearings provide support at the points S, and the load is applied at points L by the method shown in Fig. 4.3.

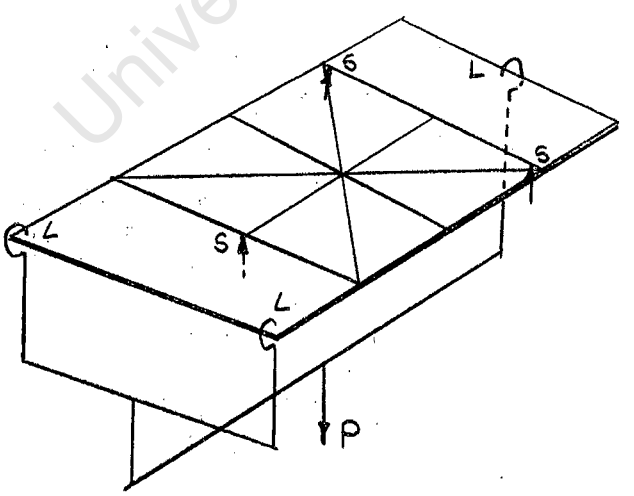

Fig. 4.3

This loading is considered to provide a uniform moment per

unit length $M_x = \frac{P}{2}.\frac{3}{6} = \frac{P}{4}$ in the centre of the plate. The moments M_y and M_{xy} are considered to be zero in the same region. Deflections are measured along the lines 1.,2.,3.,4. by means of the apparatus shown in Fig. 4.4. The foot of the gauge B is placed

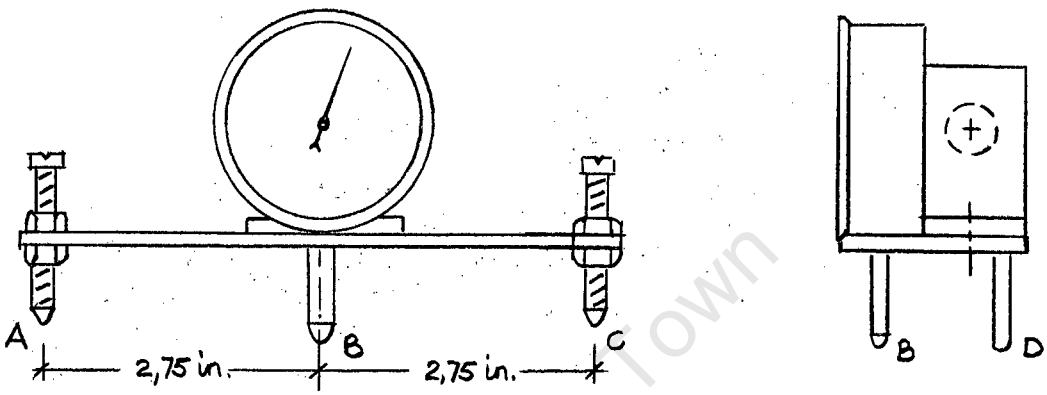

Fig. 4.4

on the central point of the plate; the feet A and C are placed along the required line; and foot D is used to steady the platform.

Now if a bending moment M_x (= P/4) only is applied to the plate ($M_y = M_{xy} = 0$) Eq 4.1 becomes

$$h^3w = 6M_x (a'_{11}x^2 + a'_{12}y^2 + a'_{16}xy)$$

Along line 1.:

$$x = 2,75 \text{ in}, \quad y = 0 \quad \therefore a'_{11} = \frac{wh^3}{11,35P}$$

Along line 2.:

$$x = 0, \quad y = 2,75 \text{ in} \quad \therefore a'_{12} = \frac{wh^3}{11,35P}$$

Along line 3.:

$$x = y = 2{,}75/\sqrt{2} \qquad \therefore a'_{11} + a'_{12} + a'_{16} = \frac{wh^3}{5{,}67P}$$

Along line 4.:

$$x = y = 2{,}75/\sqrt{2} \qquad \therefore a'_{11} + a'_{12} - a'_{16} = \frac{wh^3}{5{,}67P}$$

In the case $\theta = 0^\circ$

$$a'_{11} = a_{11} \; ; \; a'_{12} = a_{12} \; ; \; a'_{16} = 0$$

In the case $\theta = 90^\circ$

$$a'_{11} = a_{22} \; ; \; a'_{12} = a_{12} \; ; \; a'_{16} = 0$$

Notice that to find values of a_{11}, a_{12} and a_{22} a minimum of two models is needed. The simplest two values of θ to use are $\theta = 0^\circ$ and $\theta = 90^\circ$. Measurements along lines 3. and 4. are redundant; they can be taken to give better average results but are not necessary.

A strong recommendation for this bending test is that the plate is in pure bending when $\theta = 0^\circ$ or 90°. There are thus no extra terms in the theoretical formulae for D_x, D_y and D_1 according to the 8th order theory of Massonnet (Eqs 2.30 to 2.32), when asymmetrically stiffened plates are tested.

Hearmon and Adams tested three types of plywood using $\theta = 0^\circ$, $22\frac{1}{2}^\circ$, 45°, $67\frac{1}{2}^\circ$ and 90° for each. They measured deflections along all four lines 1.,2.,3.,4. . There were thus many measurements and the redundant ones along lines 3. and 4. agreed quite well with the results for lines 1. and 2. They estimate the uncertainty in the average results to be a maximum of 3%.

Note that the flexural rigidities can be calculated from

the constants a_{11}, a_{12} and a_{22} by

$$A_{11} = \frac{a_{22}}{a_{11}a_{22}-a_{12}^2} \quad ; \quad A_{12} = \frac{-a_{12}}{a_{11}a_{22}-a_{12}^2} \quad ; \quad A_{22} = \frac{a_{11}}{a_{11}a_{22}-a_{12}^2}$$

and $D_{ij} = A_{ij} \frac{h^3}{12}$.

Hoppmann (Ref. 21) did tests on three types of asymmetrically stiffened plates using the method described above. He found a_{12} and a_{21} separately, and they compare very badly. To show the relative discrepancies his results are given below in Table 4.1.

Type of stiffener	$\frac{a_{11}}{h^3} 10^6$	$\frac{a_{12}}{h^3} 10^6$	$\frac{a_{21}}{h^3} 10^6$	$\frac{a_{22}}{h^3} 10^6$
Brass rod	9,7	0,06	- 4,9	13,9
Grooved steel plate	24,5	- 8,55	- 9,3	33,5
Grooved duralumin	90	-12,8	-39,2	612

Table 4.1

Here h is the thickness of an equivalent true orthotropic plate, which need not be defined. Units are $(\text{lb in.})^{-1}$.

However in a later paper (Ref. 26) in tests on two more plates he obtained much closer values of a_{12} and a_{21}. These are shown in Table 4.2.

Type of stiffener	$\frac{a_{11}}{h^3}\ 10^6$	$\frac{a_{12}}{h^3}\ 10^6$	$\frac{a_{21}}{h^3}\ 10^6$	$\frac{a_{22}}{h^3}\ 10^6$
Groove one side	2,67	-0,76	-0,73	3,37
Groove two sides	3,96	-1,77	-1,69	7,90

Table 4.2

The results in Table 4.1 do suggest that a_{12} and a_{21} or D_{12} and D_{21} are not as well defined in this test as a_{11} and a_{22} or D_x and D_y are. In other words the test is not as sensitive to these elastic constants as one would like.

The Twisting Test

The method used is illustrated in Fig. 4.5. The test plates are square measuring 6 x 6 in. The deflections are measured exactly as in the bending test.

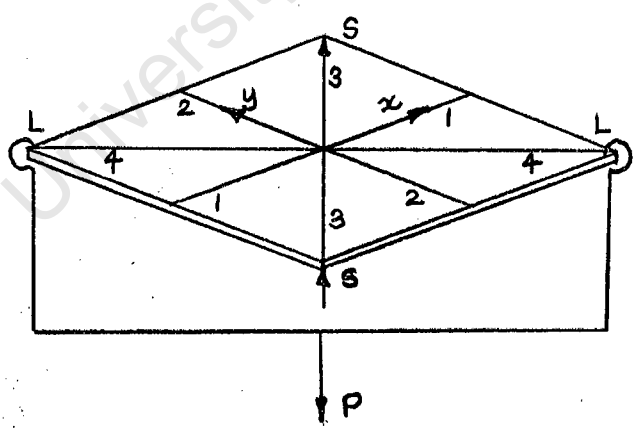

Fig. 4.5

The plate is loaded on diagonally opposite corners and supported on ball-bearings at the other two corners. The theory of this method of loading is given by Timoshenko (Ref. 1) and shows that the concentrated loads P/2 at each

corner produce a torsional moment M_{xy} per unit length along each side equal to P/4. Hence from Eq 4.1

$$2h^3w = 3P\,(a'_{16}x^2 + a'_{26}y^2 + a'_{66}xy)$$

Along line 1.: $a'_{16} = \frac{wh^3}{11,35P}$

Along line 2.: $a'_{26} = \frac{wh^3}{11,35P}$

Along line 3.: $a'_{16} + a'_{26} + a'_{66} = \frac{wh^3}{5,67P}$

Along line 4.: $a'_{16} + a'_{26} - a'_{66} = \frac{wh^3}{5,67P}$

For the case $\theta = 0^\circ$ or 90°, there should be no deflection along lines 1. and 2.

Along line 3.: $a_{66} = \frac{wh^3}{5,67P}$

Along line 4.: $a_{66} = -\frac{wh^3}{5,67P}$

It can be seen that a minimum of one measurement is needed to find a_{66}, and obviously only one plate is needed.

Then $A_{66} = \frac{1}{a_{66}}$

and $2D_{xy} = A_{66}\frac{h^3}{12}$

In general this is an accurate, simple test. It also has the advantage that, by the 8th order theory of Massonnet, the theoretical formula for D_{xy} is the same as that for the 4th order theory (see Eq 2.37). In other words, for an asymmetrically stiffened plate, the eccentricity of the ribs does not cause extra terms to be added to the theoretical formula for D_{xy}.

2. Another Method

The method given below was developed by the writer who was trying to find a way of determining the rigidities using only one model instead of three. This was done eventually and used for the experimental work in this thesis, and is described in section 3. of this chapter. Other investigators might be tempted to pursue an approach described in this section (section 2.) which appears promising at first. It is shown, however, that this approach still requires more than one model for testing.

First of all it should be pointed out that, in the method in section 1. above, it is not necessary to determine the constants a_{11}, a_{12}, a_{21} and a_{22} and then to calculate D_x, D_{12}, D_{21} and D_y from them. The rigidities can be found more directly as follows. Considering an asymmetrically stiffened plate, in Fig. 4.2 let the stiffeners run parallel to line 1. (i.e. $\theta = 0$). Then at the centre of the plate we can say

$$M_x = \frac{P}{4} = D_x \frac{d^2w}{dx^2} + D_{12} \frac{d^2w}{dy^2}$$

$$M_y = 0 = D_y \frac{d^2w}{dy^2} + D_{21} \frac{d^2w}{dx^2}$$

The values of $\frac{d^2w}{dx^2}$ and $\frac{d^2w}{dy^2}$ can be measured experimentally, and so we have two equations in the four unknowns D_x, D_{12}, D_{21} and D_y.

Now let the stiffeners run parallel to the y direction in Fig. 4.2 (i.e. $\theta = 90$), and we can say

$$M_y = \frac{P}{4} = D_y \frac{d^2w}{dy^2}' + D_{21} \frac{d^2w}{dx^2}'$$

$$M_x = 0 = D_x \frac{d^2w}{dx^2}' + D_{12} \frac{d^2w}{dy^2}'$$

The values of $\frac{d^2w}{dx^2}'$ and $\frac{d^2w}{dy^2}'$ are again measured, and now we have four independent equations in the four unknowns, which can be solved. The only experimental difference between the method of section 1. and this method is that deflections are measured in the former and curvatures in the latter.

An approach to a method of finding the rigidities is seen by considering the twisting test (Fig. 4.5). Although it is used in section 1. to measure a_{66} (or D_{xy}) only, the plate does bend as well. If the principal directions of stiffness (X,Y) coincide with the axes (x,y) in Fig. 4.5 (i.e. $\theta = 0^\circ$ or 90°) then along lines 1. and 2. there is no bending, only twisting; along lines 3. and 4. there is pure bending and no twisting. Since this bending occurs, it would seem that by making some sort of measurements, some information about the bending rigidities D_x, D_{12}, D_{21} and D_y should be able to be found. What can be found is discussed below.

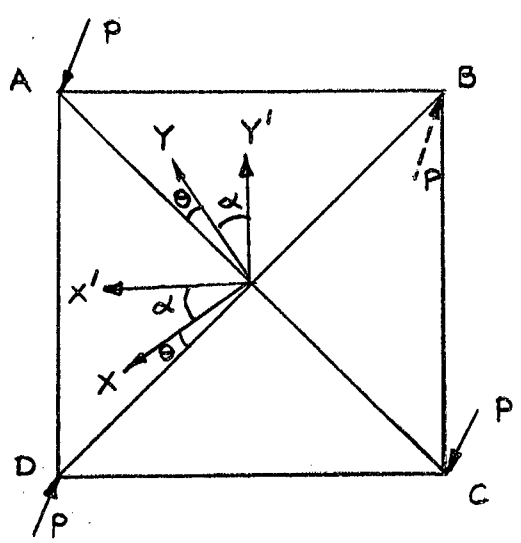

Fig. 4.6

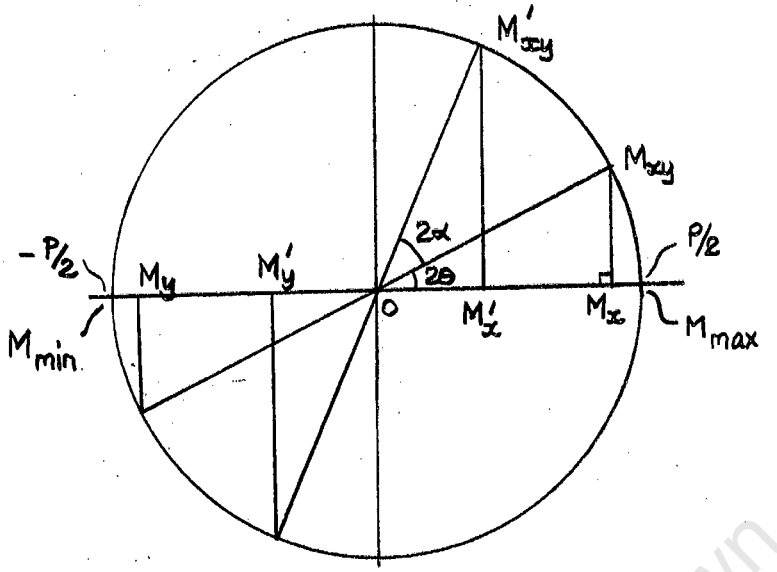

Fig. 4.7

Consider a square plate (Fig. 4.6) loaded as shown at the corners by a force P. Let the stiffeners run in the general direction X at an angle θ to the diagonal BD. As was shown in Chapter 3 (Eqs 3.13) the moments in the plate at any point can be represented by a Mohr's circle (Fig. 4.7). From statics $M_{max} = P/2$; $M_{min} = -P/2$ and the origin of the coordinates in Fig. 4.7 corresponds to the centre of the circle. It can be seen that

$$M_x = \frac{P}{2}\cos 2\theta = -M_y$$

$$M_{xy} = \frac{P}{2}\sin 2\theta \qquad \text{Eqs 4.2}$$

Now choose another general rectangular pair of axes X',Y' such that $\hat{XOX'} = \alpha$. Using Eqs 3.13 to express M'_x, M'_y and M'_{xy} in terms of M_x, M_y and M_{xy}, we have

$$M'_x = \frac{(M_x+M_y)}{2} + \frac{(M_x-M_y)}{2}\cos 2\alpha - M_{xy}\sin 2\alpha$$

$$M'_y = \frac{(M_x+M_y)}{2} - \frac{(M_x-M_y)}{2}\cos 2\alpha + M_{xy}\sin 2\alpha$$

$$M'_{xy} = \frac{(M_x-M_y)}{2}\sin 2\alpha + M_{xy}\cos 2\alpha$$

Eqs 4.3

From Fig. 4.7

$$M'_x = \frac{P}{2}\cos(2\theta + 2\alpha) = -M'_y$$

$$M'_{xy} = \frac{P}{2}\sin(2\theta + 2\alpha)$$

Eqs 4.4

Eqs 4.3 can now be used to give relationships between the rigidities, since for

M_x we substitute $D_x \frac{d^2w}{dx^2} + D_{12} \frac{d^2w}{dy^2}$

M_y we substitute $D_y \frac{d^2w}{dy^2} + D_{21} \frac{d^2w}{dx^2}$

M_{xy} we substitute $2D_{xy} \frac{d^2w}{dxdy}$

where $\frac{d^2w}{dx^2}$, $\frac{d^2w}{dy^2}$ and $\frac{d^2w}{dxdy}$ are measured by experiment. θ is fixed for a particular model.

In the general case where θ lies between 0° and 45°, we have three basic equations

$$M'_x = \frac{P}{2}\cos(2\theta + 2\alpha) = \frac{(M_x-M_y)}{2}\cos 2\alpha - M_{xy}\sin 2\alpha \qquad (1)$$

$$M'_{xy} = \frac{P}{2}\sin(2\theta + 2\alpha) = \frac{(M_x-M_y)}{2}\sin 2\alpha + M_{xy}\cos 2\alpha \qquad (2)$$

$$\frac{(M_x+M_y)}{2} = 0 \qquad (3)$$

Let us see what happens when we choose different values of α and substitute them into the above equations.

For equation (1):

$$\alpha = 0^\circ : \frac{P}{2}\cos 2\theta = \frac{(M_x - M_y)}{2} \qquad (1A)$$

$$\alpha = 45^\circ : -\frac{P}{2}\sin 2\theta = -M_{xy} \qquad (1B)$$

$$\alpha = 90^\circ : -\frac{P}{2}\cos 2\theta = -\frac{(M_x - M_y)}{2} \qquad (1C) = (1A)$$

$$\alpha = 30^\circ : \frac{P}{2}\cos 2\theta \tfrac{1}{2} - \frac{P}{2}\sin 2\theta \frac{\sqrt{3}}{2}$$

$$= \frac{(M_x - M_y)}{2}\tfrac{1}{2} - M_{xy}\frac{\sqrt{3}}{2} \qquad (1D)$$

$$(1D) = \tfrac{1}{2}(1A) + \frac{\sqrt{3}}{2}(1B)$$

$$\alpha = 60^\circ : -\frac{P}{2}\cos 2\theta \tfrac{1}{2} - \frac{P}{2}\sin 2\theta \frac{\sqrt{3}}{2}$$

$$= -\frac{(M_x - M_y)}{2}\tfrac{1}{2} - M_{xy}\frac{\sqrt{3}}{2} \qquad (1E)$$

$$(1E) = -\tfrac{1}{2}(1A) + \frac{\sqrt{3}}{2}(1B)$$

For equation (2):

$$\alpha = 0^\circ : \frac{P}{2}\sin 2\theta = M_{xy} \qquad (2A) = (1B)$$

$$\alpha = 45^\circ : \frac{P}{2}\cos 2\theta = \frac{(M_x - M_y)}{2} \qquad (2B) = (1A)$$

$$\alpha = 30^{\circ}: \quad \frac{P}{2}\cos 2\theta\,\frac{\sqrt{3}}{2} + \frac{P}{2}\sin 2\theta\,\tfrac{1}{2}$$

$$= \frac{(M_x - M_y)}{2}\,\frac{\sqrt{3}}{2} + M_{xy}\,\tfrac{1}{2} \qquad (2C)$$

$$(2C) = \frac{\sqrt{3}}{2}(1A) - \tfrac{1}{2}(1B)$$

It can be seen that equations (1) and (2) yield no more than two independent equations, namely (1A) and (1B). The conclusion is that, when the stiffeners are placed in a general direction at an angle θ to the diagonal, the total possible number of independent equations relating the rigidities that can be found is three, namely (1A), (1B) and (3).

In the case $\theta = 0^{\circ}$

We can find the following equations

$$\frac{(M_x + M_y)}{2} = 0 \qquad (3)$$

$$\frac{P}{2} = \frac{(M_x - M_y)}{2} \qquad (1A)$$

$$0 = M_{xy} \qquad (1B)$$

However, $\frac{d^2w}{dxdy} = 0$ in this case and equation (1B) therefore gives no information. Therefore only two independent equations may be found by experiment when $\theta = 0$.

In the case $\theta = 45^\circ$

Here the stiffeners are parallel to the sides AB,CD of the plate, as in the twisting test in section 1. We have the following equations:

$$\frac{P}{2} = M_{xy} \tag{1B}$$

$$\frac{M_x + M_y}{2} = 0 \tag{3}$$

$$\frac{M_x - M_y}{2} = 0 \tag{1A}$$

However when $\theta = 45^\circ$ we have

$$\frac{d^2w}{dx^2} = \frac{d^2w}{dy^2} = 0$$

Every term in the expressions for M_x and M_y has either $\frac{d^2w}{dx^2}$ or $\frac{d^2w}{dy^2}$ as a factor, and therefore equations (3) and (1A) give no information. The only information one can possibly find from a twisting test when $\theta = 45^\circ$ is from

$$\frac{P}{2} = M_{xy} = 2D_{xy}\frac{d^2w}{dxdy} \tag{1B}$$

From the above we conclude that, if one wants to find all the rigidities D_x, D_{12}, D_{21}, D_y and D_{xy} by means of a twisting test as in Fig. 4.6, one must use more than one plate model. This is because θ must have more than one value. If one of the models has $\theta = 45^\circ$, then two other models must be used (say $\theta = 0^\circ$, $22\frac{1}{2}^\circ$). If none of the models has $\theta = 45^\circ$, then two models is the total minimum

number which must be used.

3. The Writer's Method

It was decided that tests would be done on a number of technically orthotropic plates to determine the values of the rigidities D_x, D_{12}, D_{21}, D_y and D_{xy}. These values were to be compared with the values given by theoretical formulae. The type of orthotropic plate chosen was the asymmetrically stiffened plate with stiffeners running in one direction only. As has been stated, a major consideration was to find a method of determining the rigidities which involved making only one model of each orthotropic plate. The method used is described below.

The Twisting Test

The torsional rigidity, D_{xy}, is determined by means of a twisting test similar to that described in section 1. The stiffeners are made parallel to a side of the plate.

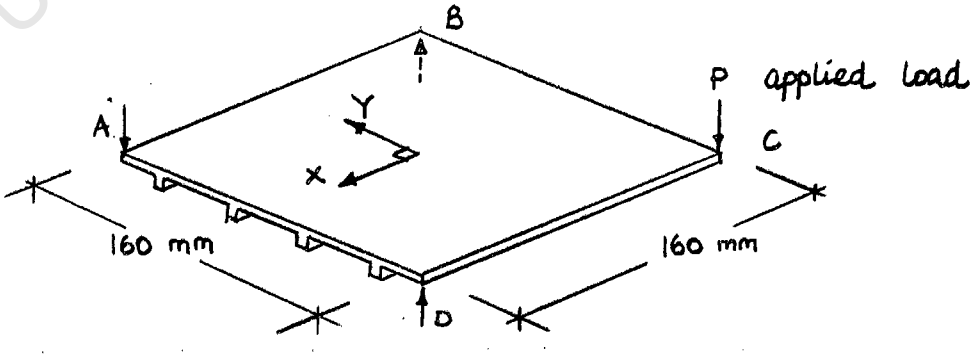

Fig. 4.8

Points B and D of the plate are supported on screws, and point A is held down by another fixed screw. The applied

load, P, is transmitted to the plate through a deflection gauge (1 div. = 0,01 mm).

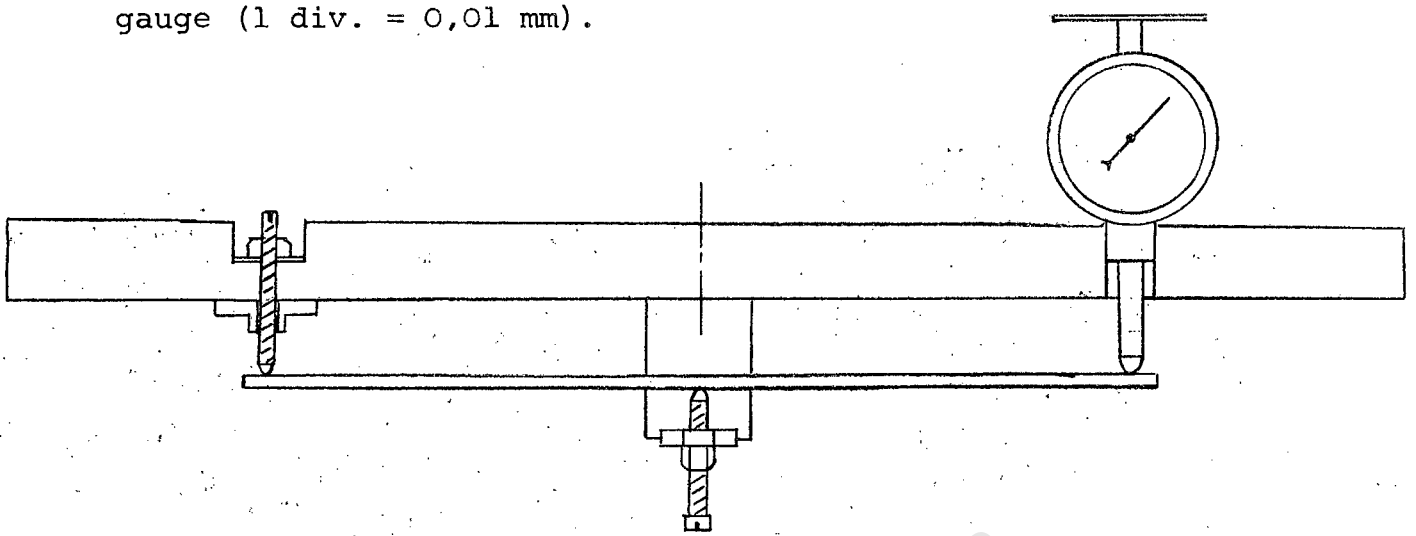

SECTION QQ

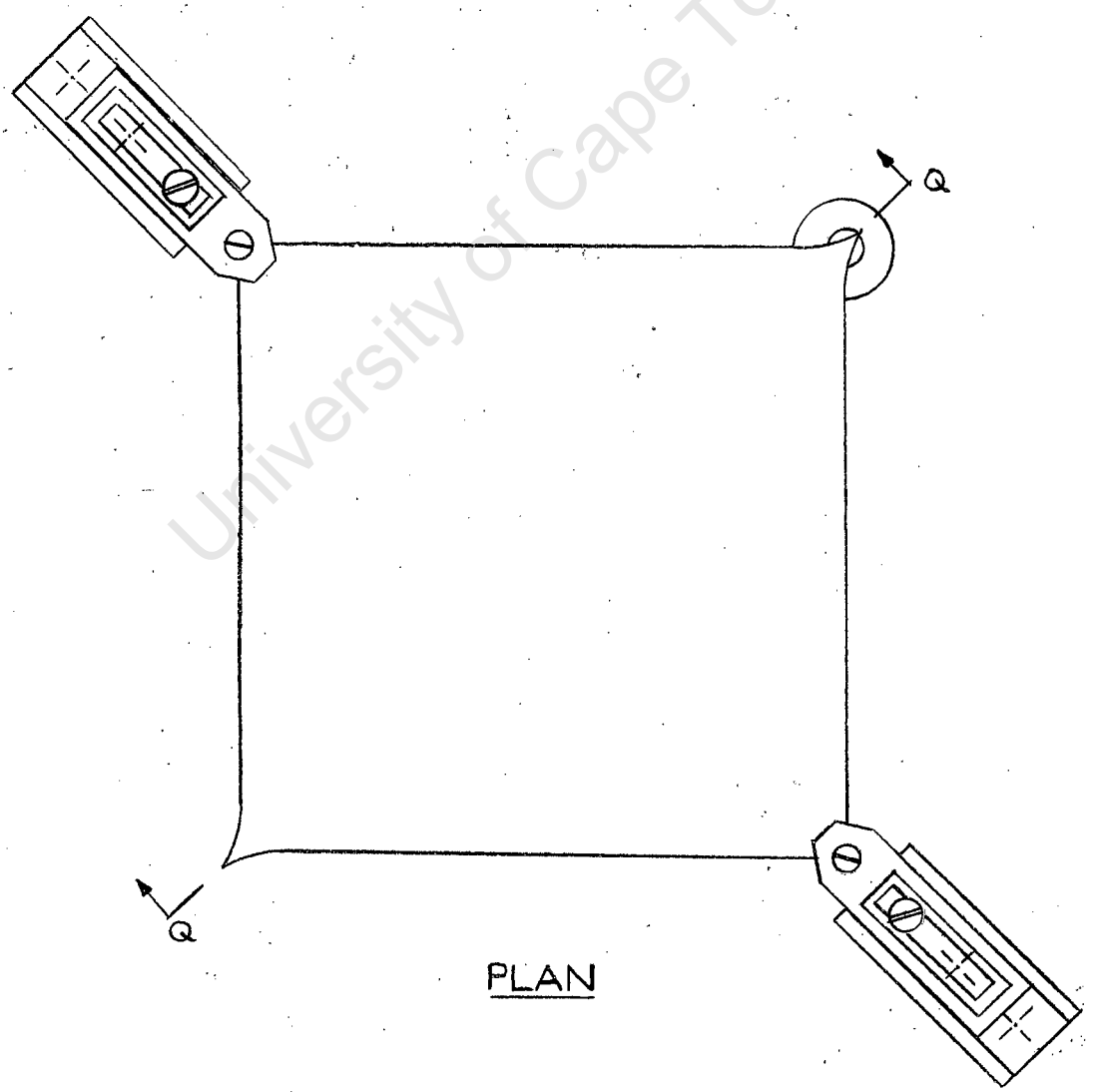

PLAN

Fig. 4.9

The fixed-screws are attached to a model-holding-board, as in Fig. 4.9, and the deflection gauge is fixed into the board. The model creeps under load, as will be discussed in Chapter 5, and the model-holding-board must be tapped lightly and continuously to keep the hand of the gauge moving steadily. The friction in the gauge is small, but it does exist and the board must be tapped for accurate results.

D_{xy} is found as follows:

$$M_{xy} = 2D_{xy} \frac{d^2w}{dxdy}$$

$\frac{d^2w}{dxdy}$ is the same at all points of the plate and is the change of slope in the X direction per unit distance in the Y direction. If w is the deflection of the corner point C in Fig. 4.8 (A,B,D being fixed), and if ℓ is the length of side of the square plate, then

$$\frac{d^2w}{dxdy} = \frac{w}{\ell^2}$$

$$\therefore \quad \frac{P}{2} = 2D_{xy} \frac{w}{\ell^2}$$

$$\therefore \quad D_{xy} = \frac{P\ell^2}{4w} \qquad \text{Eq 4.4}$$

The Bending Test

The same square model used in the twisting test is used here. It is supported on its four corner points on screws which are fixed to the model-holding-board. This board is the same one as that used in the twisting test. The conversion to the bending test requires the replacement of

the downward screw at A and the deflection gauge at C by upward fixed screws.

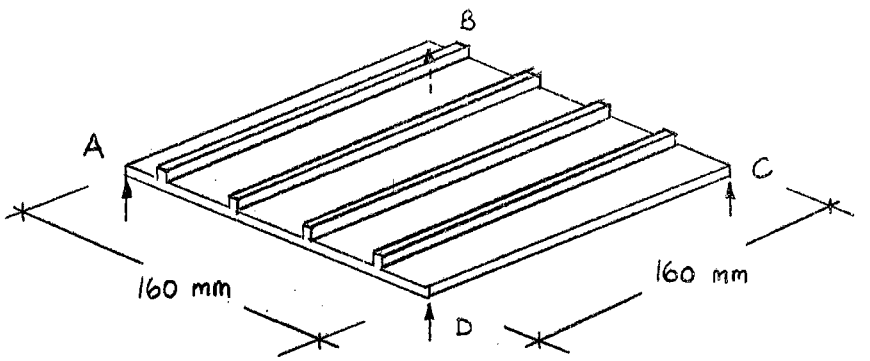

Fig. 4.10

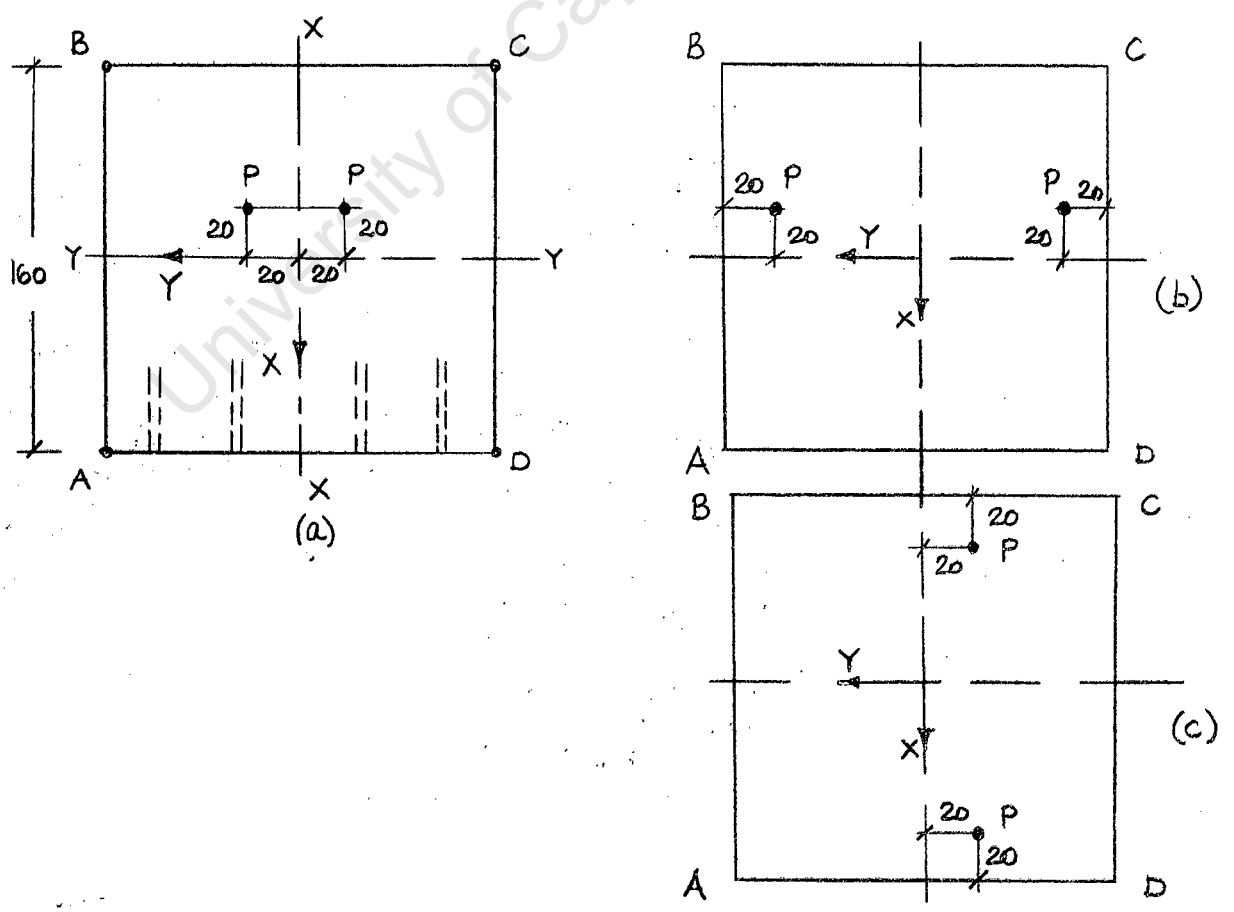

Fig. 4.11

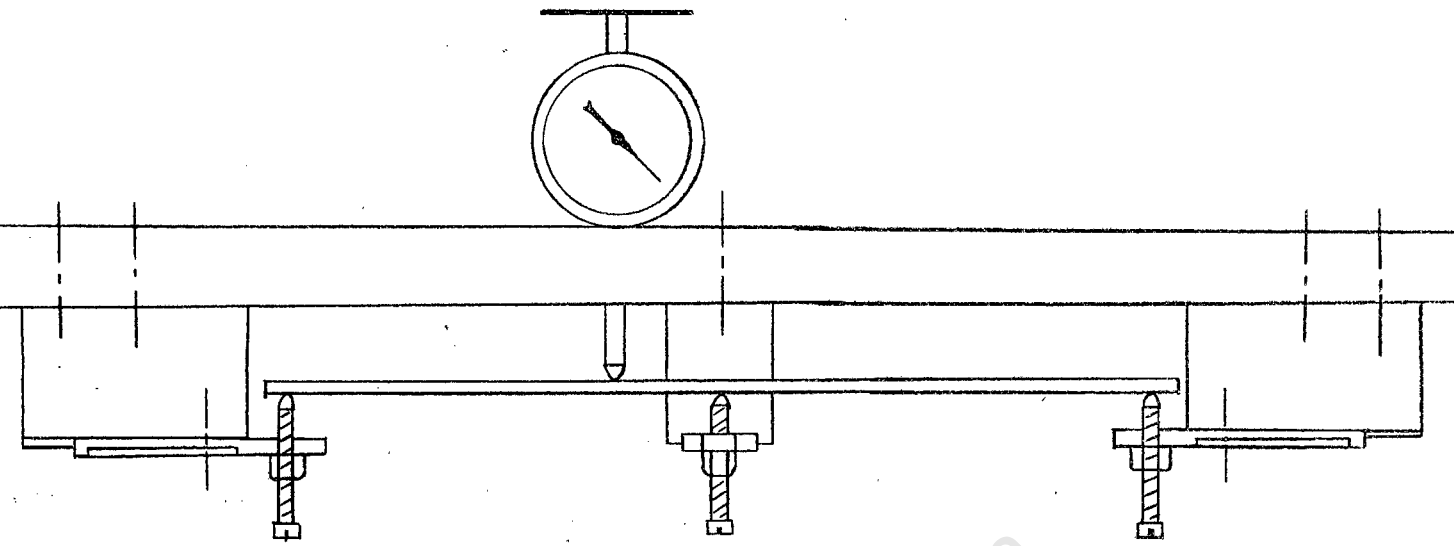

SECTION QQ

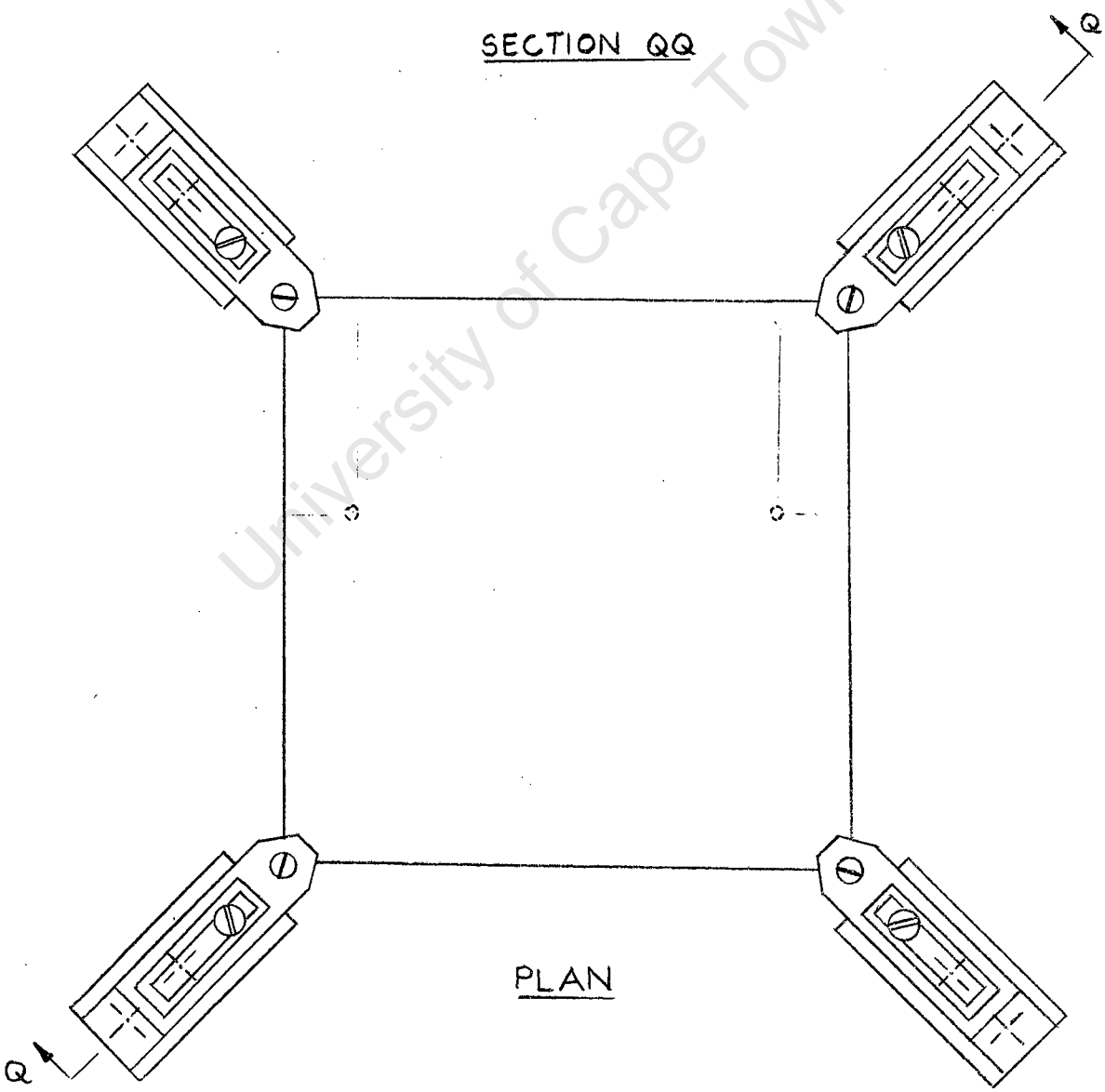

PLAN

Fig. 4.12

The model is loaded in the positions shown in Fig. 4.11, and the whole apparatus is shown in Fig. 4.12. The load is applied through deflection gauges as in the twisting test. The friction in the deflection gauges is considered to be less than the friction in a system using a plunger and platform (see Fig. 4.13).

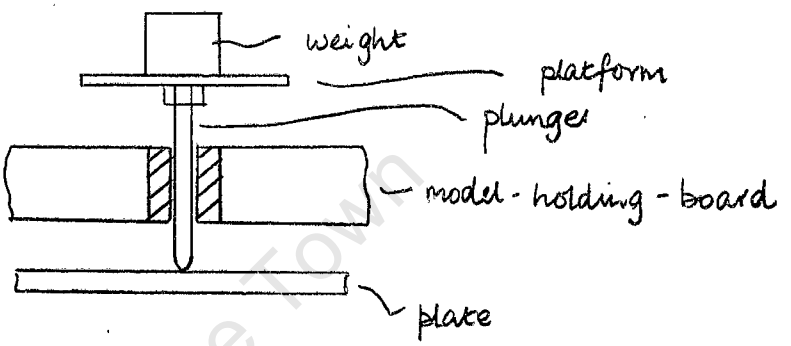

Fig. 4.13

Consider the loaded plate (Fig. 4.11). The reactions at the four corners can be found from statics. In each load case equations are found for the total statical moment at midspan. If P = 1N,

for case (a), at section YY : $M_x = 2\frac{3}{8}$ P 80 N mm

$= 60$ N mm

and at section XX : $M_y = 60$ P N mm

$= 60$ N mm

Similarly the moments are found for cases (b) and (c). The moments could be found at any section, not necessarily at midspan. If the section is too close to the loads however, the curvatures are difficult to determine accurately.

These total statical moments can also be expressed in terms of the bending rigidities. Consider the M_x equation and consider the midspan section YY (length 160 mm) divided into many small divisions, each of size dy.

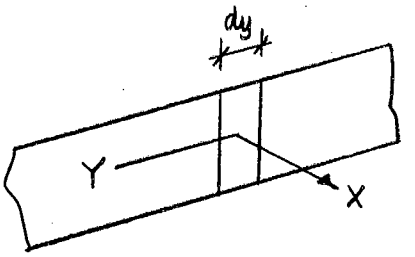

Fig. 4.14

At the centre point of this element there exist curvatures $\frac{d^2w}{dx^2}$ and $\frac{d^2w}{dy^2}$.

The moment per unit length at this point is

$$M_x = D_x \frac{d^2w}{dx^2} + D_{12} \frac{d^2w}{dy^2}$$

The units are

$$N \frac{mm}{mm} = N.mm \frac{1}{mm} + N.mm \frac{1}{mm}$$

The total statical moment over the whole length of the midspan section is

$$\int_{-80}^{80} M_x \, dy = D_x \int_{-80}^{80} \frac{d^2w}{dx^2} dy + D_{12} \int_{-80}^{80} \frac{d^2w}{dy^2} dy \qquad \text{Eq 4.5}$$

The units are now

$$N \frac{mm}{mm} mm = (N\ mm) \frac{1}{mm} mm + (N\ mm) \frac{1}{mm} mm$$

The integrated curvature terms are found as follows. The

test is done in the Moiré apparatus (see Chapter 5). From Moiré photographs by taking lines parallel to the X direction at regularly spaced intervals, the values of $\frac{d^2w}{dx^2}$ at nine points are obtained.

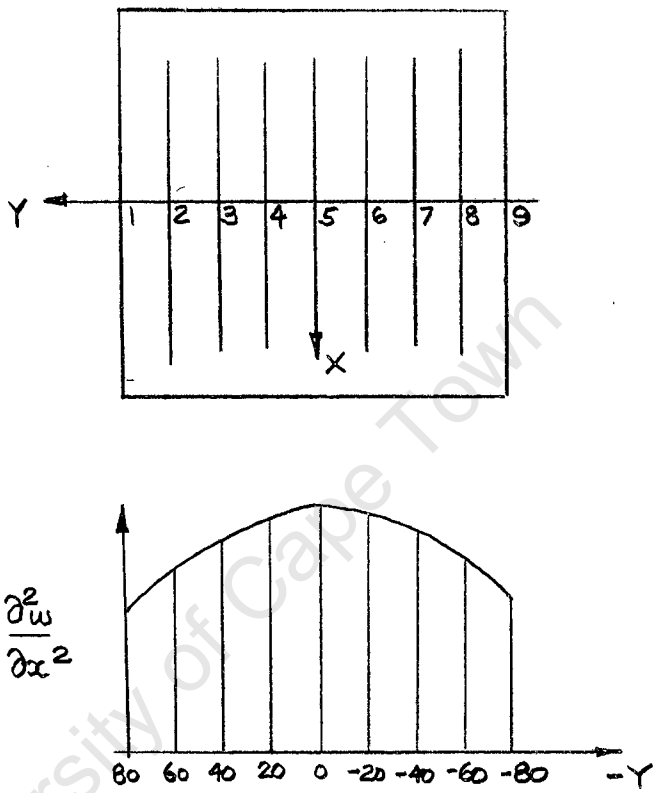

Fig. 4.15

The value of $\int_{-80}^{80} \frac{d^2w}{dx^2}\,dy$ is now found by Simpson's Rule. A point to notice is that it does not matter whether the plate is resting equally on all four supports. It may rest on only three yet it will not affect the moment equation. The values of $\frac{d^2w}{dx^2}$ will be different but the moment equation will still be valid.

The value of the term $\int_{-80}^{80} \frac{d^2w}{dy^2}\,dy$ is simple to obtain since

$$\int_{-80}^{80} \frac{d^2w}{dy^2}\,dy = \left(\frac{dw}{dy}\right)_{y=80} - \left(\frac{dw}{dy}\right)_{y=-80}$$

No curve plotting is necessary. The required values can be estimated from the enlarged Moiré photograph with reasonable accuracy.

The moment equation in the Y direction is derived similarly.

$$\int_{-80}^{80} M_y \, dx = D_y \int_{-80}^{80} \frac{d^2w}{dy^2} \, dx + D_{21} \int_{-80}^{80} \frac{d^2w}{dx^2} \, dx \qquad \text{Eq 4.6}$$

For each of the load cases in Fig. 4.11 there are two moment equations, namely for M_x and M_y at midspan. Since there are four unknowns D_x, D_{12}, D_{21} and D_y to be found, only two load cases are necessary for their solution. The third load case acts as a check and gives extra information resulting in better average values of the unknowns.

The positions of the loads were chosen with three considerations in mind.

1. The loads must not be too close to the points at which the curvatures are required as this makes the curvatures difficult to determine accurately.
2. The loading points must be on or between the ribs of all four different plate rib spacings (see Chapter 5). In other words a load cannot be applied right on the edge or just off a rib.
3. The loads must bend the plate in modes which are as different as possible. This gives well-conditioned equations which produce accurate values for the rigidities.

The limitations of this bending test are as follows. The plate is not in pure bending. According to Massonnet

this means that the theoretical formulae for the bending rigidities must have extra terms in them due to the eccentricity of the ribs. It must be borne in mind, therefore, that values of rigidities found by experiment should be larger than the theoretical values calculated on the basis of the 4th order theory. For the twisting test however the experimental values should coincide with those calculated by the 4th order theory. The other limitation is that, when the ratio of D_x to D_y is large, the plate tends to bend only in the Y-direction no matter where the point loads are put on the plate. In other words, before an appreciable curvature in the X-direction occurs, the plate may be deforming plastically in the Y-direction. The solution would be for the plate to be simply supported continuously along two opposite edges rather than on four corner support points. In the bending tests performed by the writer the model was only supported on the four corner points.

CHAPTER 5

THE BENDING TEST

1. The Models

It was decided to make 16 different orthotropic plate models for testing. These were asymmetrically stiffened plates with ribs running in one direction only. This is a common civil engineering application which is seen in concrete bridges and floor slabs of large buildings. The 16 models fall into 4 sets of 4. In each set of 4 the moment of inertia in the X (stiff) direction is the same. In other words the theoretical value of D_x is the same. The plates are shown in full scale in Fig. 5.1. In all the plates the ratio of rib spacing to rib width, s/b, is constant at 4 : 1. This is necessary to keep D_x the same in each set of 4 plates. The different rib depths give approximate ratios of D_x/D of 1,5, 3, 10 and 25.

The objective of the tests is to compare the test values with the theoretical values of the rigidities. However the objective may be more specifically defined as follows:

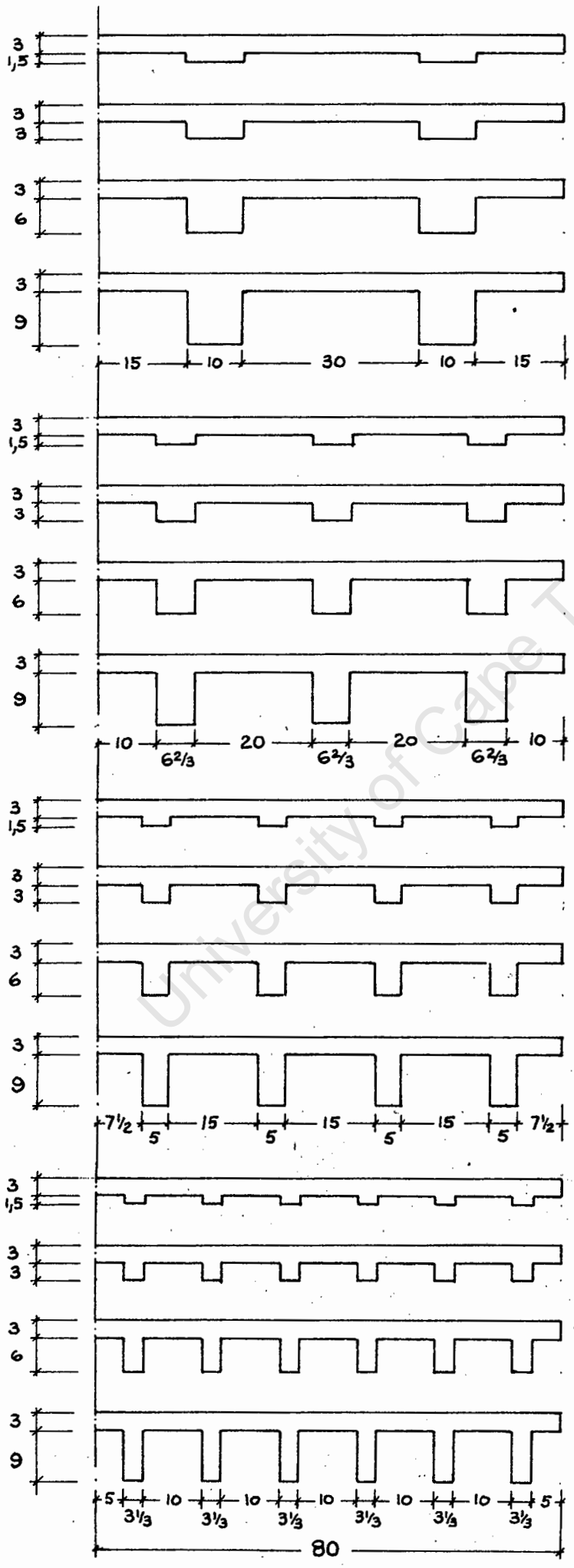

Scale : full size

Dimensions in mm

Fig 5.1

(a) To determine how well an asymmetrically stiffened plate behaves as an orthotropic plate, i.e. how far apart may the ribs be spaced before the plate becomes a system of plate elements and beam elements.

(b) To determine the influence, if any, on the rigidities D_x, D_1, D_y, of altering the spacing of the ribs of stiffened plates, which have the same theoretical values of D_x.

(c) To determine whether there is any difference between the rigidities D_{12} and D_{21}, which are the same for a true orthotropic plate and are usually assumed to be the same for an asymmetrically stiffened plate.

The bending test was done in the Moiré apparatus, and therefore the models had to have a reflecting surface. They were therefore made of black perspex which is a good reflecting material commonly used in Moiré work. Black perspex is obtainable in sheets of nominal thickness of 1/8", 3/16" and 1/4". In metric units these sizes are approximately 3,2; 4,8 and 6,4 mm. The thickness of the sheets varies considerably and the material was milled down to the required size in the case of the thinner 8 plates. For the thicker 8 plates clear perspex which comes in thicker sheets was used, also being milled to size.

It is not possible to make the plate and ribs separately and then to glue them together as the glue warps the plate which is only 3 mm thick. Models 4/6 and 12/9 were made by glueing two 1/4" sheets of black perspex together and then milling out the plate. It was found however by glueing a sheet of black to a sheet of clear perspex that air bubbles

are left between the sheets when the glue dries. These discontinuities should in general decrease the strength of the resulting plate. Model 12/9 was also made out of clear perspex. The bending test was only performed on the thinner 8 plates. The thicker models made of clear perspex can also be tested if they are painted or given a reflective coating in some way. The best method seems to be to dip the models in a fairly thin solution of high gloss black paint. More than one coat may be needed. Other methods considered were sticking a transfer on the surface or spray painting or electroplating it. No suitable transfer could be found and electroplating of this type is not done by any firm in Cape Town. The painted surface is not as flat nor as reflective as the black perspex surface and the results can not be expected to be as good with this method.

2. Variation in dimensions

The variation of the dimensions of the models from those specified is not negligible since the plates are thin. A small absolute deviation may therefore be a relatively large one. Correction factors were applied to the stiffnesses of the models to compensate for this variation. These factors are defined as follows:

$$D_x \text{ (actual)} = k_x \cdot D_x \text{ (specified)}$$
$$D_{12} \text{ (actual)} = k_x \cdot D_{12} \text{ (specified)}$$
$$D_y \text{ (actual)} = k_y \cdot D_y \text{ (specified)}$$
$$D_{21} \text{ (actual)} = k_y \cdot D_{21} \text{ (specified)}$$

In order to calculate a correction factor a theoretical

formula for the rigidity in question must be assumed. The following were the formulae taken:

$$D_y = D = \frac{Eh^3}{12(1-\upsilon^2)} \qquad \text{Eq 2.43}$$

$$D_x = \frac{EI_x}{s} \qquad \text{Eq 2.41}$$

The dimensions were measured at the points shown in Fig. 5.3. The symbols used for the dimensions are shown in Fig. 5.2.

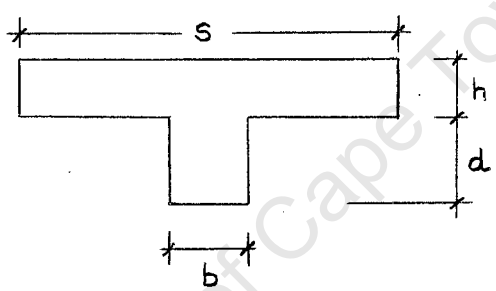

Fig. 5.2

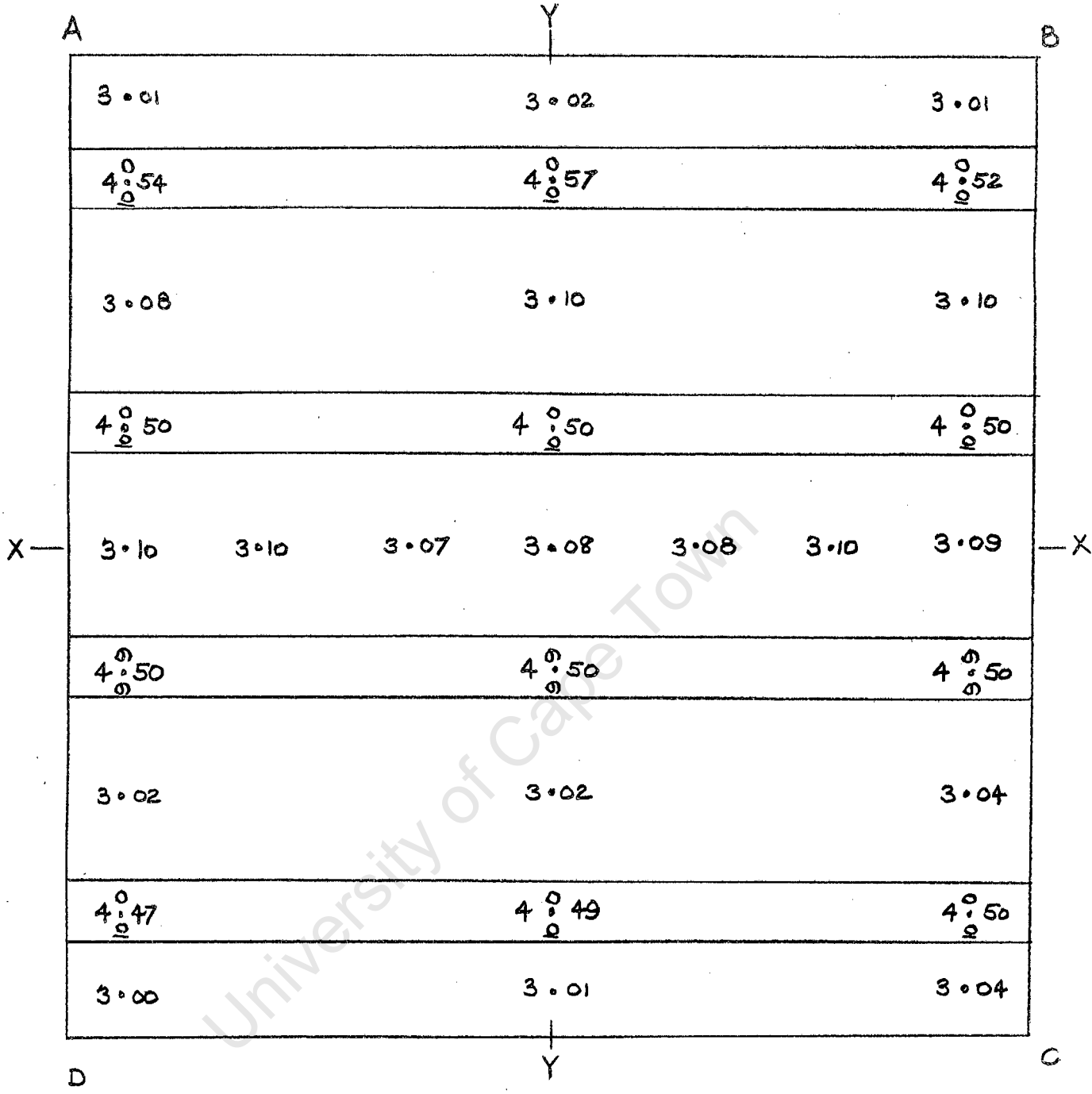

4/1,5 plate

Dimensions in mm

Fig. 5.3

Measurements are made on each rib and between each rib. The thickness of the plates was measured at the positions

shown by means of a dial gauge set above a base which was surface-ground to make it as smooth as possible. The dimension b was measured with a vernier.

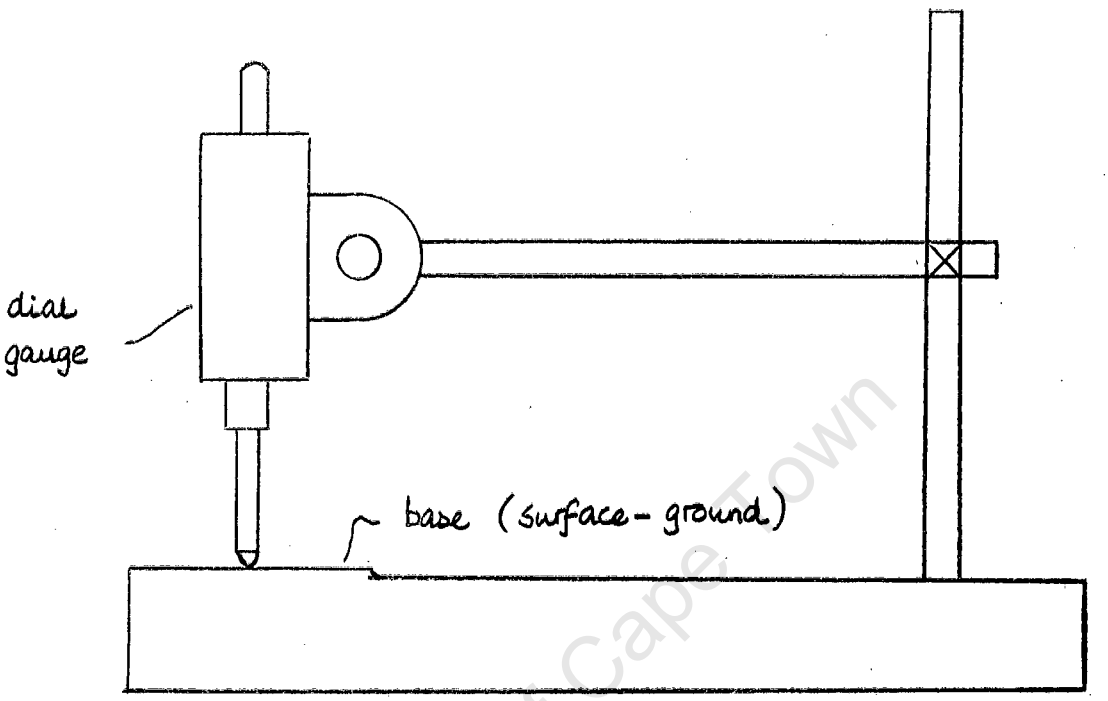

Fig. 5.4

Each thickness value was an estimated average of the thickness in the vicinity of the points shown, obtained by moving the plate around on the base.

Calculation of k_y

Since the equation for M_y in the bending test is applied at the midspan section XX, the thickness measurements along this line are used (see Fig. 5.3). For each plate 7 equally spaced points are used. Since D_y depends on the cube of the thickness h, the average value of h can be calculated as

$$h_m = \sqrt[3]{\frac{\Sigma_1^7 h_i^3}{7}}$$

It is not necessary, however, to calculate the cubes of each measurement as an approximate method is sufficiently accurate. The specified plate thickness is 3 mm for all models which, by chance, also simplifies the calculation as shown below.

	h	h^3
	$3 + \Delta_1$	$3^3 + 3.3^2\,\Delta_1 + 3.3.\Delta_1^2 + \Delta_1^3$
	$3 + \Delta_2$	$3^3 + 3.3^2\,\Delta_2 + 3.3.\Delta_2^2 + \Delta_2^3$
	$\vdots$	$\vdots \quad \vdots \quad \vdots \quad \vdots$
	$3 + \Delta_n$	$3^3 + 3.3^2\,\Delta_n + 3.3.\Delta_n^2 + \Delta_n^3$
Σ	$3n + \Sigma\Delta$	$3^3 + 3^3.\Sigma\Delta + 3^2.\Sigma\Delta^2 + \Sigma\Delta^3$
mean	$3 + \frac{\Sigma\Delta}{n}$	$3^3 + 3^3.\frac{\Sigma\Delta}{n} + 3^2.\frac{\Sigma\Delta^2}{n} + \frac{\Sigma\Delta^3}{n}$

From the above, the geometric mean is defined from

$$h_m^3 = 3^3 + 3^3\,\frac{\Sigma\Delta}{n} + 3^2\,\frac{\Sigma\Delta^2}{n} + \frac{\Sigma\Delta^3}{n}$$

The arithmetic mean is

$$h_a = 3 + \frac{\Sigma\Delta}{n}$$

$$\therefore \quad h_a^3 = 3^3 + 3^3\,\frac{\Sigma\Delta}{n} + 3^2\left(\frac{\Sigma\Delta}{n}\right)^2 + \left(\frac{\Sigma\Delta}{n}\right)^3$$

Since Δ is small, the last two terms in h_m and h_a can be neglected, giving

$$h_a = h_m \ .$$

The correction factor k_y is given by

$$k_y = \frac{h_m^3}{3^3}$$

since the specified plate thickness is 3 mm.

$$\therefore \quad k_y = \frac{3^3 + 3^3 \frac{\Sigma\Delta}{n}}{3^3} = 1 + \frac{\Sigma\Delta}{n}$$

Therefore k_y can be found from the arithmetic mean of h. For example, if h_a = 3,047 mm

then k_y = 1,047 .

This is quite accurate enough for the purpose of these experiments.

It is important to know how close the true mean value of h is to the calculated mean value h_a. For this reason we calculate standard deviations. The standard deviation of a single observation of h is

$$\text{SDSOH} = \frac{\Sigma_1^7 (h_i - h_a)^2}{6}$$

The standard deviation of the mean of h, h_a, is

$$\text{SDMNH} = \frac{\text{SDSOH}}{\sqrt{7}}$$

The standard deviation of a single observation of h, SDSOH, describes the accuracy with which we know the value of h at any point along section XX. For example, if SDSOH = 0,04 mm, then we can say with 68% confidence that at any particular point of the plate along the section XX the measured value of h will be in the range $h_a \pm$ 0,04 mm. If SDSOH = 0,04 mm, then SDMNH = $\frac{0,04}{\sqrt{7}}$ = 0,015 mm. We can now say with 68% confidence that the mean value of h lies in the range $h_a \pm$ 0,015 mm. Consider Fig. 5.5.

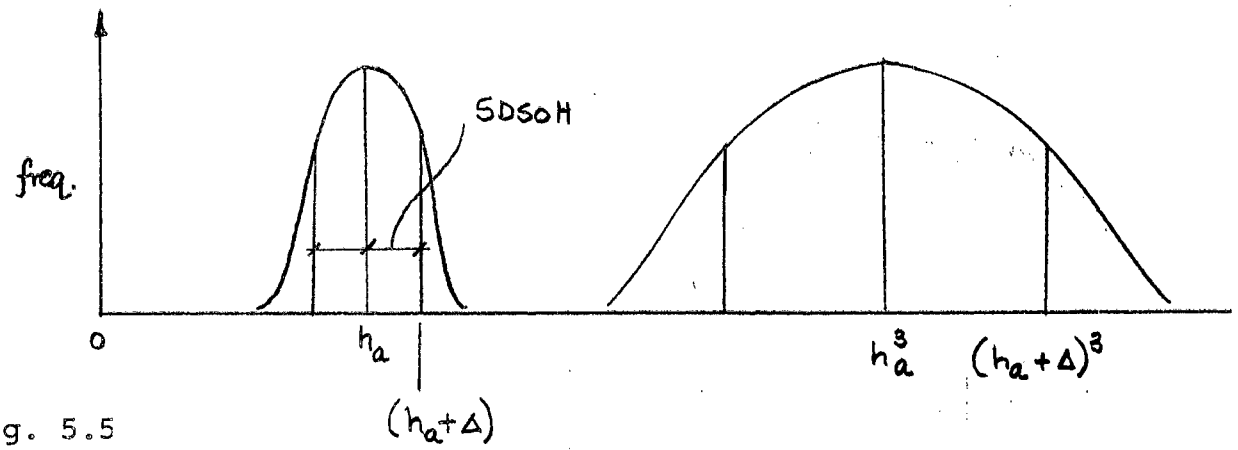

Fig. 5.5

In the above calculations it has been assumed that h is normally distributed. This should be so from the Central Limit Theorem of statistics because each measured value of h was an average value for its surrounding area. We would expect h to be normally distributed anyway in the absence of evidence to the contrary. By cubing each value of h, we obtain the distribution of h^3. Strictly speaking it will be log-normally distributed, but the proof that $h_a \doteqdot h_m$ implies that it is approximately normally distributed too.

Consider a value of h of $(h_a + \Delta)$. Cubing this we get

$$(h_a + \Delta)^3 = h_a^3 + 3h_a^2 \Delta + \ldots.$$

Now let Δ = SDSOH.

Then we may say that the standard deviation of h^3 is

$$h_a^3 + 3h_a^2 \Delta - h_a^3 = 3h_a^2 \Delta$$
$$= 3h_a^2 \text{ SDSOH}$$

Now the standard deviation of the mean of h^3 is $3h_a^2$ SDMNH.

The relative standard deviation of the mean of h^3 is

$$RSDMNH3 = \frac{3h_a^2 \, SDMNH}{h_a^3}$$

Since $h_a \doteq 3$ mm

$$RSDMNH3 \doteq SDMNH$$

As an example of what this means, if SDMNH = 0,015 mm, then we may say with 68% confidence that the mean of h^3 lies within the range

$$h_a^3 \, (1 \pm RSDMNH3)$$
$$\text{or } h_a^3 \, (1 \pm 0{,}015)$$

In other words we are 68% confident that the true value of the mean of h^3 lies within 1,5% of our calculated value h_a^3. Note that RSDMNH3 is dimensionless but SDMNH is in mm.

Calculation of k_x

For the calculation of k_x the measurements along the midspan section YY must be used (see Fig. 5.3). First of all the quantities h_a, SDSOH and SDMNH are calculated. Then the values of d_i are obtained from

$$d_i = (h + d)_i - h_a$$

Then d_a, SDSOD and SDMND are found. Next b_a, SDSOB and SDMNB are found. The notation is the same as for h in the calculation of k_y. The theoretical formula used for D_x is

$$D_x = \frac{EI_x}{s}$$

where $\frac{I_x}{s}$ is the moment of inertia per unit width of plate.

For the T-section

$$\frac{I_x}{s} = \frac{h^3}{12} + \frac{bd^3}{12s} + \frac{bdh(d+h)^2}{4(sh+bd)}$$

By substituting h_a for h, d_a for d, b_a for b we find I_x (model). Then

$$k_x = \frac{I_x(\text{model})}{I_x(\text{specified})}$$

The relative standard deviation of the mean of I_x, **RSDMNIX**, can also be calculated. From the theory of errors if

$$F = f(a,b, \ldots ,n)$$

and the standard deviations of the dependent variables are SDA, SDB, ..., SDN, then the standard deviation of F is

$$SDF = \sqrt{\left(\frac{dF}{da}\right)^2 . SDA^2 + \left(\frac{dF}{db}\right)^2 . SDB^2 + \ldots + \left(\frac{dF}{dn}\right)^2 . SDN^2}$$

Applying this to the formula for I_x and taking SDMNS = 0,

$$SDMNIX = \sqrt{\left(\frac{dI_x}{dh}\right)^2 . SDMNH^2 + \left(\frac{dI_x}{dd}\right)^2 . SDMND^2 + \left(\frac{dI_x}{db}\right)^2 . SDMNB^2}$$

Then $RSDMNIX = \frac{SDMNIX}{I_x}$

In Appendix A the computer program which calculates k_x, k_y, RSDMNH3 and RSDMNIX will be found.

3. Creep

A factor which has to be taken into account in the bending and twisting tests is the phenomenon of creep.

When a plate is loaded it does not immediately bend to its final deflected position. It deflects rapidly at first, say over the first minute, slowing down all the time. It continues to deflect appreciably for at least the first 12 minutes after loading. Fig. 5.6 shows a graph of deflection against time obtained in a preliminary test. This was a T-beam model made of black perspex. It can be seen that the creep rate is still appreciable at 12 minutes. Presumably as the time tends to infinity the creep rate falls off to zero, and it may be unnoticeable after say 30 minutes. One cannot wait for this during the experiments so the deflections must be measured at a certain known time after the load is applied. The times used by the writer were 2 minutes or 5 minutes. It can be seen that the creep rate is not vastly different at these two times, but other investigators seem to use 4 or 5 minute creep times. It can be seen in Fig. 5.6 that when the model is unloaded, the creep rate falls off more quickly than when the model is loaded. This is because there is an initial load still on the model causing it to creep in the opposite direction. It is also possible that gravity is resisting the upward movement of the model.

In the next section will be found the writer's method of determining E and υ for black perspex. It will be realised that E must be defined as the E at a particular creep time, because as a model deflects its strength apparently decreases. Since the rigidities are calculated from E among other factors, they are also defined as the rigidities at a particular creep time.

Fig 5.6

CREEP OF BLACK PERSPEX

The twisting test was performed on the thinner 8 models using a creep time of 5 minutes. The deflections were measured at 1 minute intervals, and so it was possible to calculate the ratio between E_2 and E_5, where the subscript denotes the creep time in minutes.

$$E_2/E_5 = w_5/w_2$$

where w is the deflection of the corner of the plate. This ratio was calculated for 27 applications of a load and averaged to find $E_2/E_5 = 1{,}018$ with a standard deviation of 0,005. This value should be independent of temperature or the applied load. The writer has not found any of the other ratios corresponding to different creep times, but a rough estimate is that $w_{12}/w_2 = 1{,}05$.

In other words the strain increases by 5% between 2 and 12 minutes after loading.

4. The Moiré Method

The Moiré apparatus was used to determine the curvatures required in the bending test, and is shown in Fig. 5.8. The application of the Moiré method to plate bending analysis was first described by Ligtenberg (Ref. 27) and will not be discussed here.

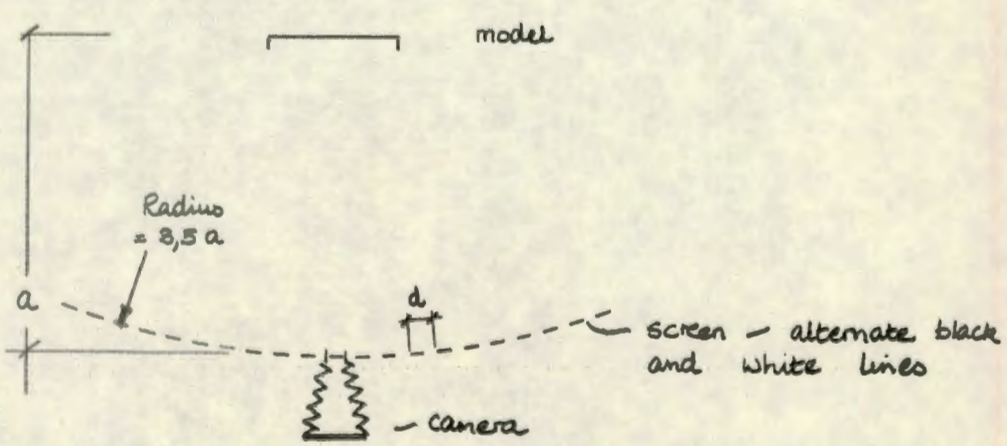

Fig. 5.7

The constant for the apparatus which is needed to calculate the curvatures is, with the notation in Fig. 5.7, the value of d/2a. In the experiments values were

d = 2,14 mm

a = 795 mm

d/2a = 0,001344

= the change in slope between two adjacent fringes.

The lighting is provided by four 500 W lights. The heat generated by these is considerable, and the model warms up quickly when they are switched on. As will be seen in Chapter 6, the values of elastic constants determined in the

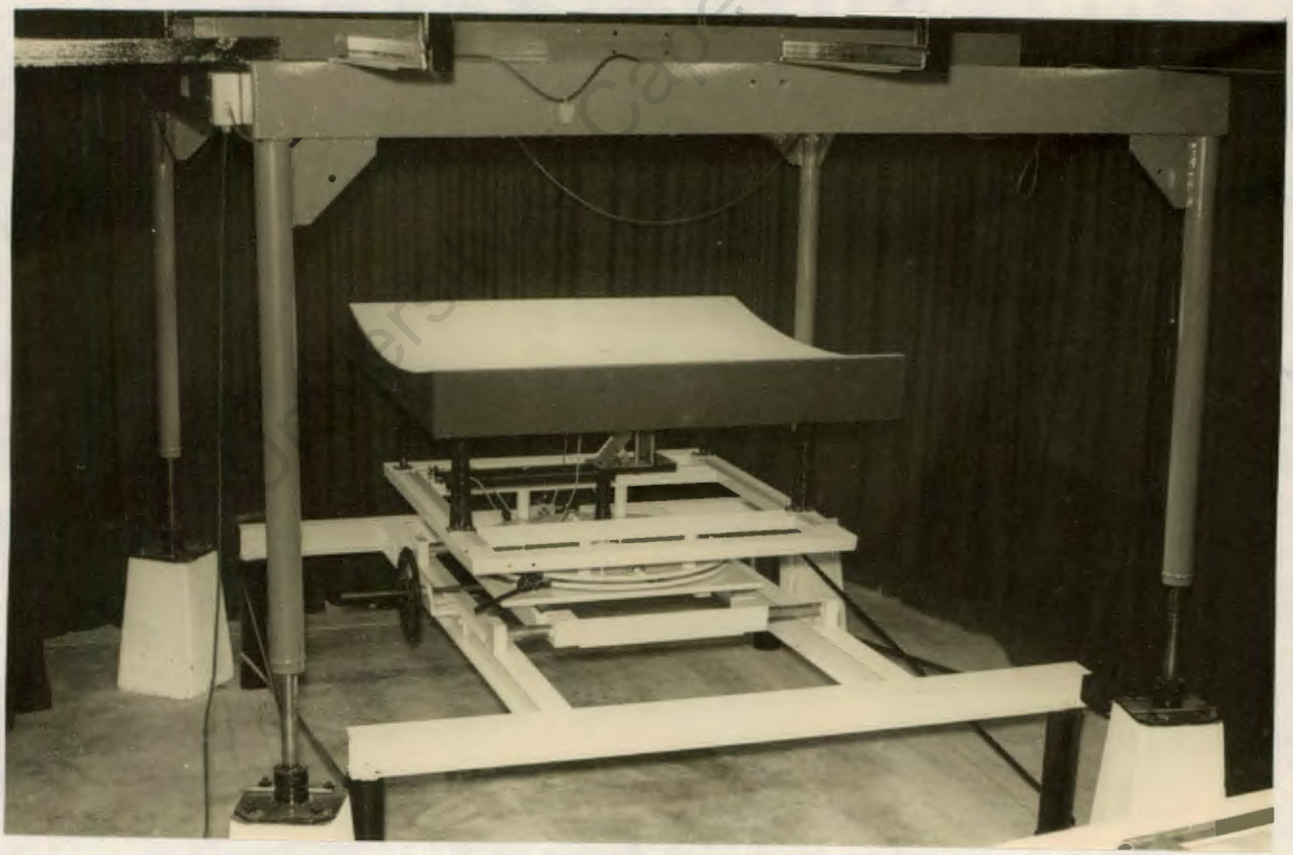

Fig. 5.8

Moiré apparatus differ appreciably from those determined in a test done at room temperature. This effect is allowed

for when comparing twisting test with bending test results.

The apparatus is enclosed by a roof and curtains when in operation. This is because the exposure times for the film would otherwise vary considerably depending on the time of day or night when photographs are taken. The screen can be rotated about a vertical axis so that the curvatures in any direction in the model may be found. The camera used is a Linhof and Professional Line copy film is used for good contrast. The negatives can be enlarged to full scale in an enlarger in the dark room.

The method used in taking the photographs using a creep time of 2 minutes is as follows:

a. The initial load due to the spring force of the deflection gauges is applied.

b. The plate is loaded through the deflection gauges with the force P required to produce sufficient fringes. P is applied for 2 minutes.

c. The plate is unloaded for 2 minutes. Steps b. and c. make up the first loading cycle during which no photographs are taken. This is to allow the model to settle in on its supports.

d. The first exposure is taken and the gauges are read.

e. The load is applied for 2 minutes. The model-holding-board is tapped at intervals to free the deflection gauge spindles of friction.

f. The second exposure is taken and the gauges are read. The deflection difference between the loaded and unloaded states is used to correct P since the force exerted by the deflection gauge spring decreases with

extrusion of the spindle. This change in force is constant at 3 g wt per mm extrusion, and is almost negligible in the bending test but not in the twisting test. In all bending tests the deflection of the plate required to produce sufficient fringes was less than 1/3 of the thickness of the plate (i.e. less than 1 mm).

g. Steps c., d., e. and f. are repeated twice so that 3 photographs are obtained for the particular load case and screen orientation. For the plates with 3 mm deep ribs only one photograph was taken, and a creep time of 5 minutes was used.

Each photograph is developed, the negative enlarged to full scale, and the fringes are traced off. Graphs of slope versus distance along the required lines are plotted.

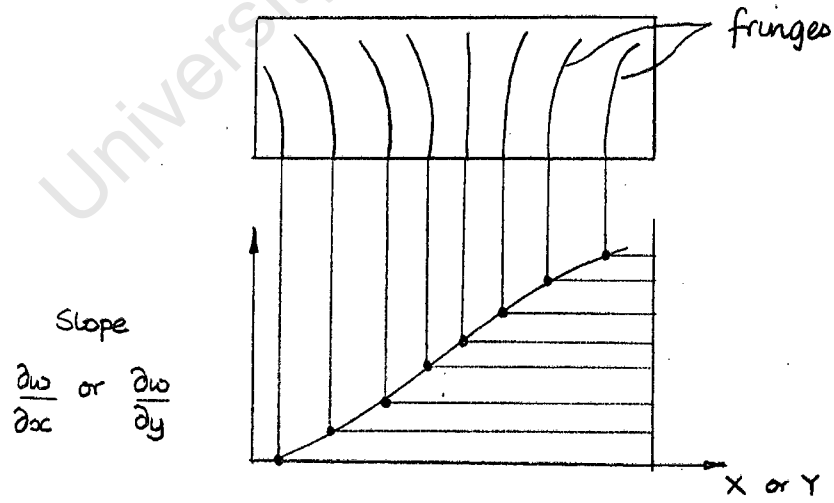

Fig. 5.9

The curvature at the required point is found by measuring the slope of the curve. Accurate graph paper and an accurate protractor are used.

An alternative to the graphical determination of the curvatures is to fit a polynomial to the curve by the method of least squares using a computer. The polynomial has the form

$$\frac{dw}{dx} = C_1 + C_2x + C_3x^2 + \ldots + C_n x^n$$

The degree, n, of the polynomial can be chosen and it must be a maximum of one less than the number of points on the curve. The writer wrote and ran a programme but the results were not as satisfactory as those of the graphical method. The reasons for this were as follows. The difference between results using 3rd, 4th and 5th degree polynomials was not as small as the writer would have liked, although an average result was acceptable. Also, when a point load is on or near the line in question the curve is not representable by a polynomial. The graphical method is definitely superior in this case to the method of averaging polynomial results. Using the graphical method one can see the effects of the loads more clearly; and is safer.

5. Calculation of E and υ

The values of E and υ of black perspex are required for the calculation of theoretical rigidities for comparison with the experimentally determined rigidities. The writer has used the bending test on a black perspex plate of uniform thickness to determine E and υ. The plate was 3 mm thick being milled on one face down to size. The tests used were those shown in Fig. 4.11 (a) and (b). The one shown in Fig. 4.11 (c) is the same as Fig. 4.11 (b).

A creep time of 2 minutes was used, and 3 photographs were taken per load case and screen orientation.

The test provides 4 equations in D and D_1. Equations A1 and B1 are of the form

$$M_x = k_x \left(D.\int \frac{d^2w}{dx^2}\,dy + D_1.\int \frac{d^2w}{dy^2}\,dy\right)$$

Equations A2 and B2 are of the form

$$M_y = k_y \left(D.\int \frac{d^2w}{dy^2}\,dx + D_1.\int \frac{d^2w}{dx^2}\,dx\right)$$

Correction factors for thickness were calculated as in section 2. above.

$$k_x = 1{,}047 \qquad k_y = 1{,}076$$

The set of equations was

A1	8600	=	$D + 0{,}355\ D_1$
A2	8570	=	$D + 0{,}343\ D_1$
B1	7440	=	$D - 0{,}0803\ D_1$
B2	14700	=	$D + 2{,}70\ D_1$

where D and D_1 are in (N mm).

Equations A1 and A2 are not solved together being very similar. All combinations of the 4 equations, with this exception, are solved. Means are found for D and D_1. υ is then calculated as $\upsilon = D_1/D$.

The value of $D(1-\upsilon)/2$ is then calculated for comparison with the result of the twisting test. E is calculated from

$$E = D.12.(1-\upsilon^2)/h^3$$

Note that this value of E is the value only for a creep time of 2 minutes and at the Moiré apparatus temperature.

Solving equations

A1 and B1	:	D_1	=	2570 N mm	;	D	= 7640 N mm
A1 and B2	:	D_1	=	2600 N mm	;	D	= 7680 N mm
A2 and B1	:	D_1	=	2670 N mm	;	D	= 7650 N mm
A2 and B2	:	D_1	=	2600 N mm	;	D	= 7680 N mm
B1 and B2	:	D_1	=	2610 N mm	;	D	= 7650 N mm

Mean D_1 = 2610 N mm

Mean D = 7660 N mm

$\therefore \quad \upsilon$ = 0,34(1)

$D(1-\upsilon)/2$ = 2520 N mm

E_2 = 3,01 GPa

The agreement between the experimental values for D and for D_1 can be seen to be good. The variation in D_1 between the highest and lowest values for D_1 is 4%, and for D is 0,5%. The value for E_2 compares well with that obtained in a preliminary beam test (see section 3.) where the value obtained was E_2 = 3,00 GPa, after correcting for the temperature difference.

6. A study of the errors in the experiments

The statement 'The error in the Moiré method is 5%' has two interpretations. One is that if a single Moiré photograph is taken and the curve is plotted along a particular line and the curvature is measured at a particular point, then we expect our result to be within 5% of the true curvature (with say 95% confidence). This is the most

likely meaning. The percentage error will depend on the following sources of error:

a. Error in d/2a.

b. Model not perpendicular to camera axis.

c. Error inherent in the curvature of the screen. The radius of the screen is made equal to 3,5a to minimise this error.

d. Error in enlarging the negative.

e. Error in tracing the fringes.

f. Error in the graph paper.

g. Error in the protractor.

h. Error in estimating the slope with the protractor.

i. Error due to temperature difference in the model when taking more than one photograph.

The other interpretation of the statement applies when more than one photograph is taken and results are averaged. Besides the expected error in the mean result calculated by the standard deviation of the mean, there is also a constant error which is caused by the Moiré method. The second interpretation is that this constant error is 5%.

In these experiments the second interpretation is used. In order to compare theoretical and experimental results a study of the errors in the results is necessary to determine how confident one is of one's conclusions.

Consider the sources of error listed above. In the experiments the constant error in the Moiré method is caused by errors a. to d. It is assumed that the enlarger was set up once and not reset at all. It was in fact reset occasionally, but in the test for E and υ it probably was not.

Errors e. to i. are not constant but vary from photograph to photograph. They are the main source of the standard deviation of the mean of the result found.

Suppose that we are measuring D. Then

$$D_{true} = k_m D_{mean}$$

D_{mean} is the experimental mean

k_m is the constant error in the Moiré method and can be expressed as

$$k_m = k_a . k_b . k_c . k_d$$

All k are close to unity.

From the theory of errors

$$(TSDMND)^2 = (D . SDKM)^2 + (k_m . SDMND)^2$$

SDMND is the standard deviation of the mean of D calculated from the experimental results.

SDKM is the standard deviation of k_m.

TSDMND is the true standard deviation of the mean of D.

Also

$$(SDKM)^2 = (k_b . k_c . k_d . SDKA)^2 + ... + (k_a . k_b . k_c . SDKD)^2$$

The writer estimates SDKA, ..., SDKD as the following values. Errors a. and b. can be taken together as k_a, and k_b left out.

$$SDKA \doteqdot 2/800 = 0,0025$$

$$SDKC \doteqdot 0$$

$$SDKD \doteqdot 1/160 = 0,0063$$

$$\therefore (SDKM)^2 \doteqdot (1.0,0025)^2 + (1.0,0063)^2$$

$$= (0,0068)^2$$

In other words it is estimated with 68% confidence that, due to the constant error in the Moiré method, the mean value of D is within 0,7% of the calculated mean of D. Or, it is estimated with 95% confidence that it is within 1,4% of the calculated mean of D.

The error due to the variation in the dimensions

It will be realised that the variation of the model dimensions is a source of uncertainty in the results. More specifically, when a correction factor k_x or k_y is calculated, there is a degree of uncertainty in the value obtained. However, it is not necessary to do extra calculations to allow for this as the uncertainty is taken into the individual results for D, D_x, D_y or D_1. When these results are averaged, part of the standard deviation is due to the uncertainty in the dimensions. There is no constant error like that of the Moiré method. RSDMNIX and RSDMNH3 as described in section 2. above are only used to show that the number of dmiension measurements is sufficient; they are not used for further calculation.

Standard deviations of D, υ, and E

Using the results in section 5. above, the following values have been calculated:

Mean D = 7660 N mm

SDMND = 9,4 N mm

TSDMND = 53 N mm

$$\text{RSDMND} = \frac{\text{TSDMND}}{\text{D}} = 0{,}007$$

Mean υ = 0,341

SDMN υ = 0,0024

RSDMN υ = 0,007

E = 3,01 GPa

SDMNE = 0,021 GPa

RSDMNE = 0,007

In the calculation of these values allowance has been made for variation in experimental results and for the constant error in the Moiré method. The conclusions may be stated as follows:

a. We can say with 95% confidence that D of the black perspex plate 3 mm thick lies in the range D = 7660 (1 $\pm$ 0,014) N mm.

b. We can say with 95% confidence that υ of the black perspex plate 3 mm thick lies in the range υ = 0,341 $\pm$ 0,005.

c. We can say with 95% confidence that E of the black perspex plate 3 mm thick lies in the range E = 3,01 $\pm$ 0,04 GPa.

Notice that the relative standard deviations of the three variables are all 0,007. This is the same as SDKM. This means that the variation in experimental results was so small that the constant error in the Moiré method is the overriding source of error.

Standard deviations of DX1, DX2, DX3, DX4, DY1, DY2, DY3

In Appendix A will be found the theoretical values for D_x and D_y which are compared to the experimental values.

These are:

$$DX1 = \frac{EI_x}{s} \qquad \text{Eq 2.41}$$

$$DX2 = \frac{E}{s}\left(\frac{bd^3}{12} + bde_2^2\right) + \frac{E}{(1-\upsilon^2)}\left(\frac{h^3}{12} + he_1^2\right) \qquad \text{Eq 2.39}$$

$$DX3 = \frac{EI_x}{s(1-\upsilon^2)} \qquad \text{Eq 2.42}$$

$$DX4 = DX2 + e_1^2 E\left(h + \frac{bd}{s}\right) \qquad \text{Eq 2.40}$$

$$DY1 = D \qquad \text{Eq 2.43}$$

$$DY2 = \frac{Eh^3}{12}\,\frac{s}{(s-b+\alpha^3 b)} \qquad \text{Eq 2.44}$$

DY3 is from Eq 2.45.

Since E, D and υ are used to calculate these values, there is an uncertainty in them. We now find values for the uncertainties. With the same notation as before

RSDMNDX1 = RSDMNE = 0,007

RSDMNDX3 = RSDMND = 0,007

Since RSDMNDX2 must lie between RSDMNDX1 and RSDMNDX3:

RSDMNDX2 = 0,007

RSDMNDX4 = RSDMNDX2 = 0,007

RSDMNDY1 = RSDMND = 0,007

RSDMNDY2 = RSDMNE = 0,007

RSDMNDY3 = RSDMND = 0,007

For all the above variables we may therefore say with 95% confidence that the values lie within 1,4% of the calculated values.

7. Results for the Stiffened Plates

The bending test on the stiffened plates is conducted in exactly the same way as the test on the plate of uniform thickness described in section 5. above. All three loading cases as shown in Fig. 4.11 are used. A typical set of the 6 different photographs per plate are shown in Fig. 5.10. The photographs are those for the 4/1,5 plate. Fig. 5.11 shows the curves plotted for the two photographs in Fig. 5.10 (a).

The derived equations for the plates 4/1,5 and 4/3 are set out on page 142. The equations for the 3 other 1,5 mm deep ribbed plates are similar to those for the 4/1,5 plate, and the equations for the 3 other 3 mm deep ribbed plates are similar to those for the 4/3 plate.

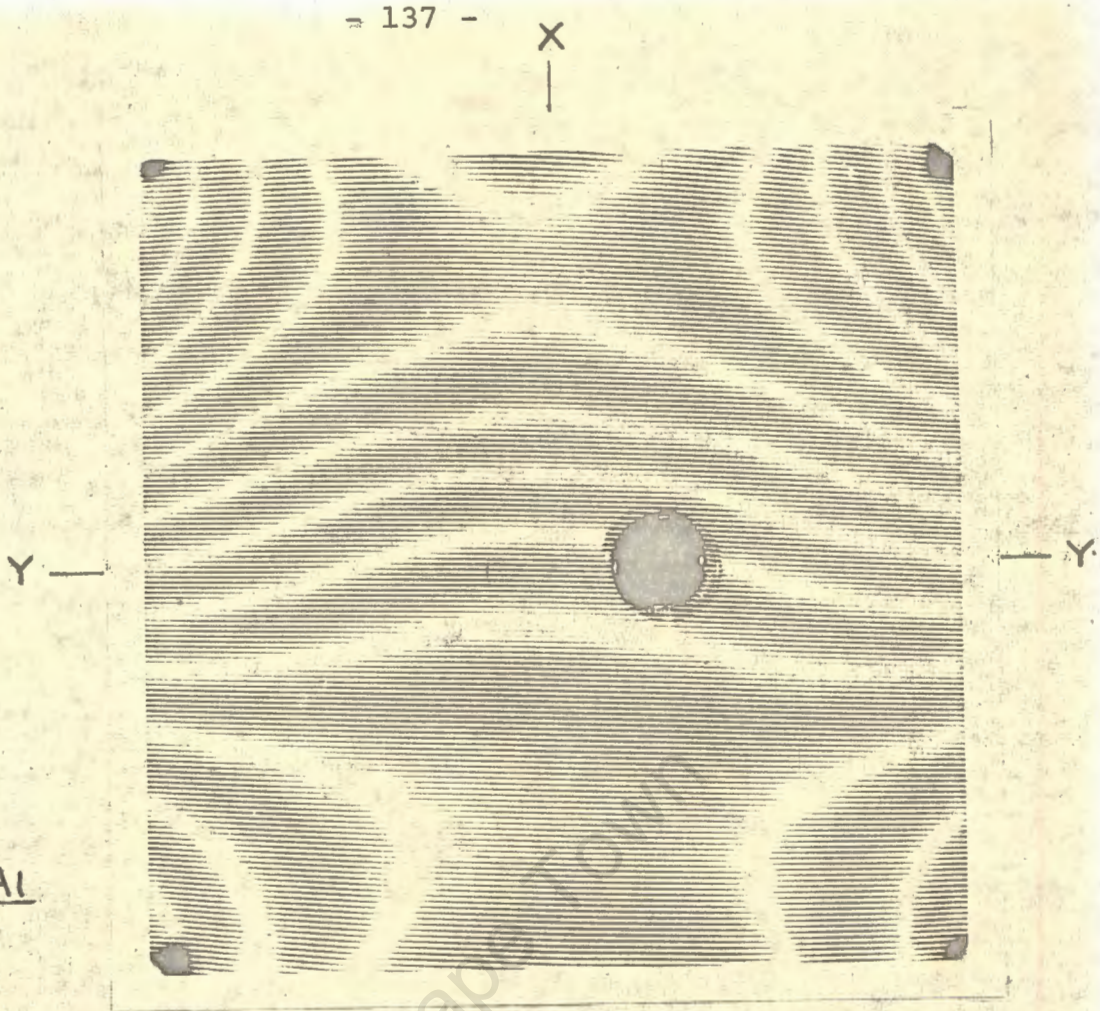

Fig. 5.10 (a) corresponding to Fig. 4.11 (a)

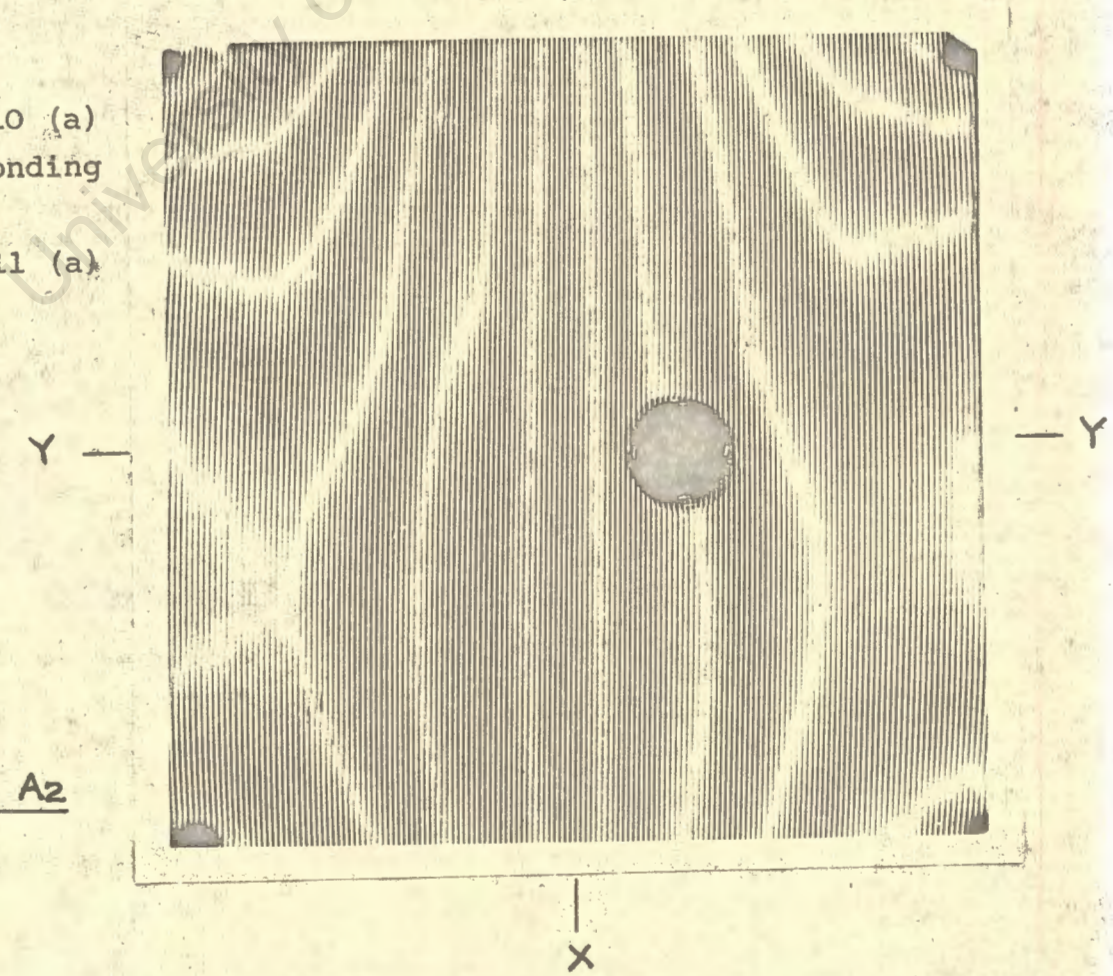

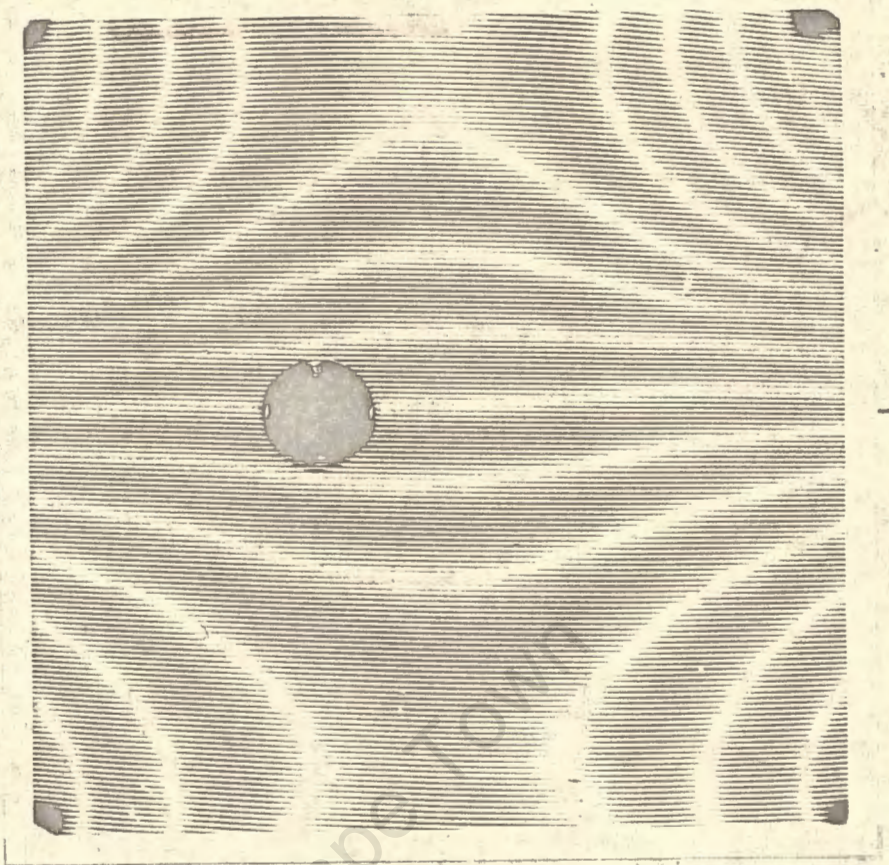

Photo B1

Fig. 5.10 (b) corresponding to Fig. 4.11 (b)

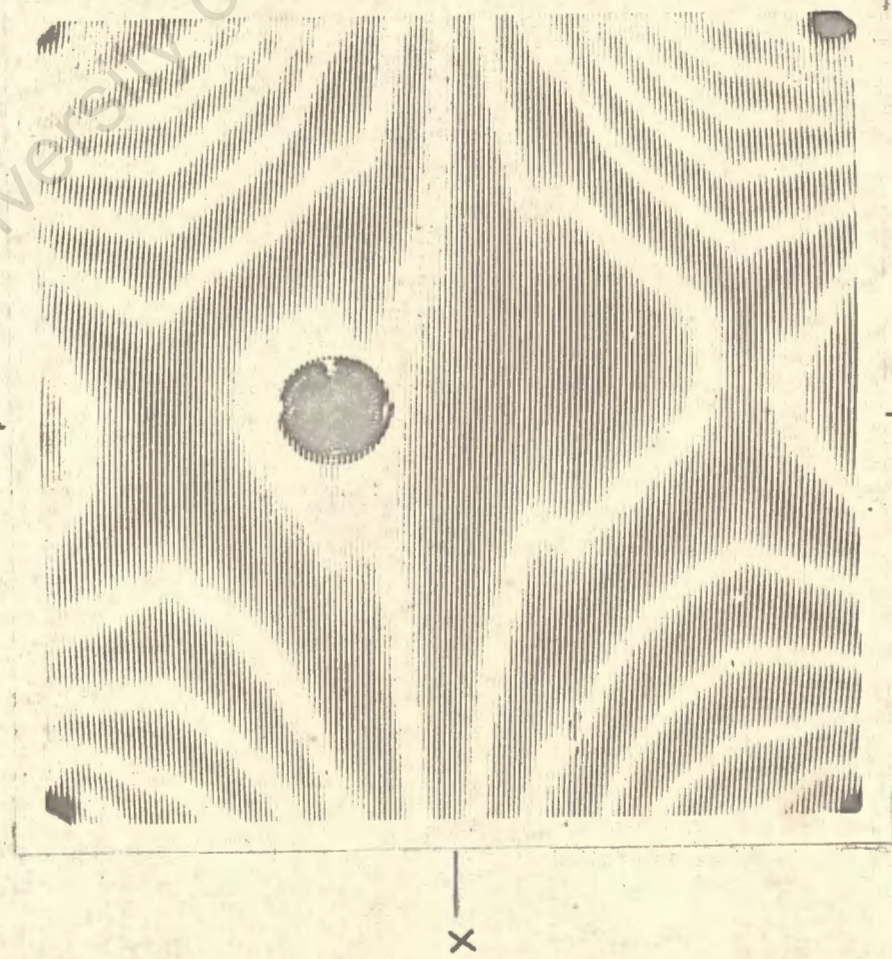

Photo B2

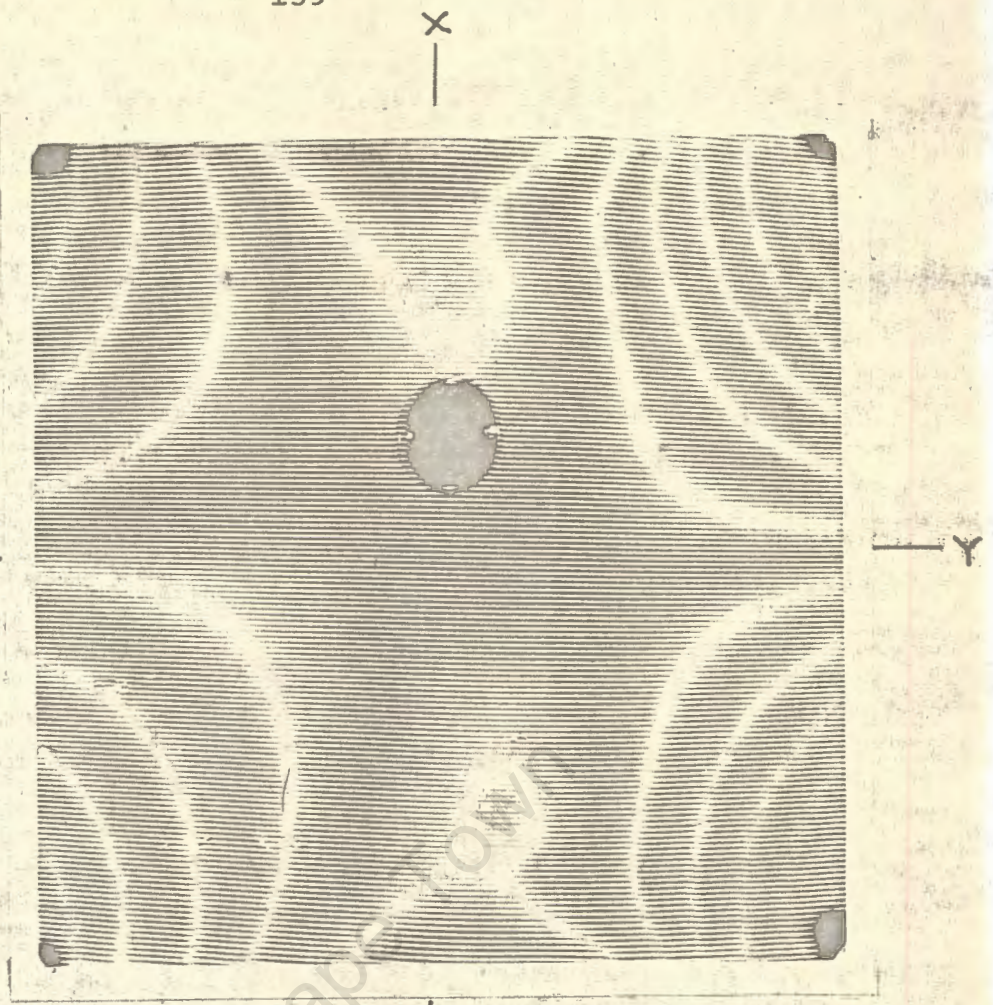

Photo C1

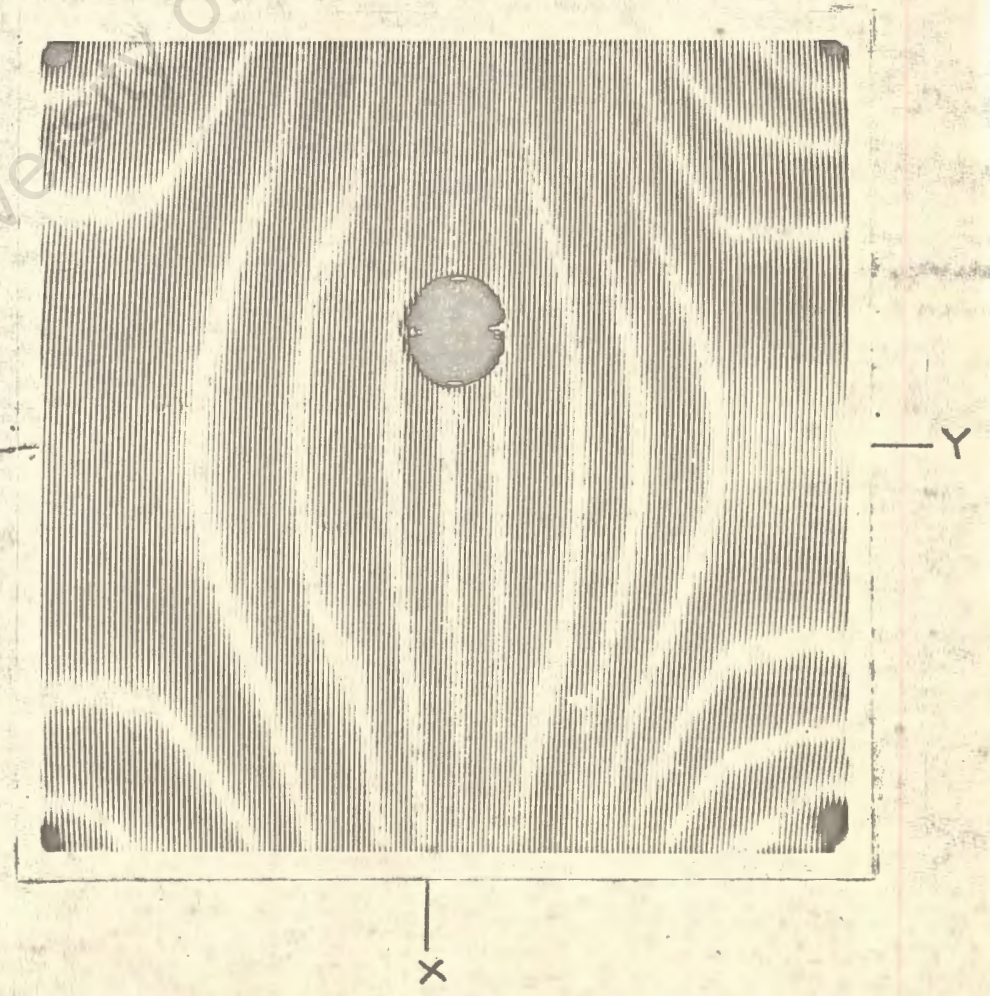

Photo C2

Fig. 5.10 (c) corresponding to Fig. 4.11 (c)

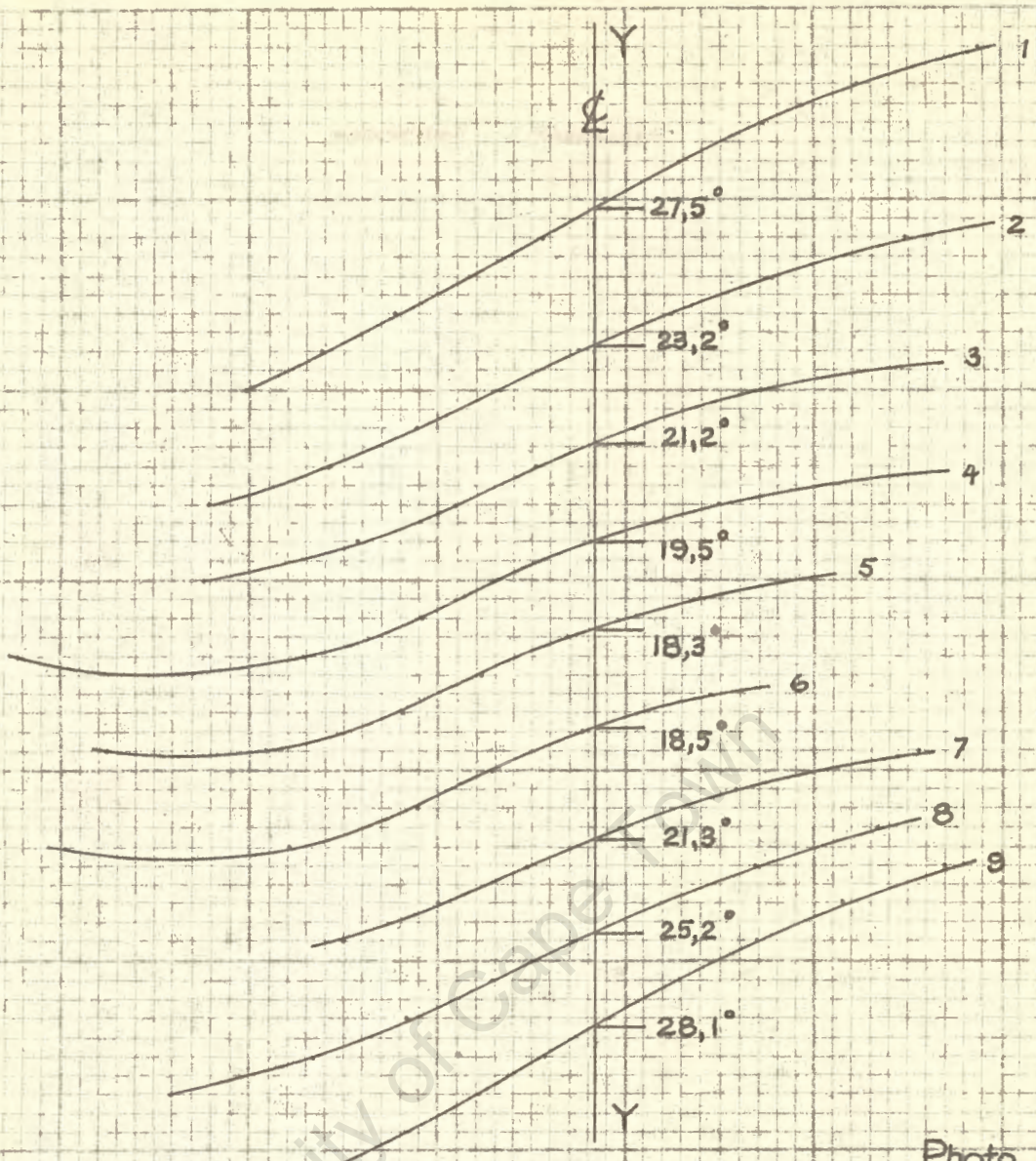

Photo A1

P = 4,35 N

$\frac{\partial w}{\partial x}$ — x

Change of slope between fringes

$$\frac{d}{2a} = 0{,}1344 \times 10^{-2} \equiv 0{,}2 \text{ inches}$$

Line	$\angle^\circ$	tan $\angle$	SM	Prod.
1	27,5	,520	1	,520
2	23,2	,428	4	1,712
3	21,2	,387	2	,774
4	19,5	,354	4	1,416
5	18,3	,330	2	,660
6	18,5	,334	4	1,336
7	21,3	,390	2	,780
8	25,2	,470	4	1,880
9	28,1	,534	1	,534
				9,612

$$\int_{-80}^{80} \frac{\partial^2 w}{\partial x^2}\, dy = 9{,}612 \times \frac{20}{3} \times \frac{0{,}001344}{0{,}2 \times 25{,}4} = 16{,}97 \text{ (dimensionless)}$$

Fig. 5.11

4 ribs, 1,5 mm deep

The equations are:

$$A1. \quad 14900 = D_x + 0{,}628\ D_{12}$$
$$B1. \quad 13000 = D_x + 0{,}015\ D_{12}$$
$$C1. \quad 24300 = D_x + 3{,}77\ D_{12}$$

$$A2. \quad 8210 = D_y + 0{,}178\ D_{21}$$
$$B2. \quad 10600 = D_y + 1{,}00\ D_{21}$$
$$C2. \quad 7900 = D_y - 0{,}094\ D_{21}$$

4 ribs, 3 mm deep

$$A1. \quad 31600 = D_x + 1{,}53\ D_{12}$$
$$B1. \quad 26180 = D_x + 0{,}302\ D_{12}$$
$$C1. \quad 55400 = D_x + 8{,}14\ D_{12}$$

$$A2. \quad 8800 = D_y + 0{,}058\ D_{21}$$
$$B2. \quad 8550 = D_y + 0{,}302\ D_{21}$$
$$C2. \quad 8050 = D_y - 0{,}095\ D_{21}$$

The solutions of the equations are as follows:

Ribs	Rib depth	D_x N mm	D_{12} N mm	D_{21} N mm	D_y N mm	Eqs
4	1,5	12950	3100	2900	7700	A,B
		13020	2990	(1160)	8000	A,C
		12960	3010	2480	8120	B,C
6	1,5	13020	3220	2980	8350	A,B
		13190	2980	3540	8250	A,C
		13020	3020	3130	8210	B,C
8	1,5	13080	3760	3580	7760	A,B
		13720	2840	(-160)	8370	A,C
		13080	2980	2700	8640	B,C
12	1,5	13260	3420	2910	8390	A,B
		13270	2960	4220	8170	A,C
		13640	2880	3240	8070	B,C
4	3	24850	4410	-1050	8700	A,B
		26100	3600	3140	8620	A,C
		25060	3730	600	8370	B,C
6	3	26010	3390	2730	8550	A,B
		26950	2780	3960	8480	A,C
		26200	2870	3200	8410	B,C
8	3	24050	4870	4160	7930	A,B
		26800	3290	-140	8020	A,C
		24500	3520	2580	8410	B,C
12	3	25380	2960	2280	8130	A,B
		24900	3250	1220	8200	A,C
		25300	3200	1800	8260	B,C

Table 5.1

The values in brackets have been ignored in taking the means.

The mean results for each plate are as follows:

Table 5.2

Ribs	Rib depth	D_x N mm	D_{12} N mm	D_{21} N mm	D_y N mm
4	1,5	12980	3030	2690	7940
6	1,5	13080	3070	3220	8270
8	1,5	13290	3190	3140	8260
12	1,5	13390	3090	3460	8210
Mean		13180	3100	3130	8170
SDMN		74	75	160	77
RSDMN		0,006	0,024	0,051	0,009
True RSDMN, σ		0,009	0,025	0,051	0,011

Table 5.3

Ribs	Rib depth	D_x N mm	D_{12} N mm	D_{21} N mm	D_y N mm
4	3	25780	3980	(920)	8710
6	3	26860	3060	(3260)	8630
8	3	25570	3960	(2240)	8270
12	3	25640	3190	(1800)	8350
Mean		25960	3550	-	8490
SDMN		262	178	-	69
RSDMN		0,010	0,051	-	0,008
True RSDMN, σ		0,012	0,051	-	0,011

In the table above for the 3 mm deep ribbed plates the means are for a 2 minute creep time, found by multiplying the actual means by 1,018 (see section 3. above). SDMN is calculated as before and

$$RSDMN = \frac{SDMN}{Mean}$$

The constant error in the Moiré method must be taken into account

$$\therefore \quad (\text{True RSDMN})^2 = \sigma^2 = (RSDMN)^2 + (SDKM)^2$$

σ represents the true uncertainty with which the variable in question is known.

8. Discussion

a. D_x results

For the thinner 4 plates it is seen that the experimental value for D_x increases with the number of ribs. However the total increase is only 3%. It may be said that D_x does not vary in the range of rib numbers tested. For the thicker 4 plates D_x can not be said to either increase or decrease with the number of ribs.

The 4 theoretical values of D_x have been calculated in Appendix A. They are compared to the mean experimental values below.

	1,5 mm rib	$\frac{(DX - D_x)}{D_x}$	3,0 mm rib	$\frac{(DX - D_x)}{D_x}$
DX1	12060	-0,085	24720	-0,048
DX2	13030	-0,011	26040	0,003
DX3	13650	0,036	27970	0,077
DX4	13660	0,036	30100	0,160
D_x	13180	-	25960	-

The uncertainties in DX were calculated in section 6. To show the comparison between experimental and theoretical results most clearly the frequency distributions of the variables are shown below

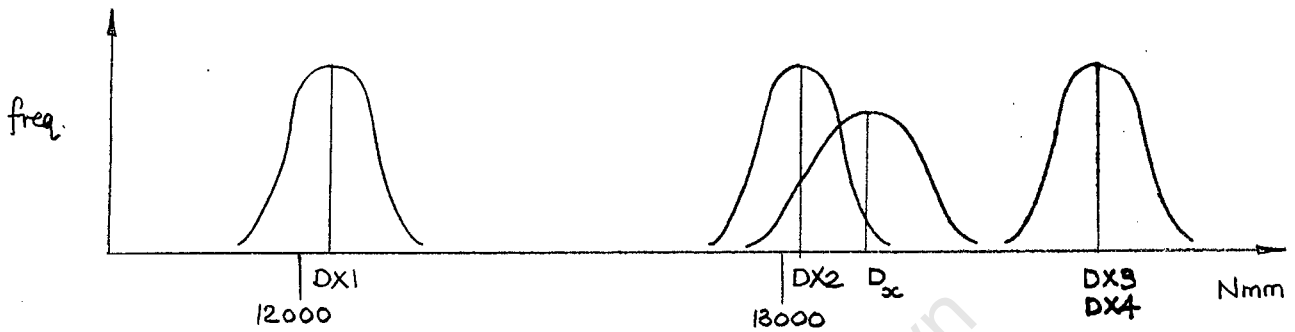

Fig. 5.12

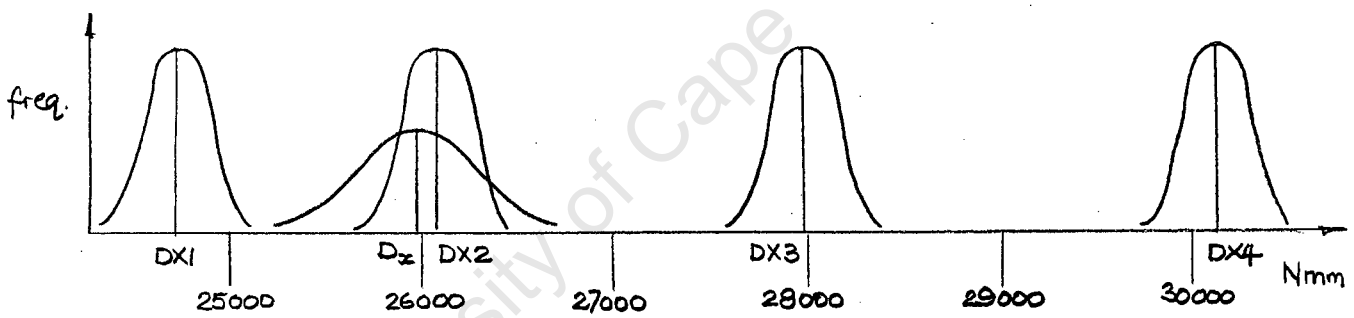

Fig. 5.13

The formulae for DX were

$$DX1 = \frac{EI_x}{s} \qquad \textbf{Eq 2.41}$$

$$DX2 = \frac{E}{s}\left(\frac{bd^3}{12} + bde_2^2\right) + \frac{E}{(1-\upsilon^2)}\left(\frac{h^3}{12} + he_1^2\right) \qquad \textbf{Eq 2.39}$$

$$DX3 = \frac{EI_x}{(1-\upsilon^2)} \qquad \textbf{Eq 2.42}$$

$$DX4 = DX2 + e_1^2\, E\left(h + \frac{bd}{s}\right) \qquad \textbf{Eq 2.40}$$

It can be seen from Figs. 5.12, 5.13 that the formulae for DX1, DX3 and DX4 are highly unlikely to be good estimates of D_x for the range of plates tested. The probability that DX2 is the true formula is high. We may say that D_x is best expressed by DX2.

As the size of the rib with respect to the plate diminishes, DX2 and DX3 converge. As the size of the rib with respect to the plate increases, DX1 and DX2 converge. Thus other formulae besides DX2 will give good approximate values in special circumstances.

The 8th order theory of Massonnet predicts that D_x lies between DX2 and DX4. For the thinner 4 plates D_x lies comfortably inside this range, but closer to DX2 (see Fig. 5.12). For the thicker 4 plates the value of D_x lies just 0,3% below DX2 (see Fig. 5.13). The conclusion is that the true value of D_x can be very little greater than the value given by DX2.

b. D_y results

The spread of the results is small as shown by the value of σ of 0,011 obtained for both the 1,5 mm and 3 mm rib plates. The test therefore determines D_y well. The value of D_y shows no significant increase or decrease with increasing rib numbers.

The theoretical formulae for D_y were:

$$DY1 = D \qquad \text{Eq 2.43}$$

$$DY2 = \frac{Eh^3 s}{12(s-b+\alpha^3 b)} \qquad \text{Eq 2.44}$$

$$DY3 = \frac{B^5}{30\int_0^B \frac{(By-y^2)^2}{D(y)}dy} \qquad \text{Eq 2.45}$$

where B is the span in the Y direction

where $D(y) = \frac{E[h(y)]^3}{12(1-\upsilon^2)}$

where h(y) is the total thickness of the plate stiffener combination subject to the following limitation. When the ratio of stiffener height to stiffener width is greater than unity a reduced height of the order of the stiffener width is used.

By the 8th order theory $D_y = D$; there is no increase in D_y due to the eccentric ribs. In Appendix A the theoretical values are given. They are compared below.

	1,5 mm rib	$\frac{(DY-D_y)}{D_y}$	3 mm rib	$\frac{DY-D_y}{D_y}$
DY1	7660	-0,062	7660	-0,098
DY2	8930	0,093	8990	0,059
DY3	9300	0,138	9810	0,162
D_y	8170	-	8490	-

The frequency distributions are as follows:

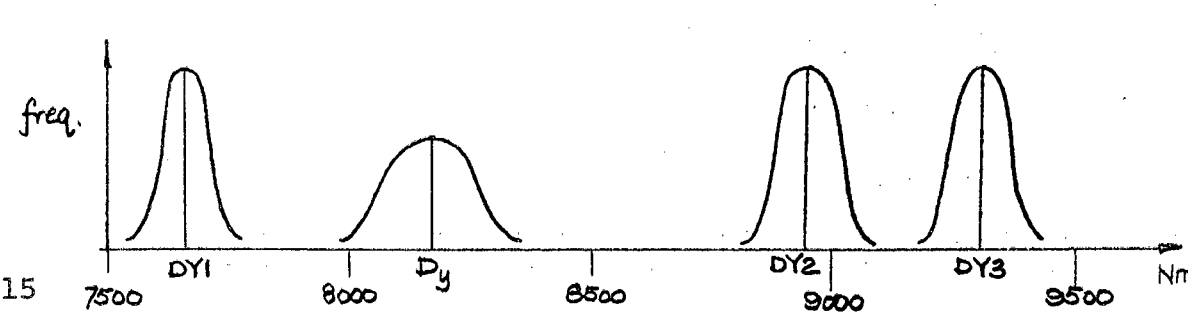

Fig. 5.15

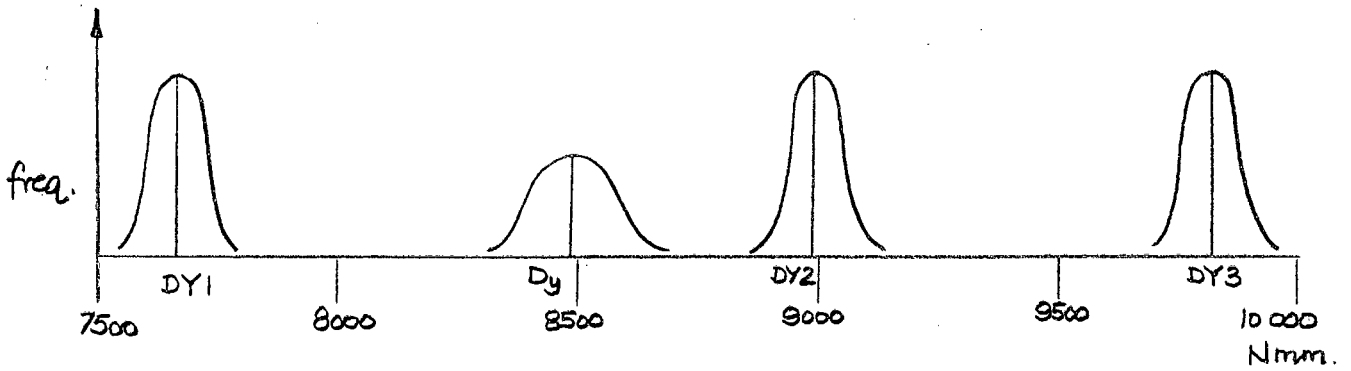

Fig. 5.16

The formula DY2 and DY3 can be rejected confidently. The mean value of D_y is very significantly larger than DY1. The cause is easily seen when tracing the curves of slope versus distance from the Moiré fringe patterns. As an example consider a 4-ribbed plate.

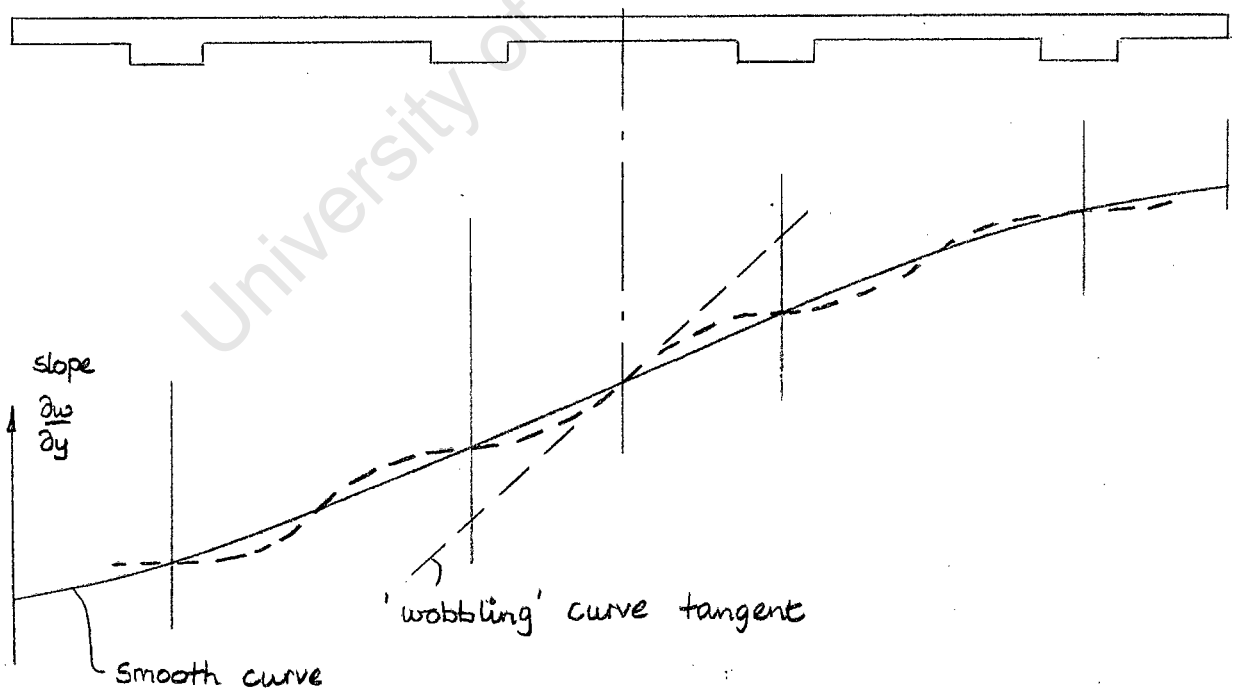

Fig. 5.17

The section taken is general and the form of the curve is a common one. The actual deflection of the plate is

represented by the dotted 'wobbling' line. The full smooth line is the one used to find the curvature at midspan for eventual use in the system of equations. The 'wobble' for an actual plate can be seen in Fig. 5.11 (Photo A2). Thus D_y is calculated by pretending that the plate is smoothly bent, or, in other words, is behaving as its equivalent true orthotropic plate would. This gives a low value to the curvature at midspan and thus a high value to D_y.

This effect is most noticeable in plates with low numbers of ribs. For high numbers of ribs not enough Moiré fringes can be obtained to see whether the 'wobble' is as pronounced as in the low rib numbered plates. Thus D_y is an arbitrary value. If the deflection of the plate is required at a point well away from the supports, then the high value of D_y may be used (D_y = 8170 or 8490 N mm). If the actual curvature at a point in the plate is required, then the low value ($D_y = D$) should be used.

c. D_{12} and D_{21} results

Values of D_{12} and D_{21} can not be said to either increase or decrease with increasing rib numbers. D_{12} is defined more precisely by the experiments than D_{21}. This is seen from the thinner plates where the values of σ were 0,025 and 0,051 for D_{12} and D_{21} respectively, and from the thicker plates where σ for D_{12} was 0,051 and D_{21} was very scattered. It was considered that it would be misleading to mean these values of D_{21} and draw conclusions from it. This scatter of results is partly due to the conditioning of the equations and partly due to the 'wobble' mentioned in the graphs in the

Y direction. This 'wobble' will interfere in any bending test devised.

For the thinner 4 plates the mean values of D_{12} (3100) and D_{21} (3130) agree very well. For these plates we may confidently take $D_{12} = D_{21}$. For the thicker 4 plates D_{21} is not well enough defined to draw a conclusion.

The theoretical values of D_1 are

$$D_1 = 0 \qquad \text{Eq 2.48}$$

$$D_1 = \upsilon D \qquad \text{Eq 2.47}$$

Eq 2.47 applies for the 4th and 8th order theories. In section 5. above it was found that

$$\upsilon D = 2610 \text{ N mm}$$

The frequency distributions of the variables are shown below.

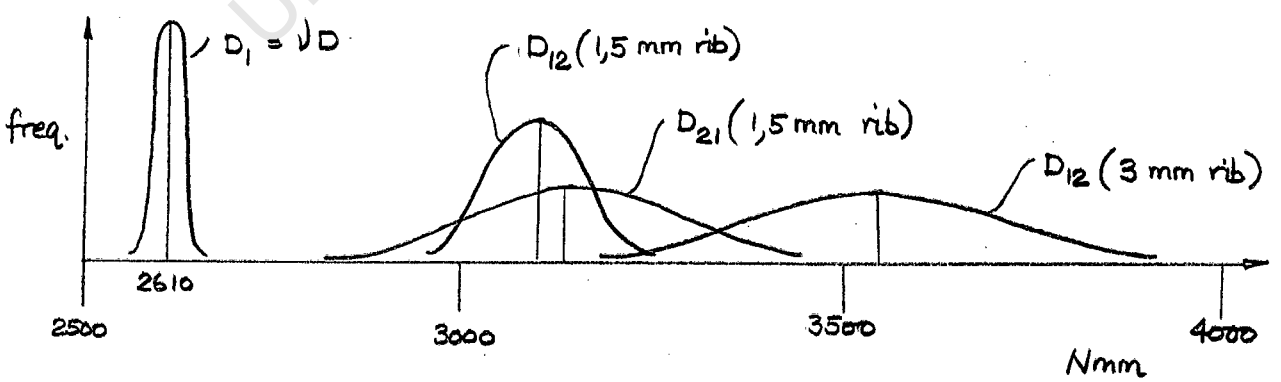

Fig. 5.14

It can be seen that the theoretical value

$$D_1 = \upsilon D$$

is well below the experimental values. There is no theoretical formula which satisfies the experimental results. Certainly $D_1 = 0$ is a poor approximation. The formula

$$D_{12} = D_{21} = \upsilon D$$

may be used as a conservative approximation.

8. Conclusions

a. The Method

It has been shown how the flexural rigidities of a stiffened plate can be determined from one model by the writer's method. It has been shown that the Moiré method is a convenient and accurate method for this purpose. Incorporated in the method is an accurate way of determining E and υ. The phenomenon of creep and the variation of the model dimensions from those specified has been catered for. A study of the errors in the experiments has been done in order to assess the confidence with which conclusions are drawn.

With the support and loading conditions used it was seen that, for the thinner 8 plates, D_x and D_y were well defined. D_{12} was not as well defined and, for the 3 mm rib plates, D_{21} was poorly defined. A survey of the literature shows that Bergsträsser's method does not give good results for D_{12} and D_{21} either.

For the plates with 6 and 9 mm deep ribs it was found that the plates were too stiff in the X direction for good results. In other words not enough fringes could be obtained in the X direction before the plate became heavily

bent in the Y direction. In order to get results for these stiffer plates the method must be modified. This may be done in several ways, which may be combined.

i. Instead of using a square plate a rectangular plate may be used. This plate must have the ribs running parallel to its long side. Only one model is necessary as the twisting test can be done on a rectangular plate. A rectangular plate will allow a greater curvature in the X direction for the same curvature in the Y direction. The conditioning of the equations may deteriorate using this method.

ii. Instead of 4 point supports two opposite sides of the plate may be simply supported. This has the same effect as i. above.

b. The Flexural Rigidities

For the range of rib numbers tested, it may be said that D_x, D_{12}, D_{21} and D_y do not vary. In this sense the plates behave as true orthotropic plates.

D_x is best expressed by the formula for DX2 (Eq 2.39). The formulae for DX1, DX3 and DX4 may confidently be rejected as being the true formulae for D_x. The 8th order theory predicts that D_x lies between DX2 and DX4. It is concluded that, for the loading and support conditions used, D_x can be very little greater than DX2.

D_y may be given two different values. This is because the plate does not bend smoothly in the Y direction; the curvature is greatly reduced over the ribs. In this sense the plate does not behave as an orthotropic plate. If it

is required that the difference in deflections between the stiffened plate and the equivalent orthotropic plate be a minimum, then the value of D_y to be used shows no agreement with any of the theoretical formulae. If it is required that the moments in the stiffened plate and the equivalent orthotropic plate be the same, then the formula $D_y = D$ should be used to find the curvatures. A high value of D_y should then be used to calculate the moment at any point in order to be on the safe side.

D_{12} may be said to be equal to D_{21} for the thinner 4 plates. In this respect the plates behave as orthotropic plates. For the thicker 4 plates the results were not precise enough for a conclusion to be drawn. There is no theoretical formula which describes D_{12} and D_{21} well. $D_1 = 0$ is a very poor approximation. The formula $D_1 = \upsilon D$ may be used as a conservative approximation.

CHAPTER 6

THE TWISTING TEST

1. General

The method used was described in Chapter 4, section 3., and the models were described in Chapter 5, section 1. Some of the models were made from clear perspex and some from black perspex. It was considered prudent to test whether the properties of black and clear perspex are the same, and therefore a square model made of each was milled down to a uniform thickness of 3 mm. The twisting test was performed on each and the results for D_{xy} compared. It was also considered prudent to test whether the milling of the models has any effect on the properties. Accordingly a square model of black perspex of nominal thickness 1/8 inch was cut and subjected to the twisting test. This model was not milled at all.

The variation in the dimensions of the models from those specified was allowed for by the calculation of a correction factor k_{xy}, as follows. The measurements made are shown in Fig. 5.3 for model 4/1,5. The measurements along the midspan line were given double the weight of the edge measurements. The mean of h, h_a, was calculated and subtracted from each value of (d + h) to find values of d. d_a and b_a were calculated. All means taken were the arithmetic means. The accuracy of this approximation was shown in Chapter 5. As was explained, a theoretical formula

for D_{xy} must be assumed. The formula is

$$D_{xy} = \frac{D(1-\upsilon)}{2} + \frac{GJ}{4s} \qquad \text{Eq 2.49}$$

Using the mean values of the dimensions, k_{xy} is calculated as

$$k_{xy} = \frac{D_{xy}\ (\text{actual})}{D_{xy}\ (\text{specified})}$$

In Appendix B the values of k_{xy} and the theoretical values of D_{xy} are calculated. In addition the two components of D_{xy} are given.

TPC = theoretical plate contribution = $D(1-\upsilon)/2$

TBC = theoretical beam contribution = $GJ/4s$

A creep time of 2 minutes was used in the experiments. Using E and υ at 2 minutes creep time and at the Moiré apparatus temperature as found in Chapter 5, G was calculated from

$$G = E/2(1+\upsilon)$$

The experiments were done at room temperature which varied between 16° and 18°C, and is considered to be constant. The results were converted to the Moiré apparatus temperature which is appreciably higher than room temperature. The effect of the temperature difference was investigated by taking one plate and doing the twisting test in the Moiré apparatus with the lights on, as well as at room temperature. The comparison is given in the results in section 3.

The testing procedure was as follows.

a. Load the dial gauge with a weight sufficient to give a deflection of approximately h/2 to 2h/3.

This deflection is larger than the usual limit of h/5 or h/3 of the small deflection theory. However the plate is supported in such a way that no horizontal support reactions are induced by large deflections. There will be small reactions caused by friction but these are considered to be negligible. The larger the deflection, the more precisely is it determined. The linearity of the load deflection graph was tested on two of the plates and found to be true within the limits of experimental error.

b. After 2 minutes unload the gauge.

This initial cycle is for the model to settle in on its supports.

c. After 2 minutes read the gauge and apply the load.

d. After 2 minutes read the gauge and remove the load.

Steps c. and d. are repeated until enough cycles have been performed to give a steady estimate of the differential downward deflection. This was usually 4 or 5 cycles. Throughout the test the model-holding-board is tapped at intervals to free the gauge spindle. Failure to do this can give erratic results, as the creep of the perspex is considerable.

As was mentioned in Chapter 5, the force exerted by the gauge spindle decreases linearly by 3 g wt per mm extrusion of the spindle. The nett force applied to the plate is calculated by subtracting the change in spindle force from the applied dead load. In the twisting test this correction is not negligible.

2. D_{xy} by Finite Differences

The theoretical formula for D_{xy} (Eq 2.49) cannot be expected to give the true value of D_{xy} for a ribbed plate. This is because the formula is the sum of the plate stiffness and the beam stiffness, acting as if they were separate members. The junction between the two must add strength to the combination.

The torsional rigidity of a T-beam, GJ_T, can be found exactly by the method of finite differences as will be described. The question is whether this result can be used to find D_{xy} of a ribbed plate made up of these T-sections. We must assume that

$$\frac{GJ_T}{s} = \gamma_x + \gamma_y = 4D_{xy}$$

in order to calculate D_{xy}. In comparing this value of D_{xy} with the experimental value, we are really testing the validity of this assumption. This was done for all the ribbed plates.

The analogy between the torsion of a beam and the deflection of a soap film under pressure is well known, and described in Ref. 6. The two problems are governed by similar differential equations. For torsion of a beam we have

$$\frac{d^2\phi}{dy^2} + \frac{d^2\phi}{dz^2} = -2G\Theta \qquad \text{Eq 6.1}$$

where $\phi(y,z)$ is a stress function and can be thought of as the deflection of a soap film stretched over the outline of

the cross-section, and where θ is the rotation per unit length of the beam

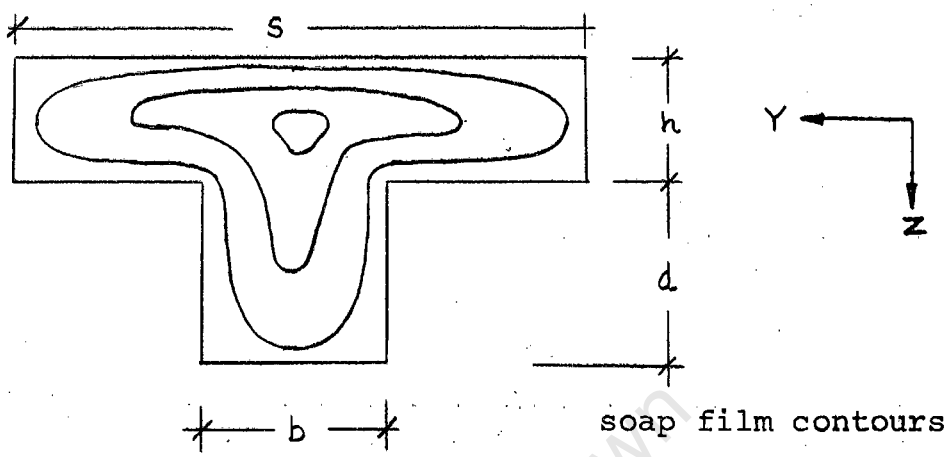

soap film contours
or contours of ϕ

Fig. 6.1

The twisting moment on the beam is

$$M_T = 2\iint \phi(y,z)\,dydz$$

$$= 2 \times \text{volume under soap film}$$

D_{xy} is then calculated as

$$D_{xy} = (\text{volume under soap film})/2s$$

The finite difference solutions were found using the computer program in Appendix C.

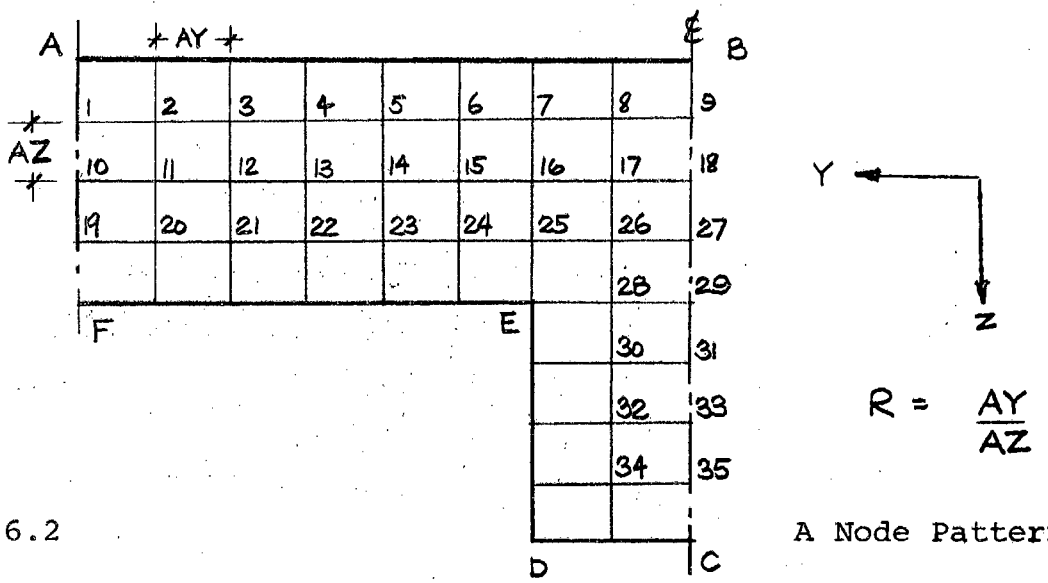

Fig. 6.2 A Node Pattern

Only an L-section is analysed because of the symmetry. The differential equation (Eq 6.1) is applied in finite difference form at each node

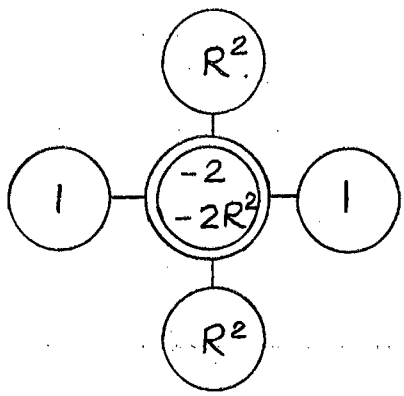

$$\nabla^2 \phi = -2G\theta \quad (AY)^2$$

General Operator Pattern

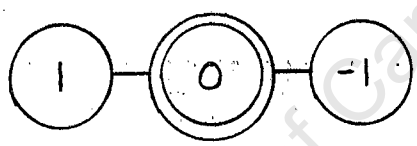

$$\nabla^2 \phi = 0$$

$$\frac{d\phi}{dy} = 0$$

Pattern

Fig. 6.3

Along lines AB,CD,DE,EF the boundary condition is that $\phi = 0$. Along line BC $\frac{d\phi}{dy} = 0$. Along line AF when $\phi = 0$ the T-beam has 'closed ends' and when $\frac{d\phi}{dy} = 0$ it has 'open ends'. D_{xy} is calculated twice giving a closed end and an open end solution. D_{xy} is then finally calculated as the weighted mean of the two results. For example, for a 4 ribbed plate

$$D_{xy} = [3.D_{xy} \text{ (open)} + D_{xy} \text{ (closed)}]/4.$$

In actual fact this refinement made very little difference to the results. It was found that

$$D_{xy} \text{ (open)} - D_{xy} = 30 \text{ N mm} \pm$$

for all ribbed plates.

The ratio of the node spacings, R, was a variable in the program. Different values of R were tested and the difference in results was negligible for ratios of between 4 and 1. The simultaneous equations were solved by Gauss diagonal reduction to save storage in the computer. This means that only the band width in the coefficient matrix of the set of equations was operated on. With this method roughly 500 nodes can be used without having to use files. The number of nodes which can be used depends on the aspect ratio, R, and the geometry of the cross-section. The university computer is a Univac 1106.

The accuracy of the solutions to the equations was checked by resubstituting the values of ϕ found back into the system of equations. The maximum difference between the left and right hand sides of the equations was then found. This error was of the order of 0,003% for 500 nodes and, in general, increased with increasing node numbers.

Finally the values of ϕ were used to calculate the volume under the imaginary membrane by Simpson's Rule. As a check the program was used to calculate D_{xy} of a uniform thickness plate 3 mm deep. The result was the same as that given by the theoretical formula.

3. Results

The results for the three uniform thickness plates were

Plate	D_{xy} (N mm)	Temp. ^{o}C
3 mm milled black perspex	2740	16,6
3 mm milled clear perspex	2710	16,3
1/8" unmilled black perspex	2710	16,1

It can be seen that it is very unlikely that black and clear perspex have different properties, or that milling has any effect on the properties. Meaning the results, it is concluded that D_{xy} of a perspex plate at 16,3^{o}C is 2720 N mm.

When the test was done in the Moiré apparatus with the lights on, the precision of the results was not as good. For the 3 mm milled black perspex plate values for D_{xy} of 2480 and 2580 N mm were obtained. The temperature of the plate was estimated as 24^{o}C. The value of D_{xy} from the theoretical formula

$$D_{xy} = D(1-\upsilon)/2$$

using the values of E and υ obtained in Chapter 5 is D_{xy} = 2525 N mm. The tests show therefore that the difference in temperature between that in the Moiré apparatus and outside it has a considerable effect on the properties of perspex. In order to correct the experimental results to the Moiré temperature a conversion factor of 2525/2720 was used. Assuming that D_{xy} (i.e. E) varies linearly with change in temperature, the estimated decrease in E per ^{o}C increase in temperature

$$= \frac{2720 - 2525}{24 - 16,3} \times \frac{100}{2620} \%$$

= 1%

It must be emphasized that this is only an estimate. More tests must be done to find a more accurate value.

A typical result sheet for the twisting test is given below.

TWISTING TEST READINGS

Plate: 3 mm milled black perspex k_{xy}: 1,044

Initial load: Dial gauge Tempre: 16,6°C

P g wt	Time min.	w mm	$\Delta w_2 \downarrow$ mm	$\Delta w_2 \uparrow$ mm	P g wt	Time min.	w mm	$\Delta w_2 \downarrow$ mm	$\Delta w_2 \uparrow$ mm
0	0	9,963							
111	1	7,635			111	17	7,500		
	2	7,568	(2,395)			18	7,478	2,280	
0	3	9,815			0	19	9,720		
	4	9,852		2,284		20	9,748		2,270
111	5	7,570			111	21	7,502		
	6	7,510	2,342			22	7,473	2,275	
0	7	9,740			0	23	9,715		
	8	9,800		2,290		24	9,730		2,257
111	9	7,550			111	25	7,480		
	10	7,507	2,293			26	7,457	2,273	
0	11	9,740			0	27	9,715		
	12	9,794		2,287		28	9,729		2,272
111	13	7,500			111	29	7,480		
	14	7,477	2,317			30	7,450	2,279	
0	15	9,730							
	16	9,758		2,281					

Mean $\Delta w_2 \downarrow$ = 2,286 mm

Nett weight, P_N, on plate = 111 - 3 (2,286) = 104,2 g wt

$$D_{xy_2} = \frac{6400.P_N.9,806}{\Delta w_2\downarrow.k_{xy}.1000} = \frac{62,8.104,2}{2,286.1,044} = 2740 \text{ N mm}$$

The experimental results for the ribbed plates are compared to the theoretical results for D_{xy} below. DXY1 is from Eq 2.49 and is calculated in Appendix B. DXY2 is from the finite difference analysis in Appendix C.

Ribs	Depth mm	DXY1 N mm	% Diff.	D_{xy} N mm	% Diff.	DXY2 N mm
Uniform 3 mm		2525	-	2525	-	2525
* 4	1,5	2600	27	3570	2	3650
* 6	1,5	2590	31	3740	-7	3490
* 8	1,5	2590	20	3240	3	3350
*12	1,5	2580	14	3000	4	3130
* 4	3	3040	33	4520	19	5370
* 6	3	2980	32	4400	7	4720
* 8	3	2920	27	4020	5	4220
*12	3	2820	19	3500	3	3590
* 4	6	5690	28	7930	29	10260
6	6	4900	27	6700	13	7580
8	6	4270	23	5570	7	5980
12	6	3540	17	4270	3	4380
4	9	10550	12	12030	36	16340
6	9	7660	17	9200	15	10630
8	9	5950	16	7100	9	7730
12	9	4310	15	5060	2	5150
*12	9	4310	13	4940	4	5150

* indicates black perspex.

The difference between the results for the two plates 12/9 is small. It will be remembered that the black perspex one was made by glueing two sheets together and then milling

out the plate. The results show that the glueing did not appreciably decrease the strength by the inclusion of air bubbles at the joint.

The D_{xy} result for plate 6/1,5 can be seen to be unreliable. From theoretical considerations D_{xy} of plate 4/1,5 must be greater than that of plate 6/1,5. It is considered that the error in k_{xy} for this plate is probably large, causing most of the error.

The uncertainty in D_{xy} is considered to be largely due to the error in assuming that Eq 2.49 is the true formula for D_{xy}. In other words, the uncertainty in k_{xy} is the dominant uncertainty. Eq 2.49 underestimates the contribution of the rib to D_{xy}. Consequently the variation in rib dimensions is not given sufficient weight in the calculation of k_{xy}. In the bending test much more accurate theoretical formulae were available for D_x and D_y and so this source of uncertainty did not arise.

It can be seen that there is a large difference between the values of DXY1 and D_{xy}. D_{xy} is consistently higher than DXY1. These differences are far too large to be accounted for by the uncertainties in DXY1 and D_{xy}. The percentage differences were calculated on the basis of D_{xy}, and follow a smooth pattern. The percentage difference can be seen to increase from zero when there is no rib to a maximum when the rib and plate depths are approximately equal. It then decreases as the rib depth increases. The percentage difference is larger for smaller numbers of ribs. The writer has not been able to find a satisfactory correction term to add to Eq 2.49 to bring it in line with

the experimental results. In the experiments the ratio of b : s was not varied, and this would limit the generality of the correction term if it were to be found.

There is also a large difference between the results for DXY2 and D_{xy}. DXY2 is consistently larger than D_{xy}. The percentage difference increases greatly with a decrease in the number of ribs. The percentage difference increases steadily as the ratio of the beam contribution to the plate contribution to D_{xy} increases. DXY2 was found from the rigidity of the T-beam, and it appears that this method does not apply to ribbed plates.

4. Conclusions

It has been shown that it is very unlikely that black and clear perspex have different properties, or that milling has any effect on the properties. The models were therefore satisfactorily made. The effect of temperature on the strength of perspex was investigated. It was estimated that the decrease in E per ^{o}C increase in temperature was 1%.

It has been shown that the equation

$$D_{xy} = \frac{D(1-\upsilon)}{2} + \frac{GJ}{4s} \qquad \text{Eq 2.49}$$

underestimates the torsional rigidities of asymmetrically stiffened plates reinforced in one direction. This formula gave values which were as much as 33% lower than the experimental values of D_{xy}.

It has been shown that the assumption that D_{xy} can be found from

$$D_{xy} = GJ_T/4s$$

where GJ_T is the torsional rigidity of the T-section of which the plate is made up is incorrect. As the size of the rib increases with respect to the plate, the results appear to diverge.

BIBLIOGRAPHY

1. Timoshenko, S. and Woinowsky-Krieger - 'Theory of Plates and Shells' - 2nd Ed., 1959.

2. Bares, R. - 'Tables for the Analysis of Plates, Slabs, and Diaphragms' - 2nd Ed., 1971.

3. Troitsky, M.S. - 'Orthotropic Bridges, Theory and Design' - 1967.

4. Bares, R. and Massonnet, C. - 'Analysis of Beam Grids and Orthotropic Plates' - 1968.

5. Leknitskii - 'Anisotropic Plates' - 2nd Ed., Moscow, 1957.

6. Timoshenko, S. and Goodier - 'Theory of Elasticity' - 2nd Ed., 1951.

7. Klöppel, K. and Yamadá, M. - 'Anisotrope Fliessbedingung' - Stahlbau, v.29, part 6, June 1960, p. 173-179.

8. Föppl, A. - 'Versuche uber die Verdrehungssteifigkeit der Walzeisentrager' - Sitzungsber, Bayr. Akad. d.W., 1921.

9. Huffington, N.J. - 'Theoretical Determination of Rigidity Properties of Orthogonally stiffened Plates' - Trans. A.S.M.E., J. of Applied Mechanics, March 1956, p. 15.

10. Adotte, G.D. - 'Second Order Theory in Orthotropic Plates' - A.S.C.E., J. of Structural Div., Oct. 1967.

11. Giencke, E. - 'Die Grundgleichungen für die orthotrope Platte mit exzentrischen Steifen' - Der Stahlbau, v.24, part 6, June 1955, pp. 128-129.

12. Massonnet, C. - 'Plaques et coques cylindriques orthotropes à nervures dissymetrique' - Intl. Ass. Bridge and Struc. Eng. (A.I.P.C.) Memoir, Zurich, v.19, 1959, p. 201-230.

13. Clifton, R.J., Chang, and Au, T. - 'Analysis of orthotropic bridge plates' - A.S.C.E., J. of Struc. Div., Oct. 1963.

14. M.T. Huber - 'Probleme der Statik Technisch Wichtiger Orthotroper Platten' - Warsaw, 1929.

15. M.T. Huber - 'Teorya Plyt' - Lvov, 1922.

16. Cornelius, W. - 'Die Berechnung der ebenen Flachëntragwerke mit Hilfe der Theorie der orthogonal-anisotropen Platte' - Der Stahlbau, v.21, parts 2,3,4; Feb., Mar., April, 1952.

17. Zienkiewicz, O.C. and Cheung, Y.K. - 'The Finite Element method for analysis of elastic isotropic and orthotropic slabs' - Proc. I.C.E., Aug. 1964.

18. Chu, K.-H. and Krishnamoorthy, G. - 'Use of orthotropic plate theory in bridge design' - A.S.C.E., J. of Struc. Div., June 1962.

19. Vitols, V., Clifton, R.J. and Au, T. - 'Analysis of composite beam bridges by orthotropic plate theory' - A.S.C.E., J. Struc. Div., Aug. 1963.

20. Bares, R. - 'Interaction transversale des constructions à poutres solidaires d'une dalle' - Acta Technica C.S.A.V., 1959, Nos. 4 & 5, 1960, No. 2.

21. W.H. Hoppmann - 'Bending of orthogonally stiffened plates' - J. App. Mech., Trans. A.S.M.E., 1955, v.77, p. 267.

22. Rowe, R.E. - 'A load distribution theory for bridge slabs allowing for the effect of Poisson's ratio' - Mag. of Concrete Research, v.7, No. 20, July 1955.

23. Leknitskii, S.G. - 'Theory of elasticity of an anisotropic elastic body', Holden-Dey, San Francisco, 1963.

24. Bergsträsser, M. - Z. techn. Phys., vol. 8, p. 355, 1927.

25. Hearmon, R.F.S. and Adams, E.H. - 'The bending and twisting of anisotropic plates' - Brit. J. Appl. Phys., v.3, May 1952, p. 150-156.

26. Hoppmann, W.H., Huffington, N.J. and Magness, L.S. - A study of orthogonally stiffened plates' - Trans. A.S.M.E., J. Appl. Mech., 1956, v.78, p. 343.

27. Ligtenberg, F.K. - 'The Moiré method' - Proc. Soc. Exptl. Stress Anal., v.12, part 2, 1955, pp. 83-98.

```
C      A P P E N D I X   A
C
C      KX AND KY FOR STIFFENED PLATES
C
       DIMENSION HM(13),HDM(12),DM(12),BM(12),TM(7)
       REAL KX,KY,NU
       WRITE(5,110)
  110 FORMAT('1H1,'NO. RIBS  R/S DEPTH     DX1       DX2       DX3       DX4
      1     KX    RSDMNIX       DY1     DY2     DY3     KY  RSDMNH3')
       WRITE(5,111)
  111 FORMAT(' ',' NM          NMM       NMM       NMM       NMM
      1                    NMM     NMM     NMM')
       DO 250 N=1,17
       READ(5,100)NR,S,BA,DA
  100 FORMAT(I2,3F7.4)
       NG=NR+1
C
C      DATA AND THEIR MEANS
C
       E=3010.
       PU=.341
       READ(6,105)(HM(I),I=1,NG)
       READ(5,105)(HDM(I),I=1,NR)
       READ(5,105)(BM(I),I=1,NR)
  105 FORMAT(16F5.2)
       SH=0
       DO 10 I=1,NG
    10 SH=SH+HM(I)**3.
       H=(SH/NG)**(1./3.)
       DO 15 I=1,NR
    15 DM(I)=HDM(I)-H
       SD=0
       SB=0
       DO 20 I=1,NR
       SD=SD+DM(I)**3.
    20 SB=SB+BM(I)**3.
       D=(SD/NR)**(1./3.)
       B=(SB/NR)**(1./3.)
C
C      CALC OF DX AND KX
C
       EIP=(S*H*H+2.*B*D*H+B*D*D)/(2.*(S*H+B*D))-H/2.
       EIT=((36.+6.*DA+DA*DA)/(24.+2.*DA))-1.5
       P1=(H**3.)/12.
       P2=H*EIP**2.
```

```
      P3=B*D**3./(12.*S)
      P4=(B*D*((H+D)/2.-EIM)**2.)/S
      DX1M=E*(P1+P2+P3+P4)
      D12=(9.+12.*EIT**2.)*DA/S
      D34=(DA**3./12.+DA*(1.5+DA/2.-EIT)**2.)*BA/S
      DX1T=E*(D12+D34)
      DX2T=E*(D12/(1.-ND**2.)+D34)
      DX3T=DX1T/(1.-ND**2.)
      DX4T=DX2T+EIT**2.*E*(3.+BA*DA/S)
      KX=DX1D/DX1T
C
C     CALC OF STD DEVS
      SH=0
      DO 25 I=1,NG
   25 SH=SH+(HM(I)-H)**2.
      SDSDH=(SH/(NG-1))**0.5
      SDMNH=SDSDH/(NG**0.5)
      SB=0
      SR=0
      DO 30 I=1,NR
      SD=SD+(DM(I)-D)**2.
   30 SR=SR+(RM(I)-B)**2.
      SDSDD=(SD/(NR-1))**0.5
      SDMND=SDSDD/(NR**0.5)
      SDSDB=(SR/(NR-1))**0.5
      SDMNB=SDSDB/(NR**0.5)
C
C     CALC OF RSDMNIX
C
      DIDH=H**2./4.+B*D*(D+B)*(2.*S*H**2.+9*D*(D+1.*H))/(4.*
     1((S*H+B*D)**2.)
      DID2=B*D**2./(4.*S)+B*H*(D+H)*(S*H*(H+3.*D)+2.*3*D**2.)/
     1(4.*(S*H+B*D)**2.)
      DIDB=D**3./(12.*S)+S*D*H**2.*(D+H)**2./(4.*(S*H+B*D)**2.)
      SDMNI=((DIDH*SDMNH)**2.+(DID2*SDMND)**2.+(DIDB*SDMNB)**2.)**0.5
      RSDMNI=SDMNI/(P1+P2+P3+P4)
C
C     CALC OF DY AND KY
C
      READ(8,105)(TM(I),I=1,7)
      ST=0
      DO 35 I=1,7
   35 ST=ST+TM(I)**3.
      T=(ST/7.)**(1./3.)
      KY=ST/189.
```

```
      DY1M=E*T**3./(12.*(1.-NU**2.))
      DY1T=E**2.25/(1.-NU**2.)
      DY2T=E**2.25*S/(S+PA*(1.-(3./(3.+DA)**3.)))
      Z=160.
      SUM=0.
      R=(S+DA)/2.
      ZZ=DA
      IF(DA.GT.BA) DA=BA
      DO 37 I=2,NR,2
      P=P-BA
      SUM=(Z**2.*R**3./3.-Z*R**4./2.+R**5./5.-Z**2.*P**3./3.
     1+Z*P**4./2.-P**5./5.)/(3.+DA)**3.+SUM
   37 R=R+S
      R=(S-DA)/2.
      P=0.
      NRR=NR+2
      DO 39 I=2,NRR,2
      SUM=SUM+(Z**2.*R**3./3.-Z*R**4./2.+R**5./5.-Z**2.*P**3./3.
     1+Z*P**4./2.-P**5./5.)/27.
      R=R+S
      P=R-S+DA
      IF(I.EQ.NR) R=80.
   39 CONTINUE
      DA=ZZ
      DY3T=E*160.**5./(720.*(1.-NU**2.)*SUM)
C
C     CALC OF STD DEVS
C
      ST=0
      DO 40 I=1,7
   40 ST=ST+(TM(I)-T)**2.
      SDSOT=(ST/6.)**0.5
      SDMNT=SDSOT/(7.**0.5)
      WRITE(5,115)NP,DA,DX1T,DX2T,DX3T,DX4T,KX,RSDMNT,DY1T,DY2T,DY3T,KY,
     1SDMNT
  115 FORMAT(1H0,3X,I2,F11.1,3X,4F9.0,2F7.3,5X,3F7.0,2F6.3)
  250 CONTINUE
      CALL EXIT
      END
```

NO.	RINGS	MIB DEPTH CM	DX1 MMM	DX2 MMM	DX3 MMM	DX4 MMM	KX	RSDMNIx	DY1 MMM	DY2 MMM	DY3 MMM	KY	RSDMNH3
*	4	1.5	12064.	13029.	13651.	13664.	1.020	.016	7664.	8932.	9306.	1.091	.005
*	6	1.5	12064.	13029.	13651.	13664.	1.044	.011	7664.	8932.	9301.	1.075	.007
*	8	1.5	12064.	13029.	13651.	13664.	1.101	.007	7664.	8932.	9300.	1.128	.007
*	12	1.5	12063.	13029.	13651.	13664.	1.118	.006	7664.	8932.	9300.	1.155	.005
*	4	3.0	24720.	26039.	27972.	30102.	1.025	.008	7664.	8988.	9818.	1.162	.005
*	6	3.0	24720.	26039.	27972.	30102.	1.027	.006	7664.	8988.	9811.	1.113	.003
*	8	3.0	24720.	26039.	27972.	30102.	1.025	.009	7664.	8988.	9810.	1.085	.005
*	12	3.0	24719.	26038.	27972.	30102.	1.024	.004	7664.	8988.	9810.	1.119	.003
*	4	6.0	81270.	84835.	91964.	115311.	1.008	.006	7664.	9018.	10104.	1.066	.006
	6	6.0	81270.	84835.	91964.	115311.	1.032	.009	7664.	9018.	10096.	1.151	.005
	8	6.0	81270.	84835.	91964.	115311.	1.009	.008	7664.	9018.	10042.	.997	.003
	12	6.0	81269.	84834.	91963.	115310.	1.038	.007	7664.	9018.	9869.	1.142	.004
	4	9.0	191807.	200555.	217045.	305045.	.976	.009	7664.	9025.	10176.	1.011	.001
	6	9.0	191808.	200555.	217046.	305045.	.987	.004	7664.	9025.	10119.	1.022	.001
	8	9.0	191807.	200555.	217045.	305045.	1.017	.007	7664.	9025.	10042.	1.054	.004
*	12	9.0	191805.	200553.	217043.	305043.	1.017	.010	7664.	9025.	9869.	1.116	.005
	12	9.0	191805.	200553.	217043.	305043.	.957	.007	7664.	9025.	9869.	1.000	.003

* INDICATES BLACK PERSPEX

```
C     A P P E N D I X   B
C
C     CALC OF DXY AND KXY
C
      DIMENSION HM(39),DANDHM(36),BM(36),DM(36)
      REAL NU,KXY
      WRITE(5,100)
  100 FORMAT(1H1,'NO. RIBS  RIB DEPTH     TPC       TBC       DXY     KXY')
      WRITE(5,102)
  102 FORMAT(' ','                MM          MMM       MMM       MMM')
C
C     DATA AND THEIR MEANS
C
      E=3810.
      NU=.341
      DO 35 IJ=1,17
      READ(2,105)NR,S,HA,DA,C
  105 FORMAT(I2,2F7.4,2F5.3)
      NH=3*(NR+1)
      ND=3*NR
      READ(2,110)(HM(I),I=1,NH)
      READ(2,110)(DANDHM(I),I=1,ND)
      READ(2,110)(BM(I),I=1,ND)
  110 FORMAT(16F5.2)
      J1=NR+1
      J2=2*(NR+1)
      K2=2*NR
      SH=0
      M=1.
      DO 10 I=1,NH
      SH=SH+HM(I)*M
      IF(I-J1)10,,
      M=2.
      IF(I-J2)10,,
      M=1.
   10 CONTINUE
      H=SH/(4.*NH/3.)
      DO 15 I=1,ND
   15 DM(I)=DANDHM(I)-H
      SD=0.
      SB=0.
      M=1.
      DO 20 I=1,ND
      SD=SD+DM(I)*M
      SB=SB+BM(I)*M
```

```
      IF(I-NR)20,,
      %=2.
      IF(I-K2)20,,
      %=1.
   20 CONTINUE
      D=SD/(4.*ND/3.)
      B=SB/(4.*ND/3.)
      G=E/(2.*(1.+NU))
      TPC=G*2.25
      APC=G*H**3./12.
      IF(D-9).,25
      TBC=G*DA**3.*BA*C/(4.*S)
      ABC=G*D**3.*B*C/(4.*S)
      GO TO 30
   25 TBC=G*DA*BA**3.*C/(4.*S)
      ABC=G*D*B**3.*C/(4.*S)
   30 DXYT=TPC+TBC
      DXY=APC+ABC
      KXY=DXY/DXYT
      %RITE(5,115)NR,DA,TPC,TBC,DXYT,KXY
  115 FORMAT(1H0,I6,F9.0,4X,3E8.0,F7.3)
   35 CONTINUE
      CALL EXIT
      END
```

NO.	RIBS	RIB DEPTH mm	IPC mm	IBC mm	OXY mm	MAX
*	4	1.	2525.	71.	2596.	1.045
*	6	1.	2525.	68.	2593.	1.031
*	8	1.	2525.	64.	2590.	1.105
*	12	1.	2525.	56.	2582.	1.127
*	4	2.	2525.	515.	3040.	1.041
*	6	3.	2525.	451.	2976.	1.069
*	8	3.	2525.	396.	2921.	1.049
*	12	3.	2525.	297.	2823.	1.068
*	4	6.	2525.	2167.	5692.	.999
	6	6.	2525.	2379.	4904.	1.052
	8	6.	2525.	1747.	4272.	1.000
	12	6.	2525.	1016.	3541.	1.045
	4	9.	2525.	8028.	10553.	.979
	6	9.	2525.	5133.	7657.	.985
	8	9.	2525.	4425.	6950.	1.002
*	12	9.	2525.	1789.	4314.	1.057
	12	9.	2525.	1789.	4314.	.970

* INDICATES BLACK PERSPEX

```
C     A P P E N D I X   C
C
C     BEAM TORSION BY FINITE DIFFERENCES
C
C     FOR CORRECT SIMPSON SUM
C     NL MUST BE EVEN, NH & NZ MUST BE ODD
C     FOR UNIFORM THICKNESS PLATE PUT NL>NY
      DIMENSION A(765,68),S(100),PHI(765)
      READ(8,4)NPL
    4 FORMAT(I3)
      G=1122.
      DO 290 KJ=1,NPL
      READ(8,5)AL,B,H,D
    5 FORMAT(4F12.6)
      READ(8,15)NY,NL,NH,NZ
   15 FORMAT(4I3)
      WRITE(5,10)AL,B,H,D,G
   10 FORMAT(1H1,'A=',F6.2,' : B=',F6.2,' : H=',F6.2,' : D=',
     1F6.2,' MM: G=',F6.1)
      WRITE(5,16)NY,NL,NH,NZ
   16 FORMAT(' ','NY=',I3,' : NL=',I3,' : NH=',I3,' : NZ=',I3)
      AY=AL/(2.*NY-2.)
      AZ=(H+D)/(NZ+1)
      R=AY/AZ
      WRITE(5,23)R
   23 FORMAT(' ','RATIO OF MESH SIZES AY/AZ=',F10.5)
      R2=R**2.
      NO=NH*NY+(NY-NL+1)*(NZ-NH)
      NE=NH+1
      ND=NZ-1
      NP=NY+1
      NR=NY*2
      NS=2*NY-NL+2
      NT=2*NY+1
      NV=2*NY+2
      NA=NH*NY
      NB=NA+1
      WRITE(5,24)NO
   24 FORMAT(' ','NO. OF NODES IS',I5)
C
C     SETTING UP THE EQUATIONS
C
      DO 290 IJ=1,2
      LL=1
   25 DO 20 I=1,NO
```

```
      A(I,NM)=-AY**2.
   20 CONTINUE
      DO 30 I=1,NO
      DO 30 J=1,NT
      A(I,J)=0.
   30 CONTINUE
      KO=0.
      DO 49 I=1,NZ
      DO 48 J=1,NY
      IF(I.GT.NH.AND.J.LT.NL)GO TO 48
      M=0.
      K=0.
      KO=KO+1
      IF(J.GT.I)GO TO 40
      IF(I.NE.J)GO TO 39
      A(KO,NM)=0.
      A(KO,NP)=1.
      GO TO 49
   39 IF(J.EQ.2) M=2
   40 IF(J.EQ.1) M=1
      IF(J.EQ.NL.AND.I.GT.NH)M=2
      IF(J.EQ.NY)M=3
      IF(J.LT.NL.AND.I.EQ.NH)K=1
      IF(J.GE.NL.AND.I.EQ.NH)K=2
      IF(J.GE.NL.AND.I.GT.NH)K=3
      IF(I.EQ.NZ)K=4
      IF(I.EQ.1)K=5
      A(KO,NP)=-2.-2.*R2
      IF(M.EQ.1)A(KO,NR)=2.
      IF(M.EQ.2)A(KO,NR)=1.
      IF(M.EQ.3)A(KO,NY)=2.
      IF(M.NE.0)GO TO 43
      A(KO,NY)=1.
      A(KO,NR)=1.
   43 IF(K.EQ.1)A(KO,1)=R2
      IF(K.NE.2)GO TO 45
       A(KO,1)=R2
      A(KO,NS)=R2
   45 IF(K.NE.3)GO TO 46
      A(KO,NL)=R2
      A(KO,NS)=R2
   46 IF(K.EQ.4)A(KO,NL)=R2
      IF(K.EQ.5)A(KO,NT)=R2
      IF(K.NE.0)GO TO 48
      A(KO,1)=R2
```

```
      A(KO,NT)=R2
   48 CONTINUE
      IF(LL.EQ.1)GO TO 90
      ERR=0.
      DO 60 I=1,NO
      DIF=-A(I,NP)
      DO 55 J=1,NT
      JJ=I-NY-1+J
      IF(JJ.LT.1.OR.JJ.GT.NO)GO TO 55
      DIF=DIF+A(I,J)*PHI(JJ)
   55 CONTINUE
   60 IF(DIF.GT.ERR) ERR=DIF
      ERR=ERR/AY**2.
      WRITE(5,65)ERR
   65 FORMAT(' ','MAX FRAC ERROR=',F14.10)
      GO TO 140
C
C     GAUSS DIAGONAL ELIMINATION
C
   90 DO 115 I=1,NO
      IF(A(I,NP))115,
      DO 95 J=NP,NP,-1
      A(I,J)=A(I,J)/A(I,NP)
   95 CONTINUE
      DO 105 L=NY,1,-1
      K=I+NY-L+1
      IF(K.GT.NO)GO TO 105
      A(K,NP)=A(K,NP)-A(K,L)*A(I,NP)
      LO=L+NY
      DO 100 J=LO,L,-1
  100 A(K,J)=A(K,J)-A(K,L)*A(I,J+NY-L+1)
  105 CONTINUE
  115 CONTINUE
      DO 120 I=NO,1,-1
      PHI(I)=A(I,NP)
      DO 117 J=NR,NT
      IF(I+J-NP.GT.NO)GO TO 120
  117 PHI(I)=PHI(I)-A(I,J)*PHI(I+J-NP)
  120 CONTINUE
      WRITE(5,125)(PHI(I),I=1,NA)
  125 FORMAT(1H0,3(F2.1))
      IF(NY.EQ.NZ) GO TO 135
      WRITE(5,130)(PHI(I),I=NR,NO)
  130 FORMAT(1H0,75(F2.1))
  135 LL=2
```

```
      GO TO 25
C
C     CALC OF VOLUME UNDER MEMBRANE
C
  140 DO 225 M=1,NH
      MA=M*NY
      MB=MA-1
      MC=(M-1)*NY
      MD=MC+1
      ME=MC+2
      MF=MC+3
      MG=MA-2
      S(M)=PHI(MD)
      MO=NY/2
      MM=NY-2*MO
      IF(MM-.2)210,,
      DO 200 I=ME,MB,2
      S(M)=S(M)+4.*PHI(I)
  200 CONTINUE
      DO 205 I=MF,MG,2
      S(M)=S(M)+2.*PHI(I)
  205 CONTINUE
      S(M)=S(M)+PHI(MA)
      GO TO 225
  210 DO 215 I=ME,MG,2
      S(M)=S(M)+4.*PHI(I)
  215 CONTINUE
      DO 220 I=MF,MB,2
      S(M)=S(M)+2.*PHI(I)
  220 CONTINUE
      S(M)=S(M)+2.*PHI(MA)
  225 CONTINUE
      IF(NH.EQ.NZ) GO TO 267
      DO 260 M=NK,LZ
      S(M)=0.
      MJ=NH*NY+(M-NH-1)*(NY-NL+1)
      MK=MJ+1
      ML=MJ+2
      MM=NH*NY+(M-NH)*(NY-NL+1)
      MN=MM-1
      MO=MM-2
      NQ=(NY-NL)/2
      MM=NY-NL-2*NQ
      IF(MM-.2)240,,
      DO 230 I=MK,MN,2
```

```
      S(M)=S(M)+4.*PHI(I)
  230 CONTINUE
      DO 235 I=ML,MO,2
      S(M)=S(M)+2.*PHI(I)
  235 CONTINUE
      S(M)=S(M)+PHI(MM)
      GO TO 260
  240 DO 245 I=MK,MO,2
      S(M)=S(M)+4.*PHI(I)
  245 CONTINUE
      DO 250 I=ML,MN,2
      S(M)=S(M)+2.*PHI(I)
  250 CONTINUE
      S(M)=S(M)+2.*PHI(MM)
  260 CONTINUE
      WRITE(5,265)(S(M),M=1,NZ)
  265 FORMAT(' ',15F8.2)
  267 SS=0.
      DO 270 M=1,NZ,2
      SS=SS+4.*S(M)
  270 CONTINUE
      DO 275 M=2,NM,2
      SS=SS+2.*S(M)
  275 CONTINUE
      V=2.*AY*AZ*SS/9.
      DXY=G*V/AL
      WRITE(5,280)DXY
  280 FORMAT(' ','DXY=',F14.6,' NMM')
  290 CONTINUE
      CALL EXIT
      END
```